

DELINEATING THE ECOLOGICAL NICHE TO PREDICT COMPETITIVE OUTCOMES  
AND THE INFLUENCE OF EVOLUTION

by

KENNETH EUGENE LEONARD

(Under the Direction of Mark A. Bradford)

ABSTRACT

Concerns with global and localized environmental change have increased interest in the course and outcomes of evolution as populations adapt to changing resource availability. Interest in populations often focuses on competitive outcomes under forcing or subsequent changes of resource availability. Changes of resource availability may be the supply of one resource in contrast to another—implicitly a change of supply ratio—or explicitly a change in the supply ratio of a pair of resources. Existing models of populations' contention for resources generally focus on development and competition over time assuming constant population characteristics, known initial states, and predictable future environmental states. We describe a simpler model to analyze evolution of populations' resource response characteristics under specific constraints and to predict expected competitive outcomes under a wide range of potential subsequent resource supplies.

We have developed, tested and applied a model of expected competitive outcomes in contention for multiple resources. We have analyzed changes of populations' requirements niches resulting from evolution in resource-limited ecological regimes. We have shown that evolution in one ecological regime not only shifts a population's requirements niche toward

greater fitness in that regime but can also shift the niche toward unexpected greater or lesser fitness in other regimes.

A population is formulated by its intrinsic growth response as a function of population-common and per-resource organismal growth response traits. The trait parameters are determined by curve fitting from demographic observations by a new Characterization Protocol. Competition is modeled in a Hutchinsonian space of resource supplies. Expected competitive outcomes are reported as per- and inter-population intrinsic growth rates throughout resource supply space. Results are displayed in qualitative and quantitative graphic forms and tabulated quantitative values of populations' response parameters.

We have applied our model to populations descended from a common ancestor in regimes of complementary restriction of two essential resources. Our model detects expected, unexpected and cryptic response trait changes and predicts intuitive and non-intuitive competitive relationships that can result from those changes in the event that any combination of ancestor, descendant or any other characterized population should come into competition anywhere in the resource supply space.

INDEX WORDS: Coexistence, Competition, Displacement, Ecological evolution, Ecological genetics, Ecological niche, Evolution, Evolutionary ecology, Genetic ecology, Hutchinsonian niche, Invasion, Microevolution, Monod model,  $R^*$ , R-star, Requirements niche, Resource ratio, Tilman model

DELINEATING THE ECOLOGICAL NICHE TO PREDICT COMPETITIVE OUTCOMES  
AND THE INFLUENCE OF EVOLUTION

by

KENNETH EUGENE LEONARD

B.S., The University of Georgia, 2005

A Dissertation Submitted to the Graduate Faculty of the University of Georgia in Partial  
Fulfillment of the Requirements for the Degree

DOCTOR OF PHILOSOPHY

ATHENS, GEORGIA

2010

© 2010

Kenneth Eugene Leonard

All Rights Reserved

DELINEATING THE ECOLOGICAL NICHE TO PREDICT COMPETITIVE OUTCOMES  
AND THE INFLUENCE OF EVOLUTION

by

KENNETH EUGENE LEONARD

Major Professor:

Mark A. Bradford

Committee:

John M. Drake  
David W. Hall  
James W. Porter  
John P. Wares

Electronic Version Approved:

Maureen Grasso  
Dean of the Graduate School  
The University of Georgia  
December 2010

## **Dedication**

This Dissertation is dedicated to my wife, Anna Louise Leonard, who has supported me in more ways than I can name. She recognized nearly a decade ago, even when I did not, that my life-long aspiration to become a researcher or professor in the natural sciences was not dead, not even moribund, but still alive and achievable. She encouraged and enabled me to restart my academic career first in Geology-Paleontology and then, when my real passion became clear, in Ecology.

She has been our financial support far beyond any obligation I can conceive. More notably and importantly, she has been my emotional and spiritual support—standing beside me or behind me at many times when I did not even notice her there. Most of all, she has loved me through everything that has happened throughout my life.

I must also give more than just a nod to our children, Norman Eugene and Stephanie Marie. Following their mother's example and loving as she taught them they have encouraged and supported their dad, and their mom, every step of the way.

I cannot think of anything more to say that would begin to suffice so I will say, just "Thank you".

## **Acknowledgments**

In addition to my Major Professor and Advisory Committee, I gratefully acknowledge the support of the following individuals:

Prof. C. Ronald Carroll, Odum School of Ecology & River Basin Center, The University of Georgia, for “If I were you, I’d do it.”,

Prof. Frank B. Golley, late of the Institute of Ecology, The University of Georgia, for conversations,

Prof. Susan S. Kilham, Department of Biology, Drexel University, for advice and encouragement in the earliest development of the graphical component of the model, and

Prof. Sally Walker, Department of Geology, The University of Georgia, for encouragement and support even before my initial matriculation at UGA.

## Table of Contents

<b>Dedication .....</b>	<b>iv</b>
<b>Acknowledgments .....</b>	<b>v</b>
<b>Table of Contents .....</b>	<b>vi</b>
<b>List of Tables .....</b>	<b>viii</b>
<b>List of Figures.....</b>	<b>ix</b>
<b>Chapter 1 , Background and Review .....</b>	<b>1</b>
<u>Figures</u> .....	<u>11</u>
<b>Chapter 2 , Modeling the Ecological Niche and Population Competition with Two Essential Resources .....</b>	<b>16</b>
<u>Summary</u> .....	<u>16</u>
<u>Introduction</u> .....	<u>16</u>
<u>Methods</u> .....	<u>20</u>
<u>Results and Discussion</u> .....	<u>25</u>
<u>Tables</u> .....	<u>30</u>
<u>Figures</u> .....	<u>31</u>
<b>Chapter 3 , Experimentally Characterizing the Ecological Niche and Validating a Model of Population Competition.....</b>	<b>41</b>
<u>Summary</u> .....	<u>41</u>
<u>Introduction</u> .....	<u>41</u>
<u>Methods</u> .....	<u>43</u>
<u>Results and Discussion</u> .....	<u>55</u>
<u>Tables</u> .....	<u>61</u>
<u>Figures</u> .....	<u>72</u>
<b>Chapter 4 , Experimental Evidence that Microevolution Reshapes the Ecological Niche... 75</b>	<b>75</b>
<u>Summary</u> .....	<u>75</u>
<u>Introduction</u> .....	<u>75</u>
<u>Methods</u> .....	<u>76</u>
<u>Results</u> .....	<u>80</u>

<u>Discussion</u> .....	86
<u>Tables</u> .....	89
<u>Figures</u> .....	95
<b>Chapter 5 , Conclusions</b> .....	<b>100</b>
<u>Validity</u> .....	100
<u>Research</u> .....	102
<u>Environmental Change</u> .....	103
<b>Works Cited</b> .....	<b>105</b>
<b>Appendix A, Mathematics</b> .....	<b>112</b>
<u>Introduction</u> .....	112
<u>Formulation Selection</u> .....	113
<u>Response Prediction</u> .....	114
<u>Plotting Code and Examples</u> .....	115
<u>Population Response Measurement</u> .....	116
<u>Response Statistics</u> .....	117
<u>Response Traits Curve Fitting</u> .....	119
<u>Figures</u> .....	123
<b>Appendix B, Yeast Strains</b> .....	<b>142</b>
<u>Tables</u> .....	143
<b>Appendix C, Biomass and Other Measurements Calibrations</b> .....	<b>144</b>
<u>Tables</u> .....	145

## List of Tables

<b>Table 2-1. Example Populations' Growth Response Parameters.....</b>	<b>30</b>
<b>Table 3-1. Yeast Characterization Nutrient Resource Supplies.....</b>	<b>61</b>
<b>Table 3-2. Typical Yeast Strain Characterization Data.....</b>	<b>62</b>
<b>Table 3-3. Yeast Strains Growth Response Parameters Summary.....</b>	<b>63</b>
<b>Table 3-4. Yeast Strains Growth Response Parameters Comparison. ....</b>	<b>64</b>
<b>Table 3-5. Yeast Strain MRG-2 Complete Response Parameters Data.....</b>	<b>65</b>
<b>Table 3-6. Yeast Strain MRG-2N Complete Response Parameters Data.....</b>	<b>66</b>
<b>Table 3-7. Yeast Strain MRG-8 Complete Response Parameters Data.....</b>	<b>67</b>
<b>Table 3-8. Yeast Strain MRG-8N Complete Response Parameters Data.....</b>	<b>68</b>
<b>Table 3-9. Results of Competitive Qualitative Outcomes.....</b>	<b>69</b>
<b>Table 3-10. Results of Competitive Quantitative Outcomes. ....</b>	<b>71</b>
<b>Table 4-1. Yeast Strains Growth Response Parameters Summary.....</b>	<b>89</b>
<b>Table 4-2. Yeast Strains Growth Response Parameters Comparison. ....</b>	<b>90</b>
<b>Table 4-3. Yeast Strain MRG-2 (Ancestor) Complete Response Parameters Data.....</b>	<b>91</b>
<b>Table 4-4. Yeast Strain Descendant-01 Complete Response Parameters Data.....</b>	<b>92</b>
<b>Table 4-5. Yeast Strain Descendant-13 Complete Response Parameters Data.....</b>	<b>93</b>
<b>Table 4-6. Phenomenological Pleiotropy for Descendant-13. ....</b>	<b>94</b>
<b>Table B-1. Yeast Strains Characteristics.....</b>	<b>143</b>
<b>Table C-1. Calibration: NTU Density <i>versus</i> Mass Density.....</b>	<b>145</b>
<b>Table C-2. Calibration: Mass Density <i>versus</i> Count.....</b>	<b>146</b>
<b>Table C-3. Calibration: NTU Density <i>versus</i> Count.....</b>	<b>148</b>

## List of Figures

Figure 1-1. One population in a Hutchinsonian resource space.....	11
Figure 1-2. Multiple populations and responses in resource space.....	12
Figure 1-3. Functional lines for a population in resource space.....	13
Figure 1-4. Populations evolving under resource supply constraints. ....	14
Figure 1-5. Two populations in competition in resource space. ....	15
Figure 2-1. The Monod Growth Response Equation.....	31
Figure 2-2. Growth Response Plot, One Population on Two Resources.....	32
Figure 2-3. Growth Response Plots, Sibling Populations.....	33
Figure 2-4. Growth Response Plots, Shifted Maximum Response. ....	34
Figure 2-5. Growth Response Plots, Further Shifted Maximum Response.....	35
Figure 2-6. Growth Response Plots, Shifted Maximum Response and Per-Resource Response.....	36
Figure 2-7. Growth Response Plots, Sibling with Flatter Per-Resource Responses. ....	37
Figure 2-8. Growth Response Plots, Sibling with Steeper Per-Resource Responses.....	38
Figure 2-9. Leibold’s FIG 6 from (1995).....	39
Figure 2-10. Leibold’s FIG. 5 from (1996).....	40
Figure 3-1. Chemostat. ....	72
Figure 3-2. Typical Yeast Strain Parameters Plot <i>versus</i> Characterization Data. ....	73
Figure 3-3. Resource-Response Traits and Surface Plots. ....	74
Figure 4-1. OPLs for Ancestor and Descendant Populations. ....	95
Figure 4-2. Differential growth Response, MRG-2 <i>versus</i> Desc-01.....	96
Figure 4-3. Differential Growth Response, MRG-2 <i>versus</i> Desc-13.....	97
Figure 4-4. Growth Response Comparison Plots, Desc-01 <i>versus</i> Desc-13.....	98
Figure A-1. Growth Response Plot Code, <i>Mathematica</i> ®.....	128
Figure A-2. Growth Response Plot Code, Annotated Section .....	129
Figure A-3. Response Surface Plots .....	130
Figure A-4. Shaded and-Contour Response Plots.....	131

<b>Figure A-5. Monod Curve Fitting.....</b>	<b>132</b>
<b>Figure A-6. Sigmoid Switch .....</b>	<b>133</b>
<b>Figure A-7. Curve-Fitting Code.....</b>	<b>136</b>
<b>Figure A-8. Curve-Fitting Output.....</b>	<b>138</b>
<b>Figure A-9. Curve-Fitting Code, Annotated Core.....</b>	<b>141</b>

## Chapter 1, Background and Review

The principal hypothesis of this present work is:

*A population's ecological niche is reshaped by evolution in response to changes in its ecological environment but trait changes which are adaptive under immediate selection may be accompanied by others which can be either adaptive or maladaptive in other environments.*

The Hutchinsonian, ecological, requirements niche of a population is a complex of many individual response traits which can be synergistically or antagonistically coupled by underlying genetic covariance. When a change in one trait is selected in response to a change in the ecological environment, genetic covariance, which may be very difficult to detect in an ecological context, may result in other trait changes which are not under immediate selection. These cryptic trait changes may be significantly adaptive or maladaptive in other environments. If these cryptic changes are to be detected as actual events in a controlled, experimental approach or as typical events in a simulation approach there is need for a modeling approach which meets five objectives not presently well addressed in any one system:

- formulation for prediction of populations' response relationships and likely competitive outcomes across an entire  $n$ -dimensional Hutchinsonian space of resource availability or other effects—as in the post-Hutchinson concept of the *requirements niche*;
- absence of formulation for development over time, to obviate speculation and reduce the complexity of the model;

- formulation of populations' response functions in terms of inherent, organismal traits, rather than in terms of only observed, demographic variables;
- formulation of individual populations' responses from which competitive relationships may be determined by comparison, rather than inferred from observed, demographic relationships between populations; and
- formulation in terms of traits sufficient to include the effects of underlying subtle, cryptic and non-intuitive genetic covariance.

The concept of a population's or species' *niche* in the study of ecology can be traced from Grinnell (1917) ≈“necessary conditions for a species' existence”, through Elton (1927) ≈“a species' functional role within the food cycle”, and Gause (1936) ≈“competitive exclusion” to the definition of *ecological niche* by Hutchinson (1957) as ≈“the locus of a population within an *n*-dimensional hypervolume”. Pulliam (2000) proposed an insightful assessment of the transition of the niche concept from Grinnell and Elton to Hutchinson—from “...a place or 'recess' in the environment that has the potential to support a species.” to “the environmental requirements of a species”—which he summarized as “According to Hutchinson, species, not environments, have niches.” (Pulliam 2000, p. 351). See also the discussion of Elton *versus* Grinnell *versus* Hutchinson in Leibold (1995).

Following these foundational steps are MacArthur (1958, 1972), Hutchinson (1959, 1978), Williams (1964) and Levin (1970), all of which are operationally comparable to the Hutchinsonian requirements niche. More recent work by Tilman (1982, 1988), Chesson (1991, 2000a, b), Leibold (1995), Weiher and Keddy (1999) is, when reduced, operationally centered on the requirements niche.

Tilman's (1980) *Graphical-Mechanistic Approach* dynamic (*i.e.*, time-development) model is, at its core, formulated on resource requirements and responses although it includes the complications of "consumption" and "supply" vectors etc.. It is the parent of other models which often apply certain simplifying assumptions or variations in terminology (*e.g.*, "impact vectors") *cf.* Chase and Leibold (2003). Pulliam's (2000) *NICHE* spatial model and synthesis of "...niche width, habitat availability and dispersal ... interspecific competition *per se.*" into the niche concept includes species resource requirements and responses to resource availabilities as essential elements. According to Pulliam's own explanation, the *NICHE* model will usually work with some utility if only resource requirements and responses are in the formulation but will usually not work if resource requirements and responses are excluded no matter what else is included. These two models intersect in formulation and operation in spite of their apparent dichotomy of space (Pulliam) *versus* time (Tilman). Pulliam's model cannot avoid some time-dependent elements in its formulation even if they are not expressly acknowledged in a particular application and Tilman's model has direct implications (if not express functions) for resource supply gradients and resulting population response distributions across space.

We must also note that there has been disagreement about the relevance of the niche concept to community assembly and maintenance, favoring absence of response-per-supply mechanisms, neutral processes, as asserted by Hubbell (2001) and reviewed by Bell (2001). Hubbell's "*Unified Neutral Theory...*" was challenged, or at least asserted to be overkill, almost as soon as it was published, as by Condit...*and Hubbell* (Condit *et al.* 2002) or by Chisholm and Burgman (2004) with a reply by Hubbell and Borda-de-Agua (2004) and has continued to be challenged as by Wiegand *et al.* (2007) and Chase (2007). If the *Unified Neutral Theory* is literally correct then our work and all the others cited, attempting one or another form of

mechanistic modeling, are moot but we do not believe this is the case. Clark (2010), working in a forest environment comparable to the one in which Hubbell realized the core of his neutral theory seems to have put the debate over neutral *versus* differential mechanisms to an end with direct confirmation of competitive mechanisms operating at a finer grain than Hubbell considered.

We hold that neutral theory is a valuable checkpoint or counter-reference model for more complex theories of or incorporating the ecological niche concept. In his famous *Concluding Remarks*, Hutchinson (1957) said:

“It is not necessary in any empirical science to keep an elaborate logicomathematical system always apparent, any more than it is necessary to keep a vacuum cleaner conspicuously in the middle of a room at all times. When a lot of irrelevant litter has accumulated the machine must be brought out, used, and then put away.”

Hubbell’s *Unified Neutral Theory* can be viewed as an example of Hutchinson’s vacuum cleaner to be applied to the residue frequently left by mechanistic theories—residue not due to any failure of the theories themselves but accumulated from our over-simplified or over-complicated applications of them. We would say further that our present formulation-hypothesis-model-theory is another example of Hutchinsonian cleaning-up. Our model, with our five objectives given above, is intended to avoid the residue generated when spatial models such as Pulliam’s or time-development models such as Tilman’s are applied to questions of competitive relative response-capability-expectation, in instant conditions of resource supplies, with instant characteristics of response per resource, in light of evolutionary (or even variation-selective) changes in response characteristics, across a Hutchinsonian space. Our approach and model, in addition to direct application, may be taken as a way to improve the determination of population characteristics to be used in more complex models such as Pulliam’s or Tilman’s or in investigation of inter- *versus* intra-species effects as in Clark *et al.* (2007, 2010).

Our definition of the ecological requirements niche owes much to the definition of *ecological niche* by Holt *et al.* (2005) as “...that suite of environmental conditions within which populations of that species are expected to persist deterministically...”. Beyond this we emphasize what Chase and Leibold (2003) called the *requirements niche*, especially in the context of populations competing for shared limiting resources. We focus on competitive relationships and their expected outcomes of displacement, coexistence etc. at any point in resource supply space, at any time, without modeling *development over time* as with Tilman’s *supply and consumption vectors* (1980 *et al.*), *cf.* Chase and Leibold’s *impact factors* (as in, for example 2003) and without expressly modeling across geographic space *cf.* Pulliam (2000).

Figure 1-1 through Figure 1-5 may help to explain what we are attempting to do here. There are four essential points in all of these figures:

- Resource space is not physical space; it is mathematical. Location in resource space represents present conditions and movement in resource space represents changing conditions of a population which need not be moving in physical space.
- Response to resource supply may be intrinsic or demographic growth rate, or standing population census, or standing population biomass, or some other measure which varies with the supplies of the resources concerned.
- Resource supply may be concentration in a stationary medium like nitrogen in soil, or concentration in flowing medium as in our chemostats, or mass supply by time as in anthropogenic contribution, or some other measure which we wish to deal with.
- This representation of resource space and populations may be measured and formulated in whatever units and by whatever mathematical function constitute a consistent set for the ecological function and purpose at hand.

Figure 1-1 shows our concept of a population in a Hutchinsonian resource space. Figure 1-2 shows how we locate a population and its growth response in resource space. Figure 1-3 illustrates “lines” in the resource space relevant to a single population’s response. Figure 1-4 shows our concept of what happens when populations evolve under resource supply constraints. And Figure 1-5 shows two populations coming into competition in resource space.

Supply vectors and their development over time are speculative at best. Consumption vectors are dependent on relative population size and combined population size as they develop over time. Modeling with these vectors, the requisite speculation and the requisite complex parameters, is still a fruitful endeavor for certain purposes but not for ours (cf. complexity problems in Miller et al. 2005). This distinction between modeling competitive relationship, relative growth response in any regime across a resource space, on one hand, and modeling competitive development over time, relative growth outcome in a specified-predicted resource regime, on the other hand, should lead to two distinct classes of models for which there is clear distinction between the different objectives—with our model being an instance of the former case. Another distinction we make is between models which operate essentially on formulation from demographic, observed phenomena such as per-resource supply and realized growth, on one hand (cf. parameter problems in Miller et al. 2005), and formulation from inherent, organismal-population traits such as self-limited intrinsic growth capability and per-resource intrinsic growth response on the other hand—with our model being an instance of the latter case. The former case models may be “ecologically easier” but are difficult, if possible at all, to formulate realistically over a broad range of ecological regimes—an essential objective of our work.

There are, in the literature, virtually no distinctive models, strongly similar to ours, which comprehensively address the objective of predicting populations' relative growth response throughout an arbitrary Hutchinsonian space. There have been several models, however, which address the objective of predicting relative growth outcome over time in specific resource or resource-and-predation regimes, virtually all of which are replicas or derivatives of Tilman's *Graphical-Mechanistic Approach* (1980). This approach and many of its successors are reviewed by Miller, *et al.* (2005) and it is used by Chase and Leibold (2003) in the *requirements niche* context. Tilman's approach was not entirely new, as he readily acknowledged, but was based primarily on the consumer-resource models of MacArthur (1972). MacArthur, in his turn, acknowledged work going back to Lotka and Volterra (ca. 1920s). Other models replicating or extending Tilman's can be found in (Tilman 1982, Holt *et al.* 1994, Leibold 1995, 1996, Grover 1997, Leibold 1998). We believe, however, that Tilman's is a useful reference point for across-resource-space model as others find it for time-extended models.

The apparent unpopularity, in ecological research, of modeling populations' responses across an entire Hutchinsonian space seems to be because these models are not continuous in time and prediction of outcomes through time seems to be an unspoken objective in spite of the shortcomings of time-development models. One frequent problem of time-development models, the essence of most of the problems noted in Miller, *et al.* (2005), is that they require a large number of parameters (*i.e.*, per population, per resource response, per predation effect, per resource supply) all predicted-projected over time—and these multiple *a priori* predictions-projections, “external to” a model, render its veracity, its statistical strength, and its ecological significance, highly suspect.

A second frequent problem of present ecological models is that they seldom, if ever, formulate populations' responses to influences in terms of inherent organismal traits but rely on responses as a function of demographic phenomena without regard to unintuitive, cryptic, complex intra-population processes—which means that results (predictions) are not reliably functions of what is actually occurring at any time. See Chase and Leibold (2003) for a non-exclusive example of phenomenological response formulations as commonly used. In addition to these problems, it is operationally, algorithmically, difficult to apply a single core formulation to both across-space and along-time modeling—in spite of the apparent similarity of the two applications in superficial reading of Tilman (as in 1980, 1982) or even Grover (as in 1997).

The idea of modeling populations' responses and expected relationships across a Hutchinsonian space without regard to time can be justified by the simple observation that ecological regimes of resource availability may change *in natura* faster than populations' relationships can stabilize, for example to exclusion or coexistence. Examples of this can be seen, implicitly at least, in (MacArthur 1972, Velicer and Lenski 1999, Ciroso-Perez *et al.* 2001, Holt *et al.* 2005, Hall and Colegrave 2007). The ability of a resource space model to predict relative growth response in whatever the environmental regime may be, and as the regime may change, can offer more insight (one of the two purposes of modeling) than a time-development model can offer in either prediction (the other purpose of modeling) or insight because of the latter's dependence on an assumed specific future ecological regime.

Most models of population responses in either an “ecological”, “evolutionary” or “genetic” context (Elton 1927, Tilman 1982, Paquin and Adams 1983b, Adams *et al.* 1985, Berendse 1994, Leibold 1996, Grover 1997, Velicer 1999, Chase and Leibold 2003, etc.) are formulated in terms of observed, demographic phenomena, resource supplies or other effects,

driving directly to population growth or size, and resulting growth or size relationships, without expressly considering organismal-population inherent response traits which generally have a complex, usually nonlinear, often self-limited effect on population growth (Hsu et al. 1977, Tilman 1981, Grover 1997). Even a function as supposedly simple as one population's growth response to a sole limiting resource is better described by the Monod formulation (1949), a hyperbolic-asymptotic function of two trait parameters on the resource supply concentration, than any linear or simpler nonlinear function. A model which is to somehow realistically-mechanistically represent multiple populations' responses to multiple resources, or even a single population's realistic response, must formulate populations in terms of organismal traits such as Monod's maximum capable growth response and per-resource half-saturation constant. This means that the complete model system must include a means, a well-defined but simple Characterization Protocol, for determining the per-population trait parameters from observed, demographic resource supply values, or other quantifiable influences, and population intrinsic responses. One of the earlier works emphasizing distinction between ecological phenomena and organismal traits was by Hsu *et al.* (1981), directly presaging our work here, which in twenty-nine years has been cited forty-seven times in "mathematical" or "modeling" publications but only nine times in "ecological" publications.

Beyond representation of obvious ecological-phenomenological processes a model of populations' responses to resources or other effects must allow for the influence on trait parameters, must permit characterized trait parameters to reflect, underlying genetic covariance of the kind implied but not quantified in work such as Adams and Paquin (Paquin and Adams 1983b, Adams 2004), Goddard and Bradford (2003a), Lenski *et al.* (Lenski 1989, Cooper *et al.* 2003, Elena and Lenski 2003) or Rutgers *et al.* (1990). This can only be achieved by a

formulation, such as Monod's, which includes sufficient trait parameters and formulation behavior, *i.e.*, the asymptotic form, to permit these effects to materialize—and with a Characterization Protocol which accurately quantifies trait parameters.

Finally, a model system for predicting the desired influence-response characteristics of individual populations and relative responses between populations must include a display, or plotting, component which represents the responses in readily interpreted qualitative (for insight) and quantitative (for prediction) form. It should present something on the order of a Hutchinson-like two-dimensional Cartesian resource supply space with a third response dimension, as if a three-dimensional extension of Tilman's *Graphical-Mechanistic Approach* (1980).

Figures

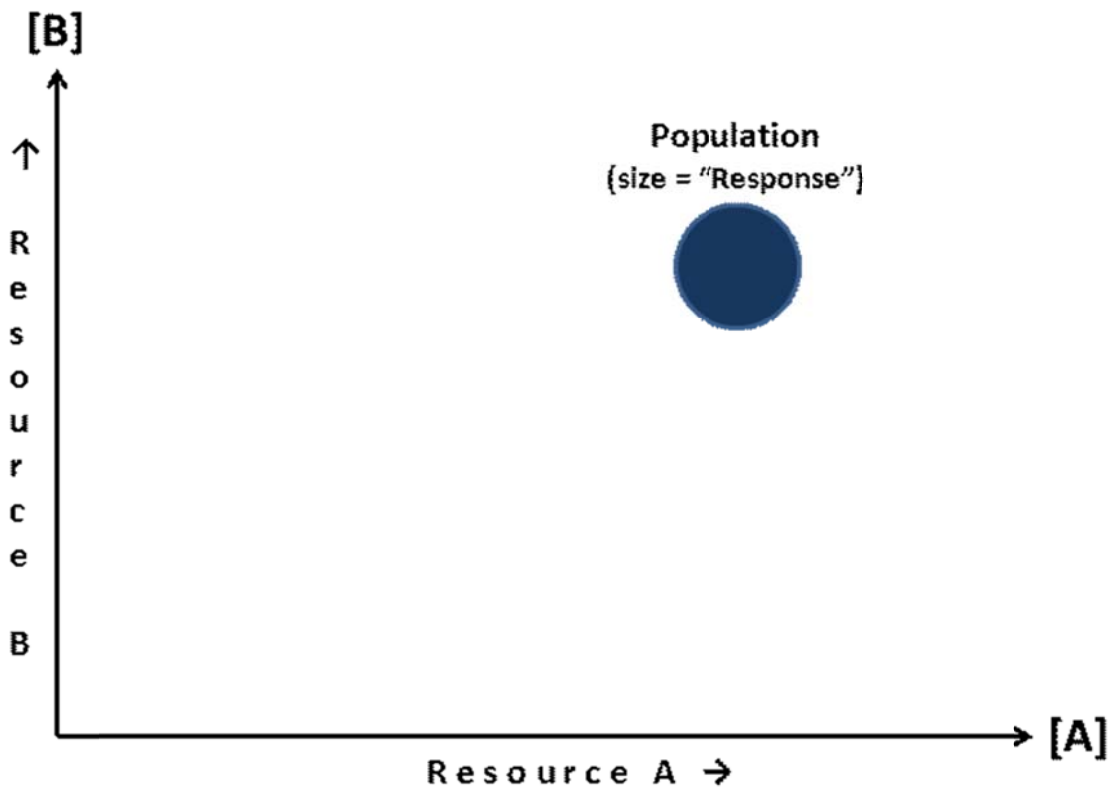


Figure 1-1. **One population in a Hutchinsonian resource space.**

The axes labeled **[A]** and **[B]** in our work here represent the variable concentration (hence the chemist's brackets) of resource supply at a steady medium flow rate but could just as well represent the medium or carrier flow rate at some stated or observed concentration or the mass flow rate to a given observed area or volume. The location (of the center) of the population is the instant location in the space of possible resource supplies and the relative size of the population's "dot" represents its response whether that is growth rate or standing population or any other measure.

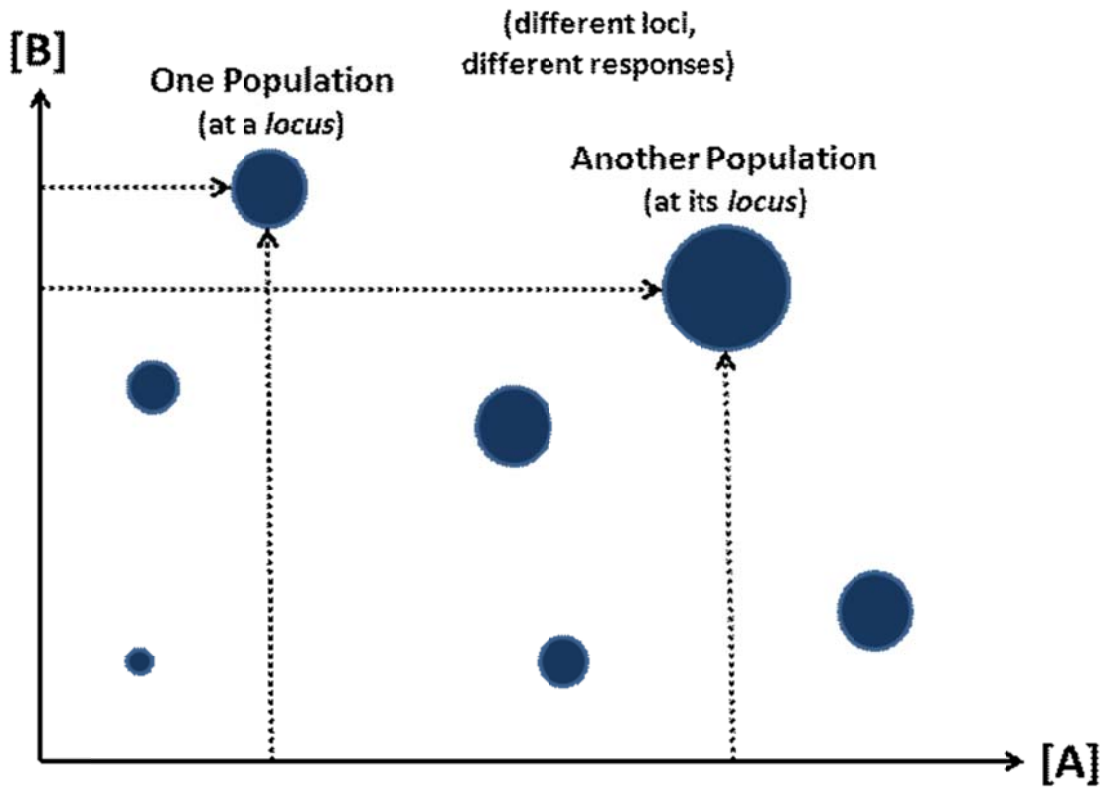


Figure 1-2. **Multiple populations and responses in resource space.**

Here we simply have several populations, as from Figure 1-1, at quantified loci in resource space with varying graphic “dot” sizes corresponding to their ecological-functional or –numerical responses to the resource supply at each particular locus.

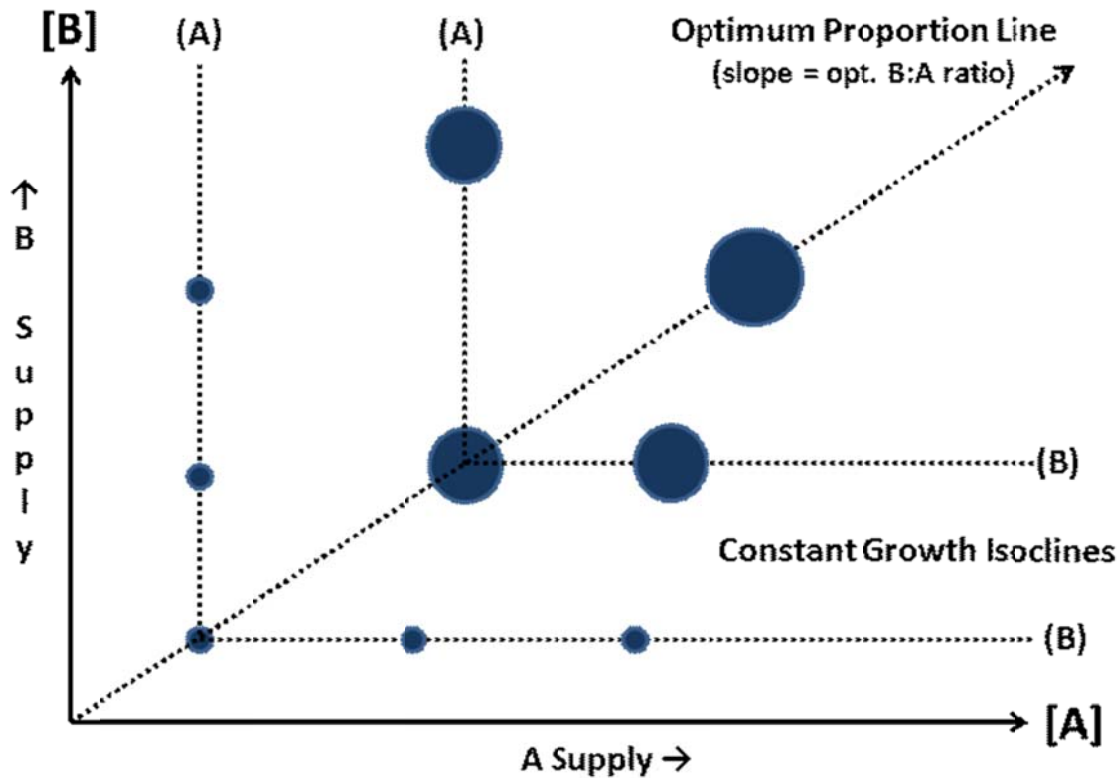


Figure 1-3. **Functional lines for a population in resource space.**

Here we represent a single population, its variable response (“dot sizes”) at loci in resource space and two types of lines relevant to its response. The general concept of response in a space of two resources and our particular formulation provides that the population’s realized response will be limited by whichever resource is in lowest supply relative to (as a function of) the population’s maximum response to that resource—as by von Liebig’s *Law of the Minimum*. We find then that the population’s response will be “small” wherever one resource is “low”, regardless of “high” supply of the other resource. This gives Constant Growth Isoclines (CGIs), vertical or horizontal traces as shown here. The diagonal line where the CGIs converge is called the Optimum Proportion Line (OPL) by Tilman (1980, p. 367, para. 3 et seq.) and most others who use his model or one of its derivatives. When a population’s instant locus is on the OPL, its response will remain constant for any increase of either resource (the other resource is still limiting) and will decrease for any decrease of either resource (because that resource will become “lower” limiting).

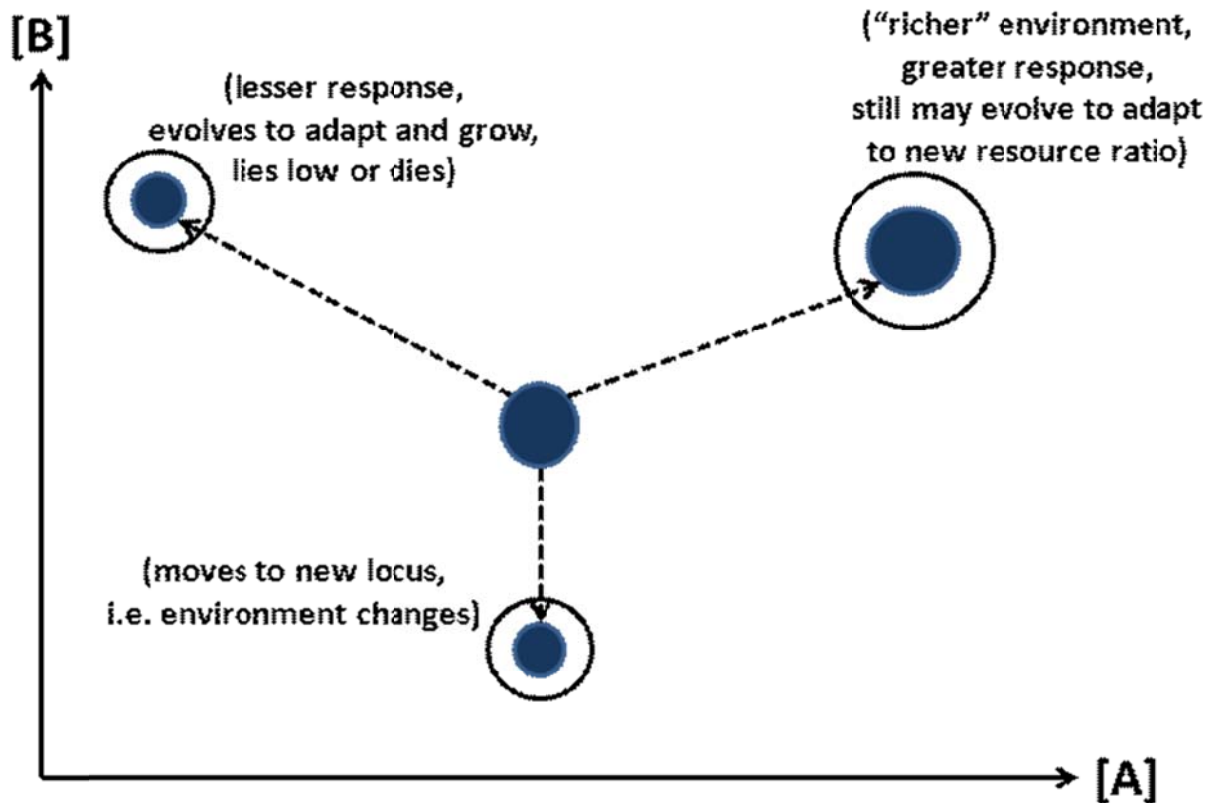


Figure 1-4. **Populations evolving under resource supply constraints.**

When a population such as the one at the center of the diverging arrows finds itself at a new locus in resource space its instant response will change, increase or decrease, according to the new resource supplies. If the new locus is a case of severely lower supply of a resource or lower supply and greater external impact such as predation then the population will likely die. If the population does not die then it is generally observed to adapt by variation and/or evolution (as the opportunity may be) and increase its response at that locus (the rings around the population "dots"). Even when the new locus (upper right) brings greater supply of both resources the population may not only grow in response to the new supplies but may adapt to the new ratio of resource supplies to an even higher response.

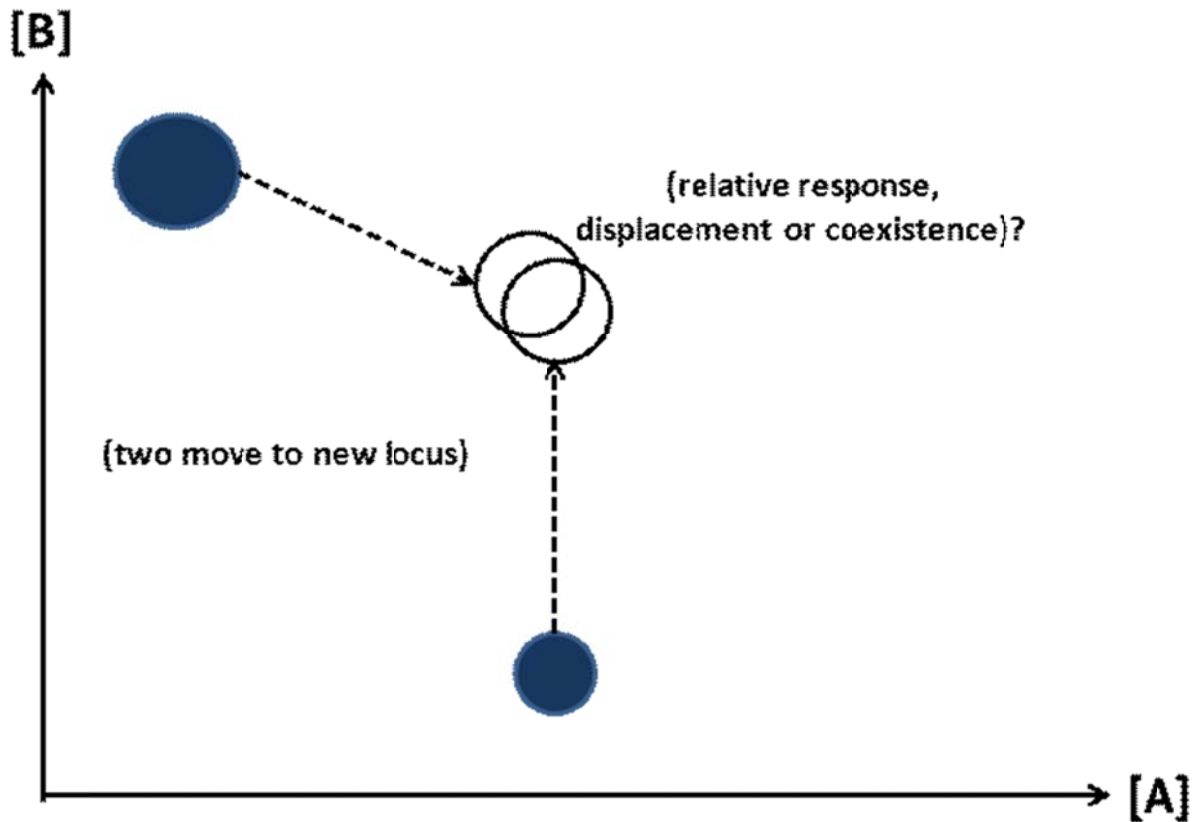


Figure 1-5. **Two populations in competition in resource space.**

Here we have cleared away the clutter of Figure 1-3 and Figure 1-4 to represent two populations evolved at different loci in resource space moving by some natural, anthropogenic-disturbing or experimental cause to the same locus. The essential thing we are attempting to predict with our method and model is which of the two will be the “superior competitor”, with the greatest response, at this locus. We particularly model two specific populations’ intrinsic growth rates and then the difference in those rates, throughout the resource space on the premise that at any instant locus at any instant time the population with the greater intrinsic growth rate will, so long as resource supply and other conditions remain constant, out-grow, out-compete and displace the other.

## **Chapter 2, Modeling the Ecological Niche and Population Competition with Two Essential Resources**

### Summary

We have developed a model of competitive population growth on two contended, limiting resources in terms of *requirements niche* in a Hutchinsonian  $n$ -dimensional space. Each population is characterized in the form of Monod's growth response model by its organismal traits of per-resource growth response, the half-saturation constants, and its maximum capable growth response trait. Realized growth response of each population and relative growth response of the two populations is modeled across a two-dimensional, Cartesian space of two resource supply concentrations as ecological-environmental phenomena and is displayed, qualitatively and quantitatively, as a phenomenological third dimension.

### Introduction

Prior and recent models of population competition for one or two (dual-limiting) resources commonly suffer from one or both of two assumptions which severely limit their utility for prediction, or even insight, to a narrow range of cases. Most of these models are based on or *de facto* comparable to Tilman's *Graphical-Mechanistic Approach* (1980). Without denigrating the value of Tilman's work as a reference model for the general case or as a specific model for particular cases the problems of resource-response modeling are well described in the review by Miller *et al.* (2005).

The first problematic assumption, usually not even acknowledged, is that a population's growth response to a resource is simply linear—that there is no variation of growth response as resource availability varies and that there is no inherent limitation of growth rate at high resource availability. We believe that this is largely the result of too-simple application of Tilman's *Graphical-Mechanistic Approach* (1980) and its descendants even though Tilman himself warned of the need to use non-linear growth functions at least as early as (1981). Even very recent theoretical work (not alone, Chase and Leibold 2003) asserts that assumption of linear response is sufficient for competitive analysis. This problem is exacerbated when measurements of resource availability and growth rate are not taken at enough points or not measured with sufficient precision (esp. the growth rate) to fit or approximate anything other than a linear response. While the measure of resource availability may be very precise the measure of phenomenological growth response is frequently very imprecise. These measures, used directly, ignore that there may be a non-phenomenological, inherent growth-response trait parameter that needs to be determined to correctly relate resource availability to growth response and a non-phenomenological growth-limit trait parameter that imposes non-linearity at all but the lowest resource availabilities. The first-resulting flat surfaces (mathematically present whether plotted or not) of growth response across resource space and the second-resulting linear isoclines (intersections of flat surfaces) make any except the very simplest predictions of competitive outcome on a single resource untenable. When two limiting resources are involved the tradeoffs (sensu Chase and Leibold 2003, pg. 41) between two populations can be much more complex than linear-response assumptions can represent at any resource availability.

The second common problem is that when evolutionary processes (in isogenic or weakly polygenic populations) or even proportionate-selective effects (in durably polygenic populations)

are considered in simple succession (ancestor Y *versus* descendant of Y), substitution succession (ancestor Y *versus* descendant of Z), or parallel succession (descendant of Y *versus* descendant of Z), underlying genetic covariance, generally not observed in “ecological” or “phenomenological” research, can fatally complicate growth responses measured and modeled solely in terms of phenomena of resource availability and population growth. Genetic covariance may manifest change of maximum capable response trait or response trait to one resource, not under selection pressure at the same time in the same population as change of response trait to the resource that is under manipulated or observed selection pressure. This covariance may appear, on closer analysis and borrowing properly genetic terms, to be “linkage-like”, “linkage disequilibrium-like” or “pleiotropy-like”—we would refer to both as simply “phenomenological pleiotropy”. The result of this underlying covariance is that a change of realized growth response may not be, at all, a one-for-one result of selection on stress of a single resource.

While examples of the problems with linearity assumptions, *inter alia*, are easy to find and well enumerated in Miller *et al.* (2005), examples of the problematic genetic covariance are more difficult to find in the literature and a very few senior authors dominate the field, most notably J. Adams with *Saccharomyces cerevisiae* and R. E. Lenski with *Escherichia coli*. An interesting aggregate discussion of phenomena of simple succession from a predominately ecological-phenomenological perspective can be found in the work of Paquin and Adams (Paquin and Adams 1983a, Paquin and Adams 1983b, Adams *et al.* 1985, Adams 2004). Velicer and Lenski (1999) provide another perspective with implications for ecological effects in parallel succession. Gerrish and Lenski (1998) examine the genetics and implicit ecological effects of descendants of a single ancestor evolved under superficially the same resource supply selection pressure. Remold and Lenski (2001) examine the genetics and implicit ecological effects of

descendants of a single ancestor evolved under different resource supply selection pressures. Travisano *et al.* (1995) and Vasi and Lenski (1999) report on true genetic pleiotropy in varying directions in populations under the same resource supply pressure.

Here, we present a mathematical model of potential competitive outcomes (*i.e.*, coexistence or exclusion) as relative growth rate between two populations growing on two dual-limiting essential resources, for example *A* and *B*. We use the Monod function (1949, pg. 343, eqn. 2), discussed in detail below, to generate the realized intrinsic growth rate (Monod's *R*) for each population per availability of resources *A* and *B*. We show that combining the Monod functions for population growth on these resources yields a two-dimensional space of niche requirements (*sensu* Hutchinson 1957). This niche space can be plotted to a surface in three dimensions where *R* constitutes the third axis. Essentially this generates a graphical representation of a response surface in niche space following the Hutchinsonian definition of niche (*cf.* Chase and Leibold 2003) across availabilities of resources *A* and *B*. We then demonstrate that niche spaces (and surfaces) of two populations can be overlaid to identify niche space where populations could either exclude or coexist with one another. Our graphical presentation owes much to the form in Tilman's *Graphical-Mechanistic Approach* (1980)—extended to show realized growth, *R*, as a third dimension. Our modeling approach is deliberately simple, requiring estimation of only three characteristics per population – Monod's  $R_K$  (maximum capable growth rate) and the responses (Monod's half-saturation constants  $C_{I\ A,B}$ ) to resources *A* and *B*. Using this model we can explore the predicted outcomes of competition across resource requirements space between two populations under multiple scenarios such as: (1) only maximum capable growth rate,  $R_K$ , differs; (2) only the half-saturation constant(s),  $C_{I\ A,B}$ , differ; (3) the half-saturation constants exhibit complementary, linkage-like or pleiotropy-

like change as a result of selection to one limiting resource—where any of these scenarios may exhibit a complex shift of tradeoff between the populations (sensu Chase and Leibold 2003, pg. 41). Our model builds on the classical, graphical models of competition on essential resources *e.g.* (Tilman 1980, Chase and Leibold 2003, others) by providing a graphically- and numerically-solvable method to predict competitive outcomes based solely on population characteristics that follow Hutchinson's (1957) notion of niche as species requirements.

## Methods

The best-known graphical models of resource competition focus on essential resources (but contrast Chase and Leibold 2003, pg. 26). In addition to using the Monod function, a fundamental departure our model makes from this prior work is that ZNGIs (Zero Net Growth Isoclines, the resource level at which births equal deaths including environmental effects such as predation) need not be estimated to predict competitive outcomes (see Chase and Leibold 2003) although one of our several plot forms does display isoclines of population realized intrinsic growth or differential realized growth between two populations. Following from this, our model does not necessitate estimation of a species impact on the environment, *i.e.*, there is no requirement to estimate the amount to which a species can deplete a resource, its  $R^*$  (sensu Tilman 1982). Instead, our approach permits prediction of competitive outcomes based on differences in realized (*i.e.*, Monod's)  $R$  of two populations for any point in the niche space created by requirements for two essential resources, where the requirements in our model are resource supply rates. Our model then relies solely on Hutchinson's (1957) conception of the niche as species requirements. We do not include Tilman's (1980) *consumption vectors* because our intent is not to trace populations' loci in resource supply space over time—see Miller *et al.* (2005) for how often this effort is unsuccessful—but to show how populations will grow,

individually or differentially, at any point in supply space at any time particular resource supply rates, effectively equivalent to Tilman's (*ibid*) *supply vectors*, occur. When and as resource supply rates are stable, or nearly so, the population which grows faster will invariably come to displace the other. When and as supply rates vary rapidly and settle to a new regime the population which grows faster in the new regime, regardless of relative population size at the time of the regime change, will come to displace the other. In any case, unless population sizes are initially well known and can be reliably tracked over time—and unless one or both resource supplies are so low as to allow one to be drawn down to where  $R^*$  applies—we find for our concerns that *consumption vectors*, *sensu* Tilman, are more often a complication than a contribution.

We do not intend criticism of more recent definitions of the ecological niche that integrate Elton's (1927) definition of species' impacts with Hutchinson's definition of requirements (cf Chase and Leibold 2003). Similarly, nor do we intend criticism of the contemporary graphical approach that relies on  $R^*$  (for example Tilman 1982, Milbrink et al. 2003). There are too many different concerns in the application of resource competition modeling to imply that any one approach should be universally applauded or denigrated. Instead, we present our model as an alternative formulation where competitive outcomes or tendencies toward outcomes might be predicted solely from species requirements. Our model can be taken as another answer to the problems of applying or extending Tilman's *Graphical-Mechanistic Approach* model, not problems with the reference model itself, as discussed by Miller *et al.* (2005).

Given that realized intrinsic growth,  $R$ , commonly increases following a saturating function as resources increase (cf Grover 1997), we use exclusively the Monod function (1949,

pg. 343, eqn. 2) to represent this relationship (Figure 2-1). The function was originally developed for bacterial population growth and the realized intrinsic growth rate ( $R$ ) is formulated as:

$$R = \frac{dN/dt}{N} = R_k \frac{C}{C_1 + C} \quad ()$$

Here  $N$  is the population size by mass (Monod's *density*),  $t$  is time,  $R_k$  is the population characteristic maximum intrinsic growth rate,  $C_1$  is the resource supply concentration required to achieve one-half  $R_k$ , also known as the half-saturation constant and  $C$  is the instantaneous resource supply concentration. This growth rate applies to a population for any one resource when all other resources are "in excess" which is the same as saying that the one resource is solely growth-limiting.

It has been shown, discussed and recommended, *e.g.* (Hsu et al. 1977, Tilman 1981, Grover 1997) that population growth response modeling across any "wide" range of a resource supply requires a non-linear, asymptotic formulation. Linear increase of the supply of a limiting resource gives an asymptotic (*i.e.* "saturating" to a limit) increase in intrinsic growth rate, which is necessarily nonlinear, and not an indefinite (*i.e.* without limit) increase, the unavoidable behavior of a linear formulation.

Linear approximations have been useful in "near zero supply" simulations as in the basic form of Tilman's *Graphical-Mechanistic Approach* (1980) or in the simplified examples of Chase and Leibold (2003) but simply do not work well elsewhere.

Our justification for choosing Monod's (asymptotic, nonlinear) function as the mathematical core of our model is, first, the fact that it is widely recognized as a reference model, *e.g.* (Ferenci 1999, Levert and Xia 2001, Lokshina et al. 2001, Higuera-Guisset et al. 2005, Tang et al. 2007, Cerucci et al. 2010) for work similar to ours—affording a basis for comparability—and, second, the fact that it is easy to comprehend, parameterize and apply—

helping to achieve our objective of a simple model with no more parameters than necessary. See Appendix A for a longer discussion of our choice.

The canonical form of the Monod equation is the simple hyperbola:

$$y = \alpha x / (\beta + x) \quad ()$$

Here, considering only Cartesian first quadrant (*i.e.*  $x > 0, y > 0$ ),  $y$  is the “response”,  $x$  is the “supply”,  $y = \alpha$  (Greek alpha) is the “asymptotic limit” parameter and  $x = \beta$  (Greek beta) is the “characteristic” parameter. There are two other simple asymptotic expressions which could be used in place of the simple hyperbola but neither one offers the prospect of more precise curve-fitting to a population’s observed growth response and neither is easier to comprehend and apply. See Appendix A for a longer discussion of the alternative forms.

It is also important to note that Monod’s formulation for realized growth rate,  $R$ , is net of life-cycle mortality but prior to environmental mortality which would involve Tilman’s **ZNGI** (Zero Net Growth Isocline) or  $R^*$ .

When a population is dual-limited by two essential resources (*i.e.*, neither can substitute for the other), all other resources being in excess supply, it’s growth can be regarded as following von Liebig’s law of the minimum (as in Tilman 1980, p. 367, eqn. 2):

$$\frac{dN}{N dt} = \min_{j=1,k} [ f(R_j) ] \quad ()$$

where *min* is the mathematical operator *minimum of*,  $f(R)$  is a resource response function and there are  $k$  resources.

*I.e.*, the realized growth rate of the population is the minimum of the per-resource growth rates. Using Monod’s notation and the case of two resources,  $A$  and  $B$ , we have:

$$R_{A,B} = \min \left[ R_{KA} \frac{C_A}{C_{1A} + C_A}, R_{KB} \frac{C_B}{C_{1B} + C_B} \right] \quad ()$$

But since  $R_K$  is common to the organism-population and  $R_{KA} = R_{KB}$  we reduce to:

$$R = R_k \min \left[ \frac{C_A}{C_{1A}+C_A}, \frac{C_B}{C_{1B}+C_B} \right] \quad ()$$

This is our complete formulation for the growth response of a single population on two essential resources. We can plot  $R$  by  $C_A$  and  $C_B$  as the population's growth-response niche surface across a resource space.

When we replicate this equation for two populations,  $Y$  and  $Z$ , in a common resource space we have:

$$R_Y = R_{KY} \min \left[ \frac{C_A}{C_{1AY}+C_A}, \frac{C_B}{C_{1BY}+C_B} \right] \quad ()$$

$$R_Z = R_{KZ} \min \left[ \frac{C_A}{C_{1AZ}+C_A}, \frac{C_B}{C_{1BZ}+C_B} \right] \quad ()$$

We can plot the two surfaces (with two colors or shades) across the common resource space as a first step to estimating competitive outcome.

Finally, we can formulate  $R_R$  (subscript  $R$  for *relative*) the simple difference of the two populations' growth rates as:

$$R_R = R_{KY} \min \left[ \frac{C_A}{C_{1AY}+C_A}, \frac{C_B}{C_{1BY}+C_B} \right] - R_{KZ} \min \left[ \frac{C_A}{C_{1AZ}+C_A}, \frac{C_B}{C_{1BZ}+C_B} \right] \quad ()$$

We plot this formulation across the common resource space as a three-dimensional surface (preferably with color- or shade-by-value), as a flat shaded-difference map or as a flat shaded-contour map. The third of these options appears much like the plot of Tilman's *Graphical-Mechanistic Approach* (1980) but with relative-growth isoclines and optional ZNGIs correctly tracking nonlinear growth responses. The second option (with the advantage of continuous variation of color or shade) can identify areas of non-obvious tradeoff (sensu Chase and Leibold 2003), and the first option is entirely new to our application area.

Tilman describes the *OPL* (Optimum Proportion Line (1980. p. 367, para. 3 et seq.) for dual-limiting essential resources equivalent to the dual-limitation ratio (cf Zinn *et al.* 2004 and

others). The significance of the OPL is that on this line and only on this line an increase in the availability of either of the two essential resources will cause no change in realized intrinsic growth rate,  $R$ , but a reduction of either resource will cause a reduction of  $R$ . The slope of the OPL is the ratio of the half-saturation constants,  $C_{1A}/C_{1B}$ , also known as the dual-limitation ratio. Comparing the OPLs of two competing populations can often (but not always, considering non-linearity and/or underlying genetic covariance) delineate areas throughout which one population consistently grows faster than the other.

### Results and Discussion

In our example plots we began with growth response parameters for Population X based on one of our experimental populations of *Saccharomyces cerevisiae*, MRG-2. The trait parameters for each example population are shown in Table 2-1 with differences greatly exaggerated for the sake of producing clear examples. The software tool we use for all of the present work is *Mathematica*®, version 7 (Wolfram Research 2008). See Appendix A, Mathematics, for details including *Mathematica*® code.

Figure 2-1 shows the basic Monod response curve in Panel (a) with growth response,  $R$ , approaching the asymptotic limit, *maximum capable growth rate* parameter,  $R_K$ , as *resource supply*,  $C$ , increases from  $0$  toward infinity. The *half-saturation constant*,  $C_I$ , is the value of  $C$  where  $R=R_K/2$  and can be thought of as a “shape” or “characteristic” parameter. Panel (b) shows the effect of reducing  $R_K$  (the asymptotic limit moves to lower  $R$ ) and/or of increasing  $C_I$  (the curve shifts to require greater  $C$  to achieve the same  $R$ .) Panel (c) shows the effect of reducing  $R_K$  and/or reducing  $C_I$  (the curve shifts to require less  $C$  to achieve the same  $R$ .) If both of these parameters should be reduced in the course of a population’s evolution we would see the effect shown in the left-hand third of Panel (c), expanded in Panel (d). Here there is a “tradeoff” of the

single population's response for a single resource. In the sense of the population "competing with itself or its ancestor", in an ecological regime of shifting or cyclic supply of the limiting resource, an increased growth response apparently evolved on "one side of" the shift would become a reduced growth response on "the other side".

Figure 2-2 shows the surface of realized growth response  $R$  when von Liebig's *Law of the Minimum* is applied to a population's responses to two resources,  $C$  and  $N$ . We have come to refer to this shape as a "dome tent" with Tilman's OPL (Optimum Proportion Line) forming the "ridge". A cross-section of the surface, parallel to either resource axis, would show the Monod response curve for that resource up to the ridge where the other resource becomes limiting.

Figure 2-3 shows the dome tents of a pair of constructed "sibling" populations which differ only in their OPLs. Panel (a) shows the two surfaces plotted on common axes with their respective ridge OPLs and a "valley" between the ridges. Panel (b) shows the difference of the two response surfaces, "positive" where one population dominates and "negative" where the other dominates. The valley between the ridges now becomes a "wall" between the two dominance regions and the entire surface flattens, the difference of growth rates decreases, as both resource supplies increase along the OPLs. Panel (c) is a "vertical" view of the difference surface, as if looking from infinite  $R$ . The color shading and the two OPLs are intentionally similar to the Tilman's basic plot (1980) and correspond directly to his regions of dominance and (potential) coexistence. Panel (d) replaces the continuous shading of Panel (c) with contour lines and stepped shading offering two advantages at the expense of continuous gradation:  $\Delta R$ , the difference in growth rates, can be read quantitatively from the contour lines and, as in the valley area, it can be seen that constant-difference isoclines are not linear—as may become significant in comparison of real populations.

Figure 2-4 shows what happens when one of the siblings decreases (or increases) its maximum capable growth rate,  $R_K$ , while the OPLs do not change. Panel (a) shows that one of the domes partially “submerges into” (or “erupts through”) the other. Panel (b) shows from the difference surface that the population with the now lower  $R_K$  loses its area of dominance to a condition where coexistence (allowing stochastic effects if not resource-per-resource tradeoff) may be possible. The wall between the two original dominance areas is still apparent. Panels (c) and (d) show the shaded and contoured plots with a notably different set of constant difference isoclines in the latter.

Figure 2-5 shows the result of further reducing or increasing the maximum capable response,  $R_K$ , from Figure 2-4. As can be inferred from Panel (a) it can require a very large change to cause one tent to completely submerge in or overwhelm the other. Panel (b), the shaded contour plot, shows that the population with greater  $R_K$  will now out-compete the other under virtually all conditions of resource supply.

Figure 2-6 shows what happens when one population decreases its  $R_K$  (to lower maximum capable growth) and increases one of its half-saturation constants (to lower response on that resource). All four panels show effects similar to Figure 2-4 or Figure 2-5, showing that certain response trait changes—the half-saturation constant in this case—can be obscured by others— $R_K$  in this case. Although this obscuration may not be of great significance in this example it can lead to competitive outcomes that are not intuitively obvious from simpler models.

Figure 2-7 shows what happens when one of the sibling populations increases the half-saturation constant,  $CI_x$ , for both resources leading to a “flatter” overall growth response. The changes in the response difference surface here are subtler than in the prior figures but,

especially as shown in Panel (d), there is a significant change in the areas of dominance and coexistence even though the apparently significant maximum growth response,  $R_K$ , has not changed.

Finally, Figure 2-8 shows what happens when the sibling which became “flatter” in Figure 2-7 now becomes “steeper” (reduced half-saturation constants,  $CI_x$ ). The results are generally complementary to those in Figure 2-7 but show subtle differences in the size of the dominant areas and the steepness of slope from one (original) area of dominance to the other.

Figures Figure 2-9 (Leibold 1995) and Figure 2-10 (Leibold 1996) illustrate the best analysis and prediction that can be achieved with present modeling approaches. Figure 2-9 former requires response parameters per population, consumption parameters per population, supply vector parameters per resource, initial population sizes and environmental mortality parameters. It is a dynamic, over-time formulation, based only on demographic values and does not address competitive relationships from resource supplies at an arbitrary, instant point in the supply space.

Figure 2-10 is much simpler than the preceding, requiring fewer and simpler parameters. It is still essentially a dynamic formulation requiring population size estimates and, as such, does not meet our concerns of prediction at arbitrary point in an  $n$ -dimensional Hutchinsonian space.

Neither these figures nor their author are taken as a bad example. They simply represent shortcomings of current best practice that our model is intended to overcome for our particular purposes.

We have a model that distinguishes in its formulation between “internal” organismal-population growth response trait parameters and “external” ecological-phenomenological resource supply values and realized growth response. It can predict and display inter-population,

competitive relationships as in Tilman's basic approach and its successors. It can also predict and display details of competitive relationships particularly resulting from nonlinearity of per-resource response traits and the limiting effect of maximum capable growth response traits that are undetectable or indistinguishable in linear-response formulations as assumed in most Tilman-like models, even as urged by some authors. And it can predict and display complex responses and relationships that can result from subtle, underlying genetic-to-phenotypic expressions.

We believe our model may be well applicable to accurate representation of invasive-competitive, displacement-competitive and evolutionary-competitive cases *in vitro*, such as with microbes or plankton. We also believe it can be applied in simulation of larger scale cases, as if *in natura*, by selected or modified populations *in vitro* and actually *in natura* by parameters abstracted from demographics observation.

Our next step (Chapter 3) in the present work will be to apply our model to competition between live populations *in vitro* to show that it works, at least, in well-controlled and quantitatively testable cases with unpredictable inter-population variation of response. The final step (Chapter 4) will be to apply the model to populations evolved under controlled "stress" of shifted resource supply ratios to assess its ability to predict, at least in a self-consistent manner, competitive outcomes between ancestor and descendant or descendant and descendant.

Tables

Table 2-1. **Example Populations' Growth Response Parameters.**

**Population:** population name; **R<sub>K</sub>**: maximum capable intrinsic growth rate; **C<sub>1C</sub>**: carbon half-saturation constant; **C<sub>1N</sub>**: nitrogen half-saturation constant; **C<sub>1C</sub>:C<sub>1N</sub>**: ratio of half-saturation constants, alias dual-limiting ratio, slope of Tilman's OPL (Optimum Proportion Line).

<b>Population</b>	<b>R<sub>K</sub></b>	<b>C<sub>1C</sub></b>	<b>C<sub>1N</sub></b>	<b>C<sub>1C</sub>:C<sub>1N</sub></b>
X	0.834	0.210	0.0130	16.2
Y	0.834	0.263 $X / 0.8$	0.0104 $X \times 0.8$	25.3 $X / 0.8^2$
Z	0.834	0.168 $X \times 0.8$	0.0163 $X / 0.8$	10.3 $X \times 0.82$
W	0.751 $Y \times 0.9$	0.263	0.0104	25.3
Z	0.834	0.168	0.0163	10.3
V	0.667 $Y \times 0.9^2$	0.263	0.0104	25.3
Z	0.834	0.168	0.0163	10.3
U	0.751 $Y \times 0.9$	0.328 $Y / 0.8$	0.0104	31.5 $> Y$
Z	0.834	0.168	0.0163	10.3
T	0.834	0.328 $Y / 0.8$	0.0130 $Y / 0.8$	25.3 $= Y$
Z	0.834	0.168	0.0163	10.3
S	0.834	0.210 $Y \times 0.8$	0.00832 $Y \times 0.8$	25.3 $= Y$
Z	0.834	0.168	0.0163	10.3

## Figures

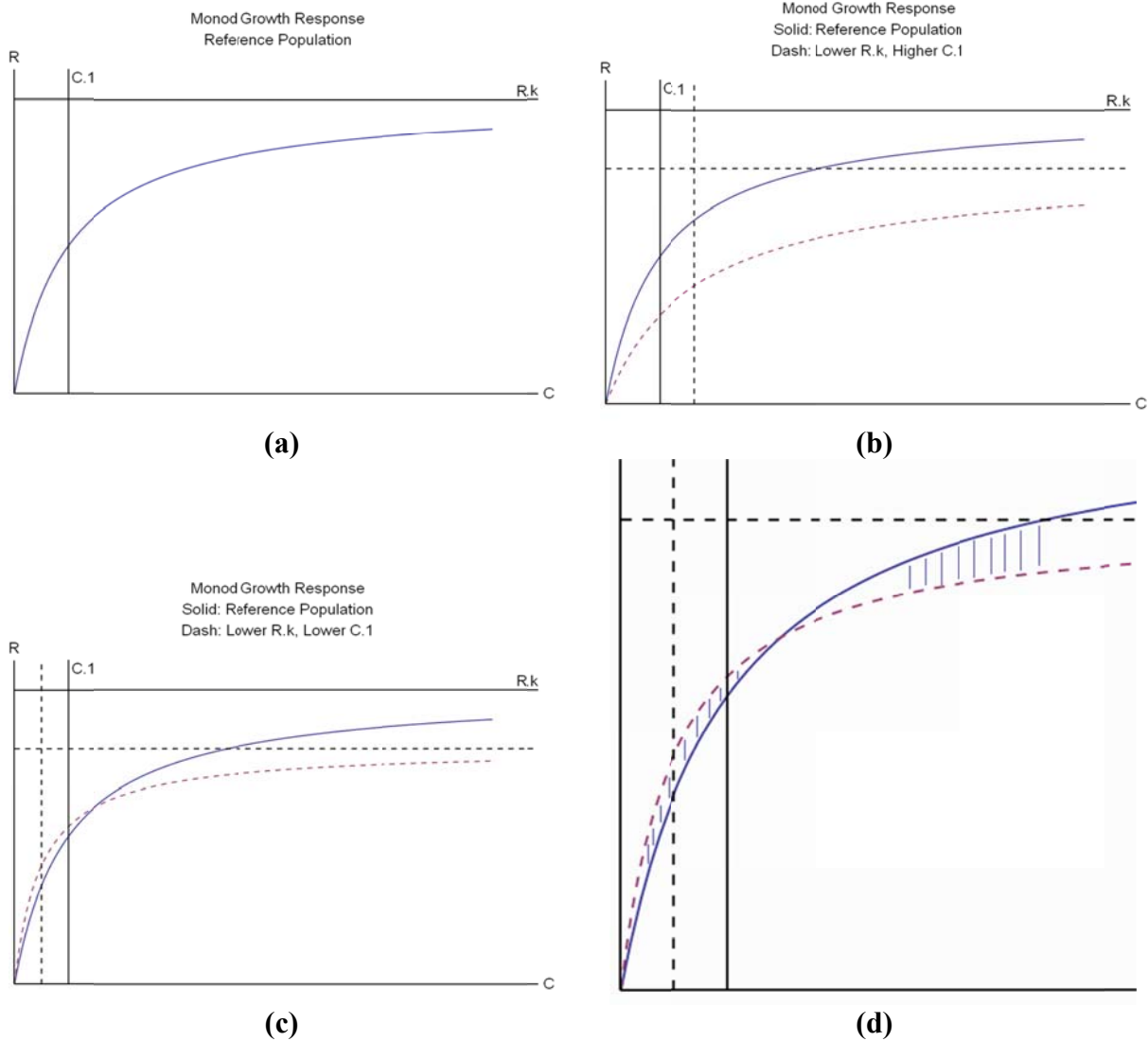


Figure 2-1. **The Monod Growth Response Equation.**

**Panel (a)** shows the Monod growth response of an arbitrary population with realized intrinsic growth rate  $R$  asymptotically approaching  $R_K$  as resource supply concentration  $C$  increases. Note  $R = \frac{1}{2} R_K$  at  $C = C_I$ ; **Panel (b)** overlays the response of a second population with lower  $R_K$  and higher  $C_I$ . Note that either of these shifts moves the response curve rightward and downward; **Panel (c)** overlays the first response with a different second population with lower  $R_K$  and lower  $C_I$ . Note that while the shift in  $R_K$  moves the response curve downward the shift in  $C_I$  moves it leftward. **Panel (d)** shows a closer view of the intra-resource tradeoff of growth response between the two populations at varying levels of just one resource, (beyond the considerations of Chase and Leibold 2003, pg. 41).

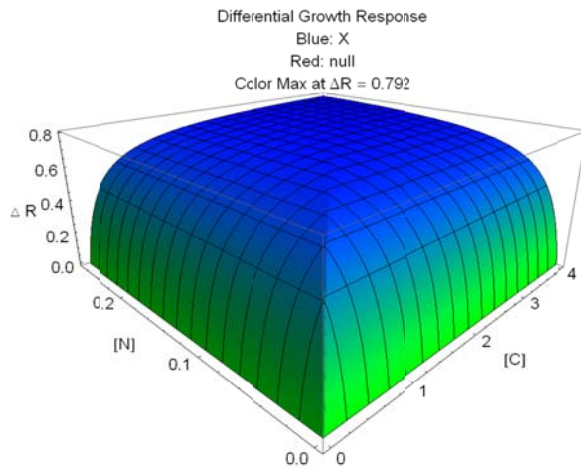


Figure 2-2. **Growth Response Plot, One Population on Two Resources.**

Example Population X based on experimental strain MRG-2

Here we have used our differential surface plot, rather than the dual surface plot, to use the shading and grid lines on the dome tent response surface for a single population on two resources. The maximum intrinsic growth rate,  $R_K$ , of this population is 0.834 and the maximum realized growth rate,  $R$ , in the plotted resource space is 0.792, indicated by “full blue”. Zero realized growth rate, at zero concentration of either resource, is indicated by “full green”.

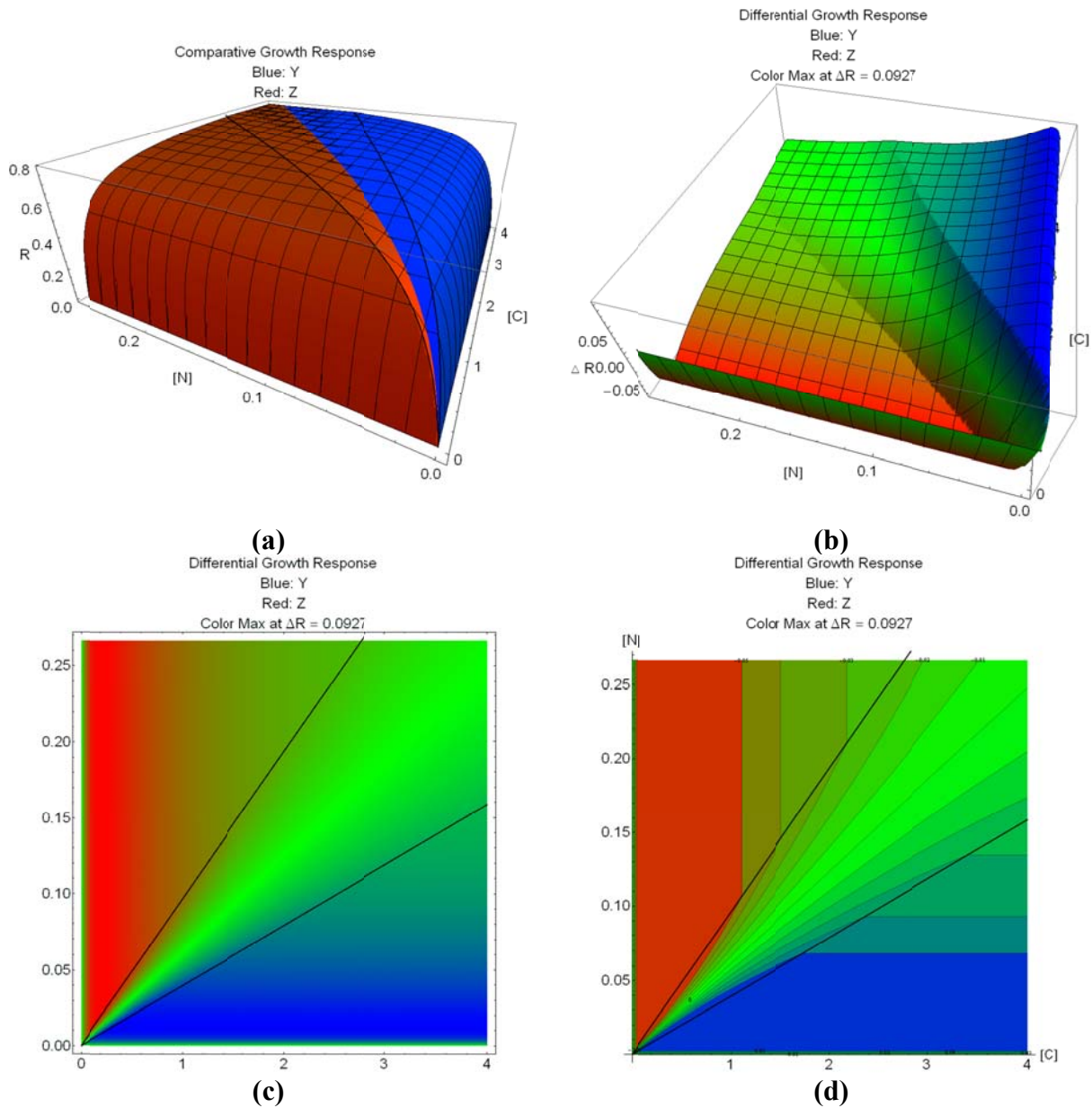


Figure 2-3. **Growth Response Plots, Sibling Populations.**

Same  $R_K$  as Pop. X in Figure 2-2,  $C_{IC}$  and  $C_{IN}$  shifted “oppositely” from Pop. X to give different OPLs.

**Panel (a)**, dual surface plot of the equal-height dome tents. The OPLs define the tent’s ridges. Pop. Y is blue and pop. Z is red. **Panel (b)**, differential surface plot of Pop. Y - Pop. Z. Y dominant shades to blue and Z dominant shades to red. Maximum absolute difference is 0.0927. **Panel (c)** shaded difference plot of the same area as Panel (b). OPLs are black. **Panel (d)** contoured-stepped difference plot of the same area. **Note:** Compare these panels to a simple Tilman-mode plot (as in 1980). The region where Tilman’s approach might allow coexistence, between the OPLs, is represented by a “cliff” in Panel (b) which effectively indicates high sensitivity to stochastic variations near the origin and tends to level close to zero as both resource supplies increase. Even in this very simple case the equal-growth isoclines between the OPLs in Panel (d) are not linear.

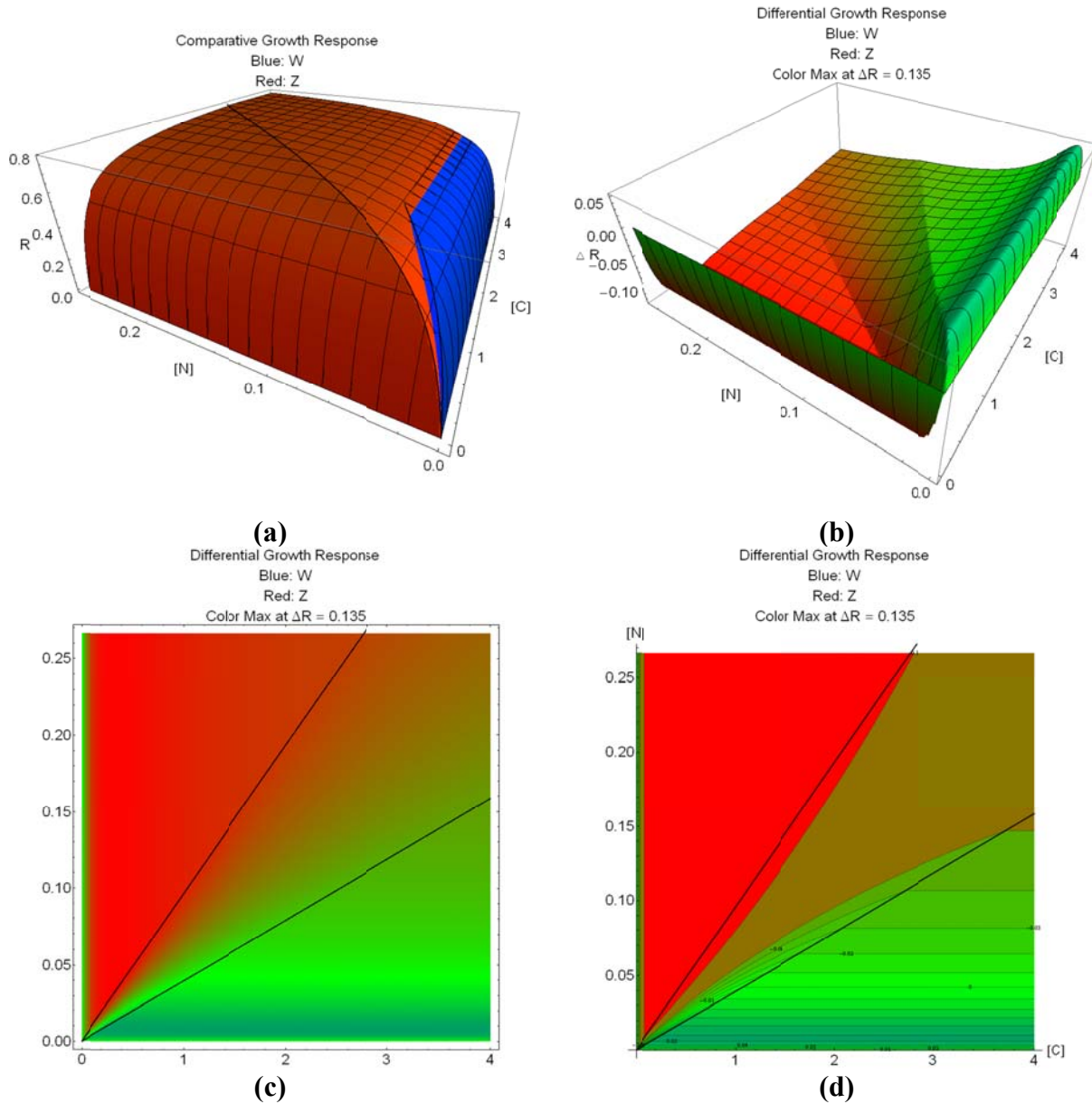


Figure 2-4. **Growth Response Plots, Shifted Maximum Response.**

The populations from Figure 2-3 with different  $R_K$  retaining the same OPLs

**Panel (a)**, dual surface plot. Blue tent, Pop. W with lower  $R_K$ , “submerges” into the red tent, Pop. Z. **Panel (b)**, differential surface plot. The maximum absolute growth rate difference is 0.135. **Panel (c)** shaded difference plot. **Panel (d)** contoured-stepped difference plot. **Note:** The area of dominance by Pop. W in Panel (a) is small in area but has a maximum value in the neighborhood of 0.5, a competitively significant amount. In a natural or anthropologically forced regime of low N supply Pop. W would be expected to dominate pop. Z. This difference, in area and degree, would never be seen in a plot with linear growth responses assumed—or might appear to extend entirely from  $[N] = 0$  to the OPL. All four panels show that the dominant range of Pop. Z extends into the coexistence range of a Tilman-like plot and Panel (d), in particular, shows the stochastic sensitivity of the entire resource space “below-right” of Pop. Z’s OPL and “close above”  $[N] = \text{zero}$ .

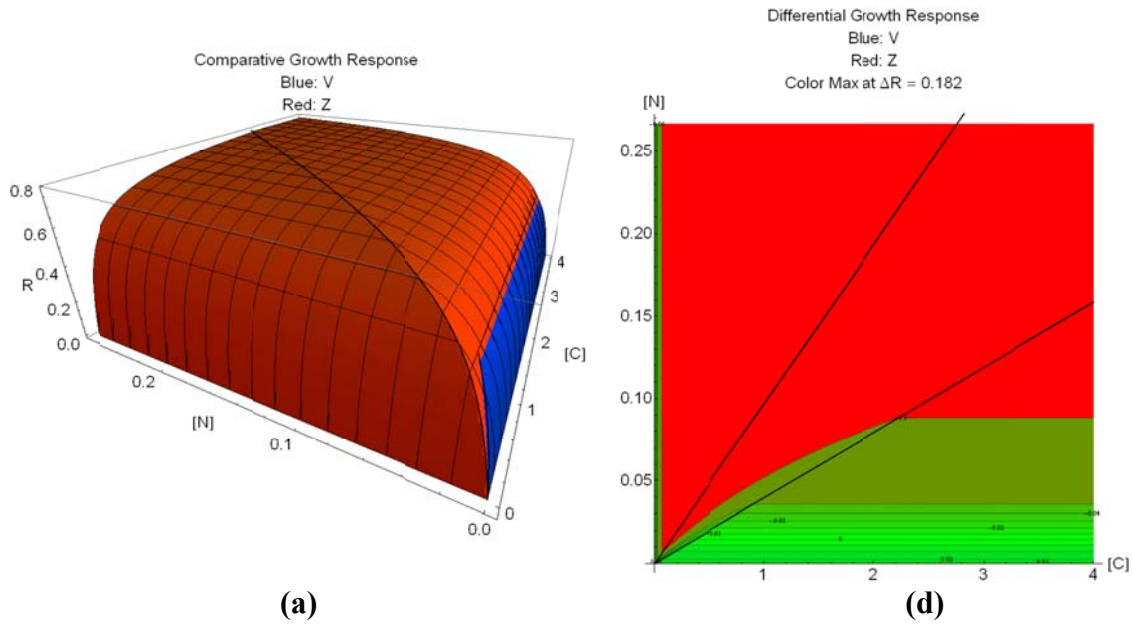


Figure 2-5. **Growth Response Plots, Further Shifted Maximum Response.**

The populations from Figure 2-4 with greater difference in  $R_K$

**Panel (a)**, dual surface plot. **Panel (d)** contoured-stepped difference plot. **Note:** In Panel (a), the blue tent, Pop. V, has submerged further below the red tent, Pop. Z. In Panel (d), The maximum difference in growth rate has increased to 0.187 and the area of dominance of Pop. Z has spread further into the “Low N” segment This figure and Figure 2-4 would appear virtually the same on a simplistic Tilman-mode flat plot of only the OPLs with assumed linear growth responses.

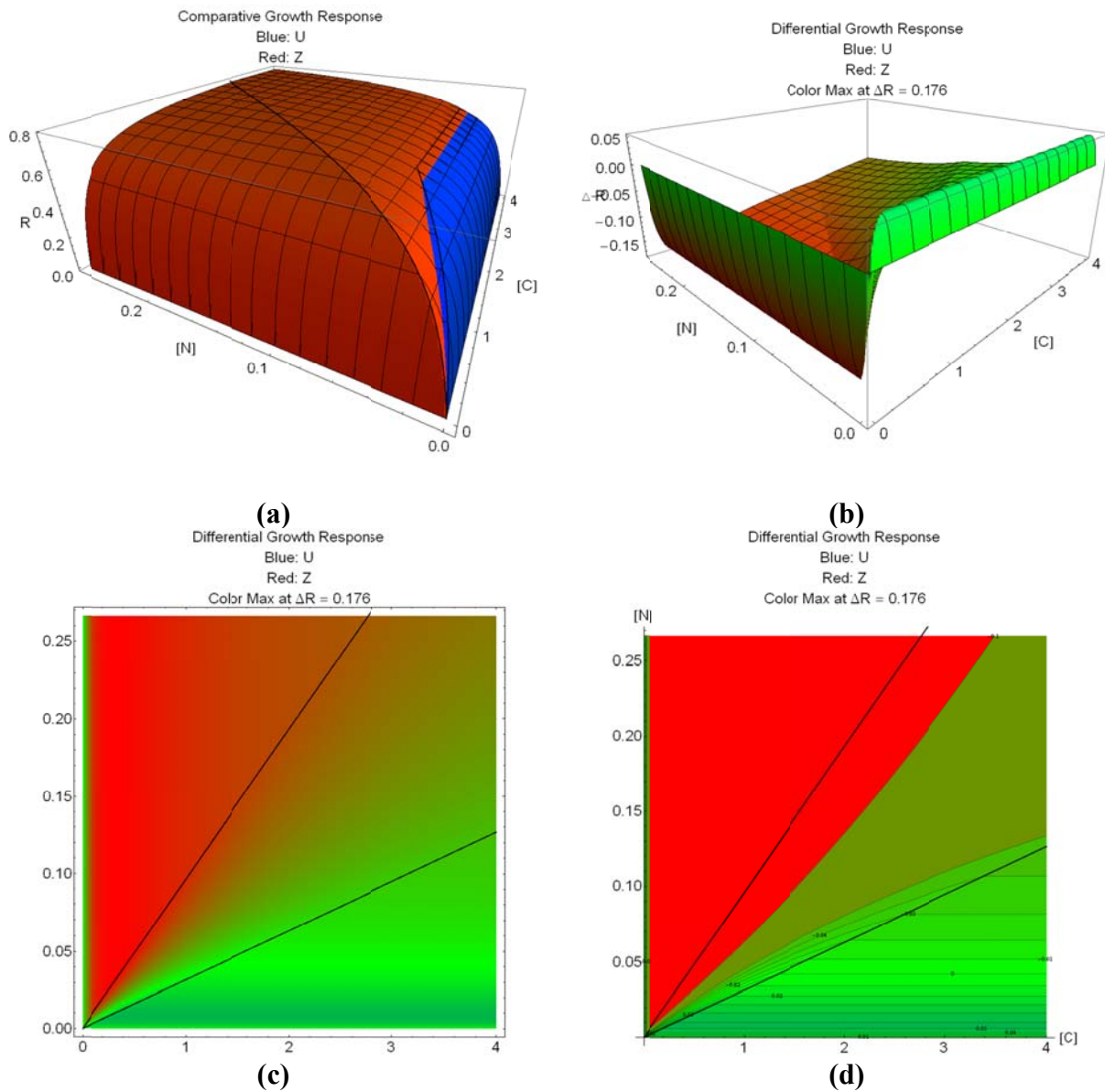


Figure 2-6. **Growth Response Plots, Shifted Maximum Response and Per-Resource Response.**

$R_K$  and  $C_{IC}$  both shifted from the prior example of  $Y$  versus  $Z$

**Panel (a)**, dual surface plot. **Panel (b)**, differential surface plot. **Panel (c)** shaded difference plot. **Panel (d)** contoured-stepped difference plot. **Note:** This plot returns to the same difference of  $R_K$  as in Figure 2-4 and shifts the carbon half-saturation constant,  $C_{IC}$ , of Pop. U higher (giving *less* growth per carbon supply) and shifting the OPL of Pop. U. The dual-surface plot of Panel (a) appears much the same as in Figure 2-4 although the OPLs are not the same as there. The difference plots of Panels (b) through (c) show much the same effect as those in Figure 2-4 although the details are different.

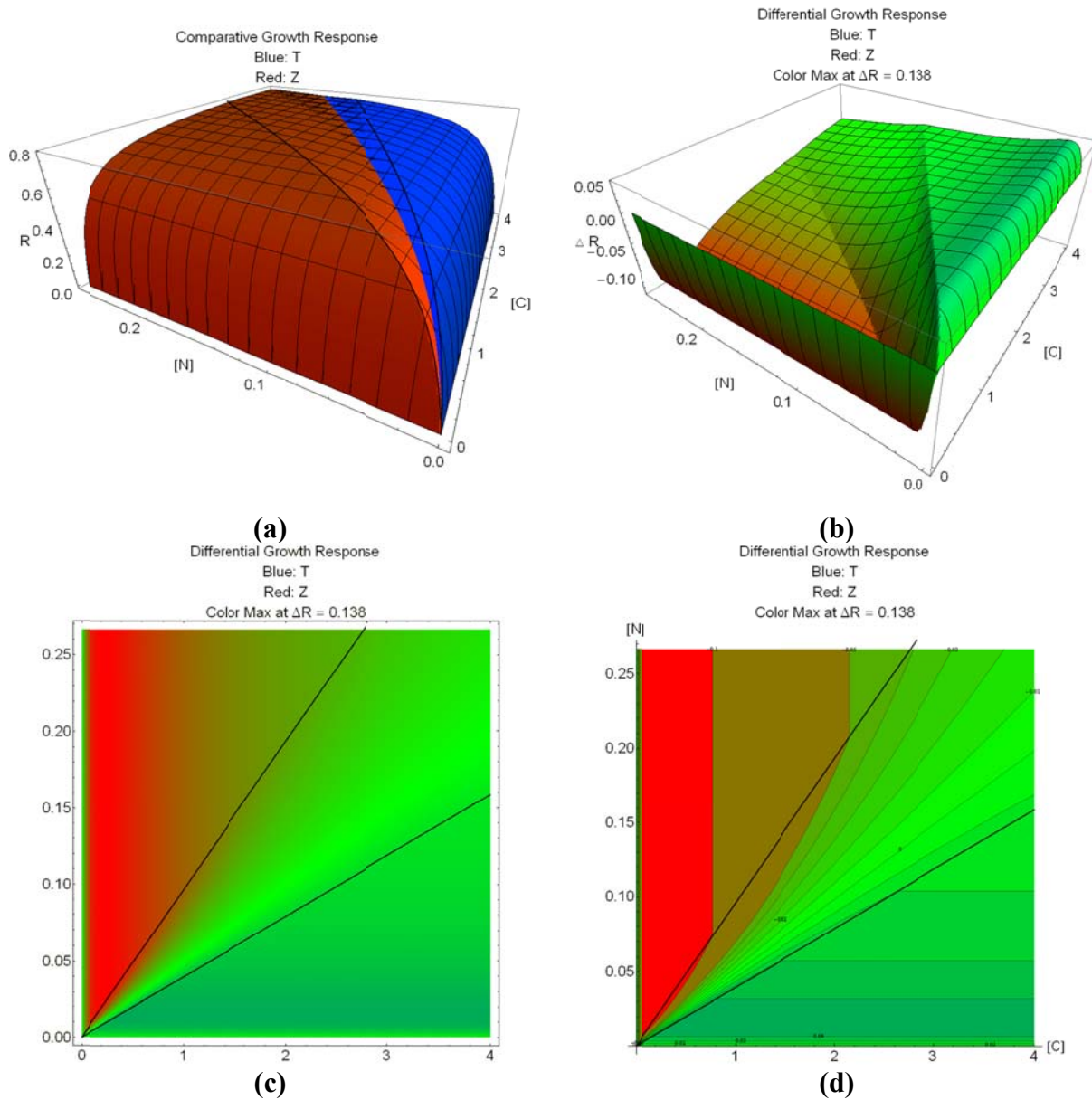


Figure 2-7. **Growth Response Plots, Sibling with Flatter Per-Resource Responses.**

Pop. T  $C_{IC}$  and  $C_{IN}$  greater half-sat. constants, same OPLs as in Figure 2-3 but “flatter” response than the prior example of Y versus Z

**Panel (a)**, dual surface plot. **Panel (b)**, differential surface plot. **Panel (c)** shaded difference plot. **Panel (d)** contoured-stepped difference plot. **Note:** Although both populations’ OPLs are the same as the “sibling” populations in Figure 2-3, the change to “flatter” per-resource responses, both  $C_{IC}$  and  $C_{IN}$ , for Population T give the competitive advantage to Population Z in the low-carbon range “above” its OPL and leave the rest of the resource supply space open to coexistence or stochastic determination of the competitive outcome. This result is complementary to that of Figure 2-8.

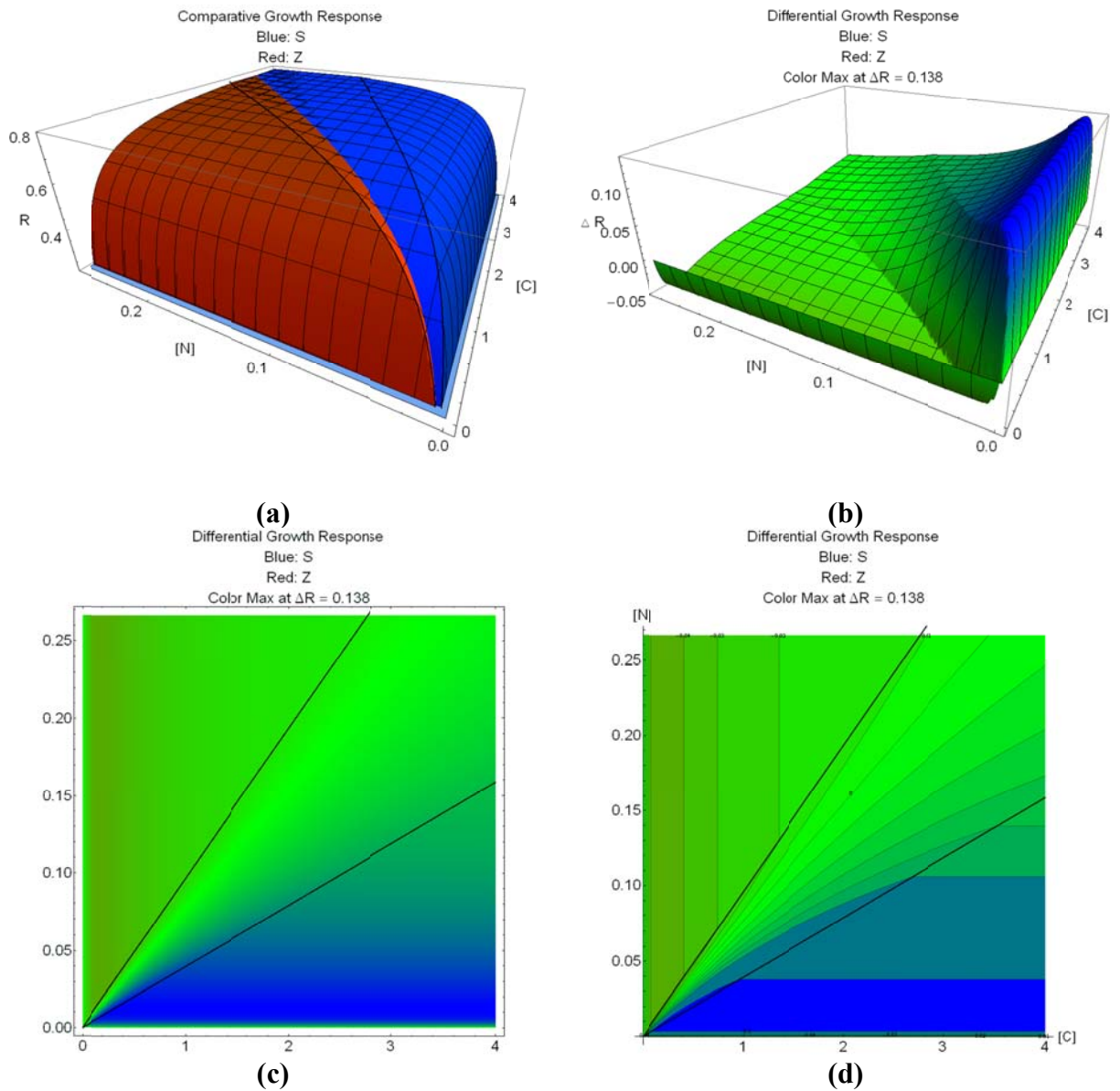


Figure 2-8. **Growth Response Plots, Sibling with Steeper Per-Resource Responses.**

Pop. T  $C_{IC}$  and  $C_{IN}$  greater half-sat. constants, same OPLs as in Figure 2-3 but “steeper” response than the prior example of Y versus Z

**Panel (a)**, dual surface plot. **Panel (b)**, differential surface plot. **Panel (c)** shaded difference plot. **Panel (d)** contoured-stepped difference plot. **Note:** Although both populations’ OPLs are the same as the “sibling” populations in Figure 2-3, the change to “steeper” per-resource responses, both  $C_{IC}$  and  $C_{IN}$ , for Population T give it the competitive advantage in the low-nitrogen range “below” its OPL and leave the rest of the resource supply space open to coexistence or stochastic determination of the competitive outcome. This result is complementary to that of Figure 2-7.

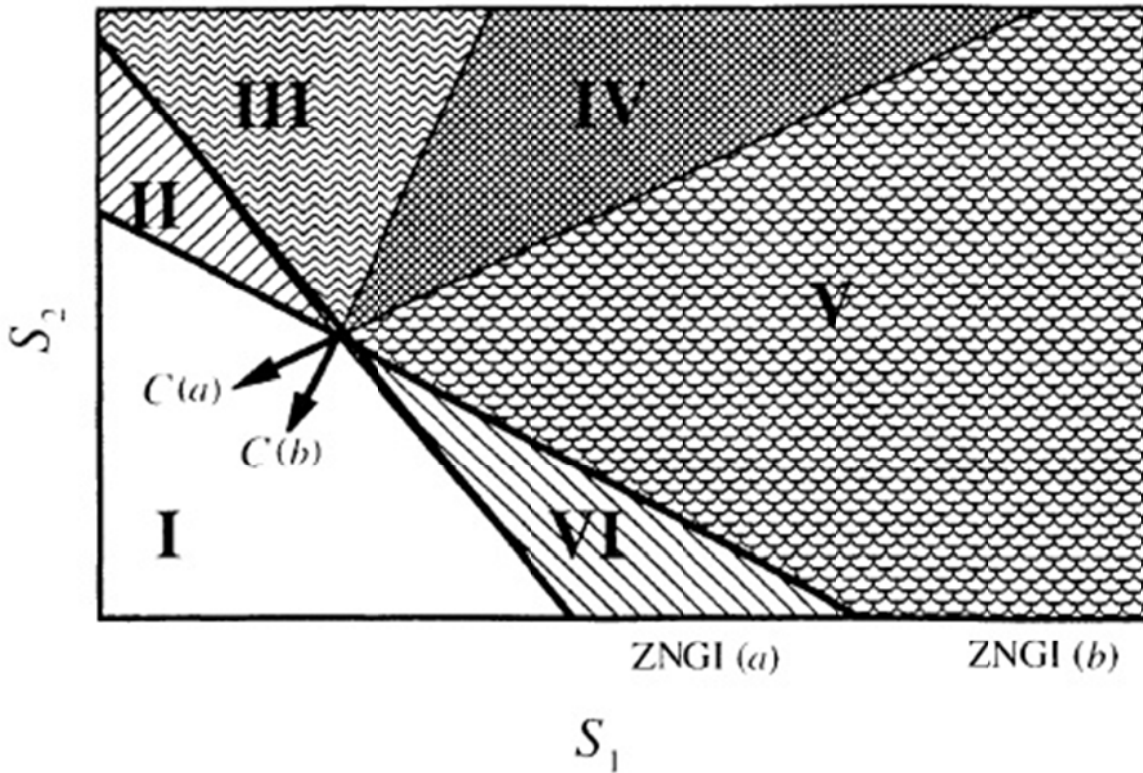


Figure 2-9. Leibold's FIG 6 from (1995)

“Environmental conditions, dependent on the Supply Point (equivalent to equilibrium resource densities in the absence of the consumers, described by the axes labeled  $S_1$  and  $S_2$ ) that determine the outcome of competition between two species competing for substitutable resources. The solid lines show the zero-net-growth isoclines of the two consumers [labeled ZNGI (a) and ZNGI (b)]. The outcome depends on their impact vectors (labeled  $C(a)$  and  $C(b)$ ) as illustrated by the extension of those shown as dashed lines. If maximum resource densities in the absence of consumers occur in Region I, neither species can exist. In Region II, only species h can exist, whereas only species a can exist in Region VI. Though both species can exist in the absence of interspecific competition in the remaining regions, species a is excluded from Region V and species h is excluded from Region III by competition. The two species coexist only if the Supply Point is in Region IV. See Tilman (1982) for a detailed discussion. Petraitis (1989) has shown that the cosine of the angle between the two impact vectors  $C(a)$  and  $C(h)$  is identical to Pianka's (1973) measure of niche overlap.”

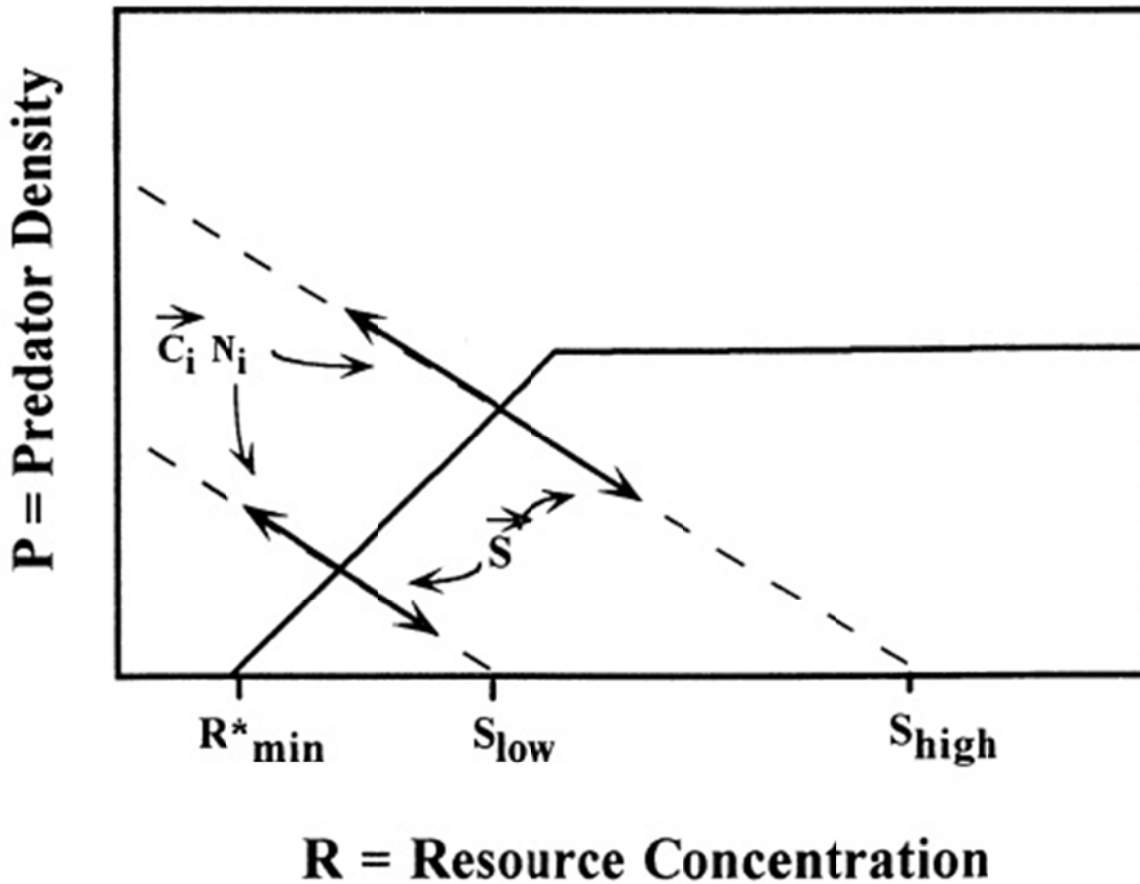


Figure 2-10. Leibold's FIG. 5 from (1996)

“The effect of increasing productivity on a simple three-level trophic chain. Two productivity levels are illustrated with different maximum resource levels ( $S_{low}$  and  $S_{high}$ ). In each case the equilibrium requires that the sum of the consumer-prey impact vectors and the STD vector be equal in magnitude but opposite in direction and that such points occur on the consumer-prey's ZNGI, as shown in fig. 2. The effect of increasing productivity is to increase the density of the predator and the resource.”

## **Chapter 3, Experimentally Characterizing the Ecological Niche and Validating a Model of Population Competition**

### Summary

We applied and tested our model, developed as in Chapter 2, to live competing populations. We also employed a new Characterization Protocol to determine organismal-population growth response traits required by the model. We took two wild-type strains of *Saccharomyces cerevisiae* and modified each of them to resist an antibiotic so that the original and modified strains could be distinguished after competition in common culture. We found that our model correctly and robustly predicted areas of both clear dominance and uncertain dominance, the latter being subject to stochastic determination of dominance or, possibly, amenable to coexistence.

### Introduction

Virtually all current and recent attempts to model population competition for resources follow Tilman's *Graphical-Mechanistic Approach* (1980) as typified by Chase and Leibold's discussion (2003) of the requirements niche (sensu Hutchinson 1957) and others. In spite of problems with implementation and interpretation (as in Miller et al. 2005) and Tilman's own cautionary comments (as in 1980, 1982) this approach remains a well-accepted reference model. Our implementation models the requirements niche in a two-dimensional space of dual-limiting resources (again sensu Hutchinson 1957). We use, beyond most other models, non-linear per-resource responses and organismal maximum capable growth response as in Monod's

formulation (1949), extended to two resources as in von Liebig's *Law of the Minimum* (ca. 1840s). We formulate our model in terms of organismal *response traits*, rather than the more frequently used phenomenological *realized rates* (as in Goldberg 1996).

In dealing with two populations competing by growth on two essential resources there are issues of properly characterizing dual-limited growth-response traits for the resources in question (as in Price and Morel 1991, Mankad and Nauman 1992, Duboc and von Stockar 1998, Clark 2001) (see esp. Rutgers *et al.* 1990, Zinn *et al.* 2004) and underlying basic issues of ecological stoichiometry (as in Sterner and Elser 2002 and others). We believe our implementation of curve-fitting phenomenological observation of a population on controlled supplies of two resources to a set of two response trait parameters and a common maximum response trait parameter is unique, never before achieved.

The objective of this study was to test experimentally a mathematical model (see Chapter 2) we developed of the requirements niches of two populations across a Hutchinsonian space of two essential resources, and to predict the outcome of inter-population competition across variation in the supply of these essential resources. To achieve this objective we propagated natural isolates of *Saccharomyces cerevisiae* under controlled experimental conditions, permitting us to characterize their realized intrinsic growth rates (Monod's  $R$ ) under different supply rates of two essential resources (*i.e.*, carbon and nitrogen). Using the mathematical model we parameterized their growth response, niche requirements across variation in the supply rates of carbon and nitrogen; such that for any point in Cartesian space across the two resource axes we could derive a population's realized intrinsic growth rate,  $R$ , on a third axis. Based on difference in  $R$  across this resource space we predicted at what resource supply rates one population might outcompete another. To test these predictions we then experimentally

competed different populations at different resource supply rates. We demonstrate that a population's growth response or niche requirements can be mapped across variation in the supply rates of two essential resources, and that differences in  $R$  between two populations within the resource space can be used to accurately predict competitive outcomes.

## Methods

### *Study organisms*

Our experimental populations were isogenic strains of wild-type *Saccharomyces cerevisiae*, a unicellular yeast found widely in the natural and domesticated environment. The strains were isolated from a “no captive cultures” winery (Kumeu River, Auckland, New Zealand) (Appendix B, Yeast Strains). Use of wild-type *versus* domesticated strains was intended to ensure the ecological relevance of the findings; specifically the responses of domesticated strains which have been perpetually propagated under artificial conditions might differ to their natural counterparts. Our isolates were <50 generations removed from the wild. In addition, use of isogenic strains removes within-population variation associated with the presence of different genotypes (polygenic populations). For the purposes of our work, we considered an isogenic strain a population and although an oversimplification it enabled unambiguous identification of niche requirements, competitive outcomes and evolutionary responses (see Chapter 4).

Our choice of *S. cerevisiae* as our experimental organism was based on the general extensive knowledge of the species in experimental environments (for example Replansky et al. 2008), our own familiarity and prior work with the species (Goddard and Bradford 2003b, Goddard 2008) and the ready availability of suitable isogenic strains (see Appendix B, Yeast Strains). Our choice of continuous culture, specifically in fully controlled chemostats, follows

the principles and logic in Hoskisson and Hobbes (2005) and is particularly driven by the need to maintain a constant (nutrient) resource environment for both Characterization and evolution (Adams et al. 1985, Goddard and Bradford 2003b, Adams 2004).

For the work presented here we used two of our wild-type, diploid isolates with differing genotypes based on micro-satellite typing of five loci (see Appendix B, Yeast Strains). These isolates are referred to as MRG-2 and MRG-8 following the original identification by Goddard. They were stored at  $-80\text{ }^{\circ}\text{C}$  with 1.7 mL of dense culture and 0.3 mL glycerol (15% v/v) in 2 mL Eppendorf tubes; this is standard practice for storage of *S. cerevisiae* cultures.

#### *Propagation of isolates*

Isolates were sub-sampled from cryo-storage into standard media for culturing *S. cerevisiae*. Specifically, they were inoculated into YPD Broth (Y1375, Sigma-Aldrich, St. Louis, MO, USA), which at  $50\text{ g L}^{-1}$  comprises  $20\text{ g L}^{-1}$  bacteriological grade peptone,  $10\text{ g L}^{-1}$  yeast extract, and  $20\text{ g L}^{-1}$  glucose. They were then grown at  $30\text{ }^{\circ}\text{C}$  for 48 h in batch culture prior to inoculation into the chemostats where they could be grown continuously in log phase under tightly-controlled resource supply rates.

Our chemostats (Figure 3-1) comprise “Multitron II” incubators (Infors HT, Bottmingen, CH) with DasGIP glassware (DasGIP AG, Jülich, DE) and “200 Series” pumps (Watson-Marlow, Wilmington, MA, USA). Each of the two chemostats maintained 16, 250 mL culture flasks concurrently at  $30\text{ }^{\circ}\text{C}$ , with gyratory agitation at 105 rpm and 25 mm throw,  $10.7\text{ mL h}^{-1}$  feed rate,  $50\pm 2\text{ mL}$  working culture volumes, and 4.69 h ( $0.213\text{ h}^{-1}$ ) culture turnover times. Each flask had separate nutrient medium supply, waste removal, and air supply. Waste removal was siphoned at 3 times the rate of media supply, ensuring that culture volumes were maintained at 50 mL and that there was no back-flow of waste. Air supply was regulated to  $0.5\text{ L min}^{-1}$  and

dried, de-oiled by expansion and carbon block adsorption, and filtered to 0.2  $\mu\text{m}$ . The outlet filter on each flask maintained a positive pressure within each flask, further preventing microbial contamination of the cultures.

Chemostat culture flasks were inoculated from the starter cultures and *S. cerevisiae* populations were grown overnight in batch culture conditions, with non-limiting nutrients. The medium (CYN5501 YNB w/o AA, w/o Ammonium phosphate, w/o Potassium Dihydrogen Phosphate and w/o Inositol; ForMedium Ltd, Norwich, UK) for these overnight cultures included 10 g L<sup>-1</sup> D-glucose monohydrate (49159; Sigma-Aldrich, St. Louis, MO, USA), 5 g L<sup>-1</sup> anhydrous (NH<sub>4</sub>)<sub>2</sub>SO<sub>4</sub> (A4418; Sigma-Aldrich, St. Louis, MO, USA), and 1 g L<sup>-1</sup> anhydrous KH<sub>2</sub>PO<sub>4</sub> (P9791; Sigma-Aldrich, St. Louis, MO, USA). This gave concentrations for C, N and P of 4.00 g L<sup>-1</sup> C, 1.06 g L<sup>-1</sup> N, 0.228 g L<sup>-1</sup> P and media was adjusted to pH 6.0 $\pm$ 0.1 using NaOH. We established in preliminary experiments and development of our Characterization Protocol that culture densities in the chemostat with this media were equivalent at the stated and double concentrations of C, N and P, confirming the formulation was not growth-limiting. To invoke resource limitation we then fed the chemostat cultures with the same base medium but with reduced concentrations of C and N.

#### *Characterizing niche requirements – step 1: empirical measures*

Characterizing niche requirements (*i.e.*,  $R$  values  $\geq 0$ , so that populations can persist deterministically without immigration) across availabilities of C and N, as representative essential, limiting resources, was a two-step process. The first step involved growing each of our two isolates at different C and N supply rates and then quantifying population biomass. We quantified biomass, instead of abundance, following MacArthur's (1972) and Monod's (1949) original conventions of population performance across availabilities of limiting resources

because one does not then have to make the assumption that all individuals are of equal mass (or resource content). Initial tests with different incubation times suggested that populations had stable biomass values after  $\geq 25$  generations and 25 generations was adopted as standard for mapping a population's niche requirements. This number of generations also limited the possibility that a beneficial mutation might sweep through any one population, thereby falsifying our assumption of isogeny across replicate populations. In addition, initial tests with different C and N supply rates suggested that concentrations of C ranging from 0.750 to 0.047 g C L<sup>-1</sup> gave ~10-fold differences in population biomass when N was not limiting (0.064 g N L<sup>-1</sup>), and that concentrations of N ranging from 0.032 to 0.002 g N L<sup>-1</sup> gave ~12-fold differences in population biomass when C was not limiting (1.5 g C L<sup>-1</sup>).

With respect to the number of generations required for a mutation to sweep our experimental populations we refer to Zeyl *et al.* (Zeyl and DeVisser 2001, Zeyl 2005) and others who estimate an adaptive (surviving) mutation rate on the order of  $1/10^{11}$  cell divisions in *S. cerevisiae*. Our Characterization cultures had a typical standing density of  $0.214 \text{ mg mL}^{-1} \times 78.5 \times 10^6 \text{ cell mg}^{-1} \times 50 \text{ mL} \times 25 \text{ h} / 4.69 \text{ h} \approx 4.48 \times 10^9$  divisions per run, approximately 1/22 the expected number of divisions to find one adaptive mutation.

Based on our initial tests, for each isogenic isolate we grew cultures at fixed, non-limiting C, with varying N supply and at fixed, non-limiting N, with varying C supply as in Table 3-1. Each supply rate was replicated 4 times. The design gave us eight points in the niche space delineated by the axes of C and N availabilities, from which we could estimate  $R$  knowing the population turnover and biomass. The latter was determined by ceasing the chemostat agitation and allowing the cultures to stand for 5 min to permit the characteristic 'cerevisiae residue' to settle to the base of the flasks and then ~45 mL of culture was removed. The sample's exact

volume was determined before it was centrifuged at 4 °C to collect the biomass ‘pellet’. The supernatant was then removed and the pellet re-suspended by vortex agitation in 1 mL DI water, transferred to a 2 mL microcentrifuge tube and the process of centrifugation and re-suspending repeated twice more to wash the biomass clean of media. The cleaned pellet was dried at 65 °C to stable mass (~24 h), and then weighed. From the mass and volume of culture sampled we estimated the population mass density to be used in the second step of the Characterization Protocol (Table 3-2).

*Characterizing niche requirements – step 2: curve fitting*

The second step used a curve-fitting process to estimate the population’s niche requirements (represented as values of  $R \geq 0$ ) across availabilities of C and N. It used the mathematical model described in Chapter 2. The process of curve fitting relies on the assumption that C and N affect population biomass additively; *i.e.*, there is dual-limitation (an assumption that held; see Results). We used Monod’s (1949, pg 343, eqn 2) growth equation for a population on a single limiting resource is:

$$R = \frac{dN/dt}{N} = R_K \cdot \frac{C}{C_1 + C} \quad ()$$

Where  $R$  is the realized intrinsic growth rate,  $N$  is the population size by mass,  $t$  is time,  $R_K$  is the maximum capable intrinsic growth rate,  $C$  is the instantaneous resource supply concentration, and  $C_1$  is the resource supply concentration at which  $R$  is half its maximum value ( $R_K$ ). It then follows that where we have two, dual-limiting resources (designated  $A$  and  $B$ ), we require two growth equations:

$$R_A = R_{KA} \cdot \frac{C_A}{C_{1A} + C_A} \quad ()$$

$$R_B = R_{KB} \cdot \frac{C_B}{C_{1B} + C_B} \quad ()$$

Since the population's growth rate must obey von Liebig's *Law of the Minimum*, we must combine the two growth equations to:

$$R = \min \left[ R_{KA} \cdot \frac{C_A}{C_{1A} + C_A}, R_{KB} \cdot \frac{C_B}{C_{1B} + C_B} \right] \quad ()$$

where *min* is the mathematical operator *minimum* of the given terms.

And since  $R_K$  is an organismal trait common to all per-resource growth responses we have a single value of  $R_K = R_{KA} = R_{KB}$ , which gives us (with collection of terms):

$$R = R_K \cdot \min \left[ \frac{C_A}{C_{1A} + C_A}, \frac{C_B}{C_{1B} + C_B} \right] \quad ().$$

We then need to find the three parameters  $R_K$ ,  $C_{IA}$  and  $C_{IB}$  by fitting the equation to experimental observations. To do this we used our empirically-generated estimates of  $R$  for the four points in niche space where carbon was limiting, as  $C_A \rightarrow C_C$ , (with nitrogen in excess), and the four points where nitrogen was limiting, as  $C_B \rightarrow C_N$ , (with carbon in excess; see above Methods). Knowing these values from the chemostat runs, we can fit numerically for  $R_K$ ,  $C_{IA} \rightarrow C_{IC}$  and  $C_{IB} \rightarrow C_{IN}$  using a curve-fitting algorithm implemented in *Mathematica*® (Wolfram Research 2008) (see Appendix A, Mathematics).

This curve-fitting provides the necessary trait parameters for computing  $R \geq 0$  across supply rates of each resource that can be plotted to delineate the niche requirements of the target population (in this instance an isogenic isolate) across the two resources investigated (carbon and nitrogen). We do this for our two wild type populations and then overlay these population-specific niche requirements to identify areas in niche space where one isolate might outcompete another.

## *Characterizing niche requirements – statistics analysis*

An overarching problem with statistical analysis of our results is that we are not dealing with conventional hypothesis testing (except, perhaps, in our direct competitions) or conventional statistical inference. We have no single parameters which are independently derived from our Characterization Protocol and the multiple data values per test point ( $\mathbf{R}$ ,  $C_C$ ,  $C_N$ ). The multiple parameters we need ( $\mathbf{R}_K$ ,  $C_{IC}$ ,  $C_{IN}$ ) for maximum capable growth response and per-resource growth response can only be determined by simultaneous curve-fitting to a single equation.

If we were to attempt to fit each per-resource response,  $C_{IC}$  and  $C_{IN}$ , from our data sets or any other measurement scheme, individually (*i.e.* without simultaneous  $\mathbf{R}_K$ ) we would be left with a linear relationship as our only alternative and we know from numerous sources previously cited *e.g.* (Ferenci 1999, Levert and Xia 2001, Lokshina et al. 2001, Higuera-Guisset et al. 2005, Tang et al. 2007, Cerucci et al. 2010) that that is not a viable option.

If we were to attempt to fit each per-resource response,  $C_{IC}$  or  $C_{IN}$ , with  $\mathbf{R}_K$  independent of the other per-resource response, we would be virtually certain to arrive at two values for  $\mathbf{R}_K$ , as if  $\mathbf{R}_{KC}$  and  $\mathbf{R}_{KN}$ , which we know from several of the immediate prior citations as well as from Grover (1997) is not realistically applicable. Simply put, if we provide a single population with sufficient supply of all resources that no further increase of any resource provides any greater growth response, then we have reached a population limit to growth rate. This can be verified by decreasing each resource, one at a time, to establish a limiting growth value for each (non-substitutable) resource and these limits will be found to be all at the same maximum growth response. So we must, in the end, fit all three of our parameters for each population,  $\mathbf{R}_K$ ,  $C_{IC}$ ,  $C_{IN}$ , simultaneously to the single Monod-and-von Leibig formulation.

We are in the situation of having no “independent variables” or “additive variables” statistical analysis available. We rely, instead, on confidence interval comparison for whatever meaning there may be to “significant difference” between competing populations’ values of each of our three parameters. Our curve-fitting program and its core *Mathematica*® function, *NonlinearModelFit*[], provide an ANOVA table for the objective variable  $x$ , our realized-observed  $R$ , but have no equivalent of independent or additive behavior to determine customary, per-variable error, residual statistics. The program does provide Standard Error, Confidence Interval (95%), t-Statistic and P-value per fitted parameter but while these are comparable to the usual statistics they are not the same and are not related by any simple function.

We show one example of manually-assembled graphical fit and residuals plot of  $C_{IC}$  and  $C_{IN}$ , Figure 3-2 for yeast strain MRG-8, as if these parameters had been individually determined. The fit and residuals for  $C_{IC}$  look good but those for  $C_{IN}$  do not. If we had recognized this syndrome early in our sequence of experiments we might have extended our range of  $C_N$ , nitrogen supply concentration, to higher values to obtain a better-appearing fit but we chose to stay with a consistent set of test points. It is not clear, however, that the  $C_{IN}$  fit would have “looked” any better by curve or by residuals as the entire fit can only deal with all three parameters.

The OPL slopes for the several populations show significant difference between all but one of the competing pairs, which runs counter to customary suspicion of “statistics of statistics”, *i.e.* because the OPL slope is a ratio of two fitted parameters which, themselves, do not appear to be significantly different. We analyzed the OPL slopes by a Monte Carlo process of dithering each of the OPL components,  $C_{IC}$  and  $C_{IN}$ , 1,000 times by its Standard Error on a Normal

Distribution, taking the ratio of each pair of dithered values, and performing a simple analysis of Mean, Variance and Confidence Interval (95%) of the 1,000 ratios.

#### *Characterizing niche requirements – statistics summary*

Table 3-3 summarizes the growth response parameters for the original and modified strains while Table 3-4 compares the statistical confidence intervals for each competing pair. Table 3-5 through Table 3-8 show the full statistical reports from the curve-fitting program. For all four competing pairs the trait parameters,  $R_K$ ,  $C_{IC}$ ,  $C_{IN}$ , appear to be statistically not significantly different per pair while the derived optimum C:N ratio, computed from the parameters, shows statistically significant difference for three of the pairs (the CIs do not overlap) and weak difference for the fourth pair, MRG-8 *versus* MRG-8N, where the CIs overlap each other but not the means. It is instructive to compare the “no significant difference” inference, except for C:N ratio, to the actual outcomes of competition shown in Table 3-9 and Table 3-10 in the Results presented below. What we infer here is validation of a point long argued, in ecology classrooms of our experience and in the literature (Graham and Edwards 2001, Di Stefano 2004, Martinez-Abraín 2007, Nakagawa and Cuthill 2007, Stephens *et al.* 2007, Martinez-Abraín 2008), that “Statistical significance does not show ecological significance—and vice-versa.”

#### *Competition assays*

By overlaying niche requirements for our two isolates we can determine regions of resource space where we might expect one isolate to always outcompete the other (specifically regions where  $R$  differed by  $\geq 0.02$ ) and areas where the outcome of competition is uncertain—where coexistence may be possible. Specifically, we used the following equation to calculate

differential growth ( $R_{rel}$ ) at any one point in resource supply space between two populations,  $Y$  and  $Z$ :

$$R_{rel} = R_Y - R_Z \text{ or} \quad ()$$

$$R_{rel} = R_{KY} \cdot \min \left[ \frac{C_A}{C_{1AY} + C_A}, \frac{C_B}{C_{1BY} + C_B} \right] - R_{KZ} \cdot \min \left[ \frac{C_A}{C_{1AZ} + C_A}, \frac{C_B}{C_{1BZ} + C_B} \right] \quad ().$$

To test the model predictions concerning competitive outcomes, we performed experimental competitions using our chemostat system. Specifically, we selected regions where difference in  $R$  was greater than 0.02 (so the outcome of competition should always be dominance by the isolate with the greater  $R$  at that point in space) and less than 0.02 (making outcomes uncertain, so we'd expect variation across replicate competitions as to the winner). As we had no simple way to differentiate one isolate from the other, we used a standard approach in *S. cerevisiae* evolution studies and marked each isolate with antibiotic resistance, permitting us to differentiate one isolate from the other by differential growth in media with and without the antibiotic.

Antibiotic-resistant populations were developed using plasmid pYL16 which inserts a gene for resistance to clonNAT brand nourseothricin (kit WERNER BioAgents 2009). The resistant isolates were grown in the standard YPD medium (described above) to  $\sim 10^7$  cells mL<sup>-1</sup>. Aliquots were stored at -80 °C as described earlier and checked for viability by initiating starter cultures and growth on agar test plates. 'Standard' plates were composed of the standard YPD medium with 20 g L<sup>-1</sup> bacteriological agar (A5306; Sigma-Aldrich, St. Louis, MO, USA), and the selection plates used same recipe plus 100 µg L<sup>-1</sup> nourseothricin antibiotic. We confirmed that the antibiotic-resistant isolates showed robust colony growth on both plate types, and that our antibiotic-naïve isolates only grew on the standard plates. This demonstrated that the two types of plate clearly distinguished between the naïve and resistant yeast strains. The naïve

strains retained the designations MRG-2 and MRG-8, and the resistant strains were named MRG-2N and MRG-8N, where  $N$  stands for nourseothricin-resistant.

The usual assumption in using antibiotic-resistant strains in competition (or fitness) assays is that the inserted resistance gene has no effect on fitness when the resistant isolate is grown without the antibiotic. We tested this assumption by characterizing the niche requirements of the resistant isolates as described above for the naïve isolates. We did find slight in  $R_K$  and  $C_I$  for each resource, and for each isolate, following resistance gene incorporation (see Results). Given these shifts we tested predicted competitive outcomes using the modeled niche requirements of the resistant *versus* naïve isolates for each distinguishable pair, giving us four possible competitions (MRG-2 *versus* MRG-2N, MRG-2 *versus* MRG-8N, MRG-8 *versus* MRG-2N, MRG-8 *versus* MRG-8N).

To perform a competition two selected strains were grown separately in standard YPD medium (described above) to between  $10^7$  and  $5 \times 10^7$  cells  $\text{mL}^{-1}$ . Each culture was adjusted (diluted) with standard YPD medium to  $5 \times 10^6$  cells  $\text{mL}^{-1}$  and 100 mL aliquots of the adjusted cultures were mixed. The resulting mixed culture was used to inoculate the chemostat flasks for the competition run: 10 mL of combined culture was added to each chemostat flask containing 50 mL of competition medium. This gave starting densities of  $\sim 4.2 \times 10^6$  cells  $\text{mL}^{-1}$  of each strain. The competition medium was the chemostat base medium (described above) with concentrations of C and N defined by the resource supply point being investigated.

Using the chemostat settings described for the Characterization runs (see above), each competition was run for 25 generations. Model predictions and initial tests suggested 25 generations was sufficient for populations with markedly different fitness values (*i.e.*,  $R_{\text{rel}}$  values  $> 0.02$ ) to differ substantially in number. For example, the poorer competitor could decline to

virtually zero abundance ( $N/2^{25} = 2.98 \times 10^{-8} N$ ), and the superior competitor could increase to dominance ( $N \times 2^{25} = 3.36 \times 10^7 N$ —subject to the asymptotic limit) from the initial 1:1 population ratio.

After 25 generations media flow and agitation were stopped and the chemostat flasks were allowed to stand for 5 min to permit the ‘cerevisiae residue’ to settle. Next ~35 mL of culture was removed and population density measured using a T100 Turbidity Meter (Oakton Instruments, Vernon Hills, IL, USA). Then each mixed culture was diluted to  $\sim 2 \times 10^4$  cells mL<sup>-1</sup> and 10  $\mu$ l (~200 cells) of this dilution was inoculated onto four, 10 cm dia. agar gel plates and distributed evenly by rolling with three, 5 mm dia. glass balls. Two plates were composed of the standard YPD medium (permitting growth of all colonies), and two were impregnated with nourseothricin at 100  $\mu$ g L<sup>-1</sup>, permitting only resistant isolates to grow. Plates were incubated for 24 h at 30 °C and examined for colony growth. If there were fewer than 50 colonies per plate then the set of four for that population pairing was incubated for an additional 24 h. For colony counts, each plate was covered with a randomly oriented counting mask—a 10 cm-dia. opaque disk with seven randomly located windows, each 0.5 mm square. The ‘windows’ showing most and fewest yeast colonies were not counted, and total colony forming units (CFUs) were enumerated for the remaining five windows. The first round of competitions competed each of the four pairs of populations at four different resource points, using two replicate competitions per population and resource supply rate. Outcomes were scored qualitatively (winner, loser, uncertain outcome). To quantify competitive outcomes more rigorously, a second round of competitions was replicated eight times for each pair of populations. For two pairings we selected resource supply points where we expected clear winners, and for the other two pairings resource supply points where competitive outcomes were uncertain. Where we expected clear

winners, we reasoned that the ratio of naïve and resistant competitors should differ significantly to one, so the 95% confidence intervals of the ratio of the abundance of these two competitors should not cross 1. For uncertain outcomes we reasoned the 95% confidence intervals should cross 1.

## Results and Discussion

### *Niche requirements*

The niche requirements of each our four competition strains were characterized first through the empirical measures of population mass density at eight different supply rates (*cf.* Table 3-1). Next we used these measures (Table 3-2) in our mathematical model to curve-fit the population growth parameters (Table 3-3) and niche requirements. There were clear differences in growth parameters between the two wild-type strains. For example, MRG-2 has an ~7% lower  $R_K$  than MRG-8, and also a higher affinity for C and N uptake (represented by the lower  $C_I$  values for both C and N). These differences translated to a broader, optimum C:N ratio for MRG-2 than MRG-8 (Table 3-3), which causes the OPL of MRG-2 to fall below that for MRG-8 Figure 3-3 (a). These differences then translate to different niche requirements of the two strains Figure 3-3 (b) and (c), so that except at low resource supply rates MRG-8 would be expected to outcompete MRG-2 Figure 3-3 (d). Given that we couldn't ascertain competitive outcomes directly between MRG-2 and MRG-8, and that antibiotic resistance may carry a fitness cost, we also characterized the growth parameters for the two resistant strains (MRG-2N and MRG-8N). These values are shown in Table 3-3, where it can be seen that induced resistance did shift the growth parameters. For example, MRG-8N had a higher  $R_K$  and  $C_I$  for carbon than MRG-8, but a lower  $C_I$  for nitrogen.

### *Competitive outcomes*

Based on differences in R across the resource space, such as shown in Figure 3-3 for MRG-2 *versus* MRG-8, we selected different resource supply points at which to compete the naïve and resistant strains. In the first round of competitions CFU counts on YPD plates with and without the antibiotic were scored qualitatively. Out of 16 competitive pairings our prediction was Confirmed 10 times, Weakly Confirmed 3 times and Contradicted 3 times. (Table 3-9). Based on this initial round of competitions, we decided we needed higher replication (n=8 instead of 2) for robust, quantitative assessment of whether observed outcomes matched those predicted. In these competitions MRG-8N outcompeted MRG-2 in six of the eight replicates, with the remaining two replicates having approximately equal representation of each strain. Nevertheless, overall MRG-8N emerged as the distinct winner (*i.e.*, 95% CI did not cross 1; Table 3-10), as predicted. For MRG-8 *versus* MRG-2N the prediction was even more robustly met (Table 3-10), and MRG-8 dominated in seven of eight replicates, with one replicate competition having equal abundances of both isolates. When the naïve and resistant isolates of the same strain were competed at resource supply rates where the outcomes were uncertain, the 95% CIs strongly overlapped one (Table 3-10), with MRG-2 winning in five competitions and losing in three, and MRG-8 (*versus* MRG-8N) winning in three competitions, losing in three and having two occasions where the ratio was ~1. Overall then, the outcomes in the second round of competitions consistently met the predictions from our model (Table 3-10) that estimated R following the assumption that dual-limitation on two essential resources suitably estimated niche requirements and competitive outcomes of natural isolates of *S. cerevisiae*.

Our primary purpose in this work was to develop a model of populations in competition for shared resources by which we could repeatably predict likely outcomes across a

Hutchinsonian resource space and not just at or close to a few demographically observed points. This required extension of Tilman's *Graphical-Mechanistic Approach* to use : 1) organismal growth-response traits rather than simple (generally linear) phenomenological relationships; and 2) an accepted non-linear, saturating model of growth responses such as the Monod function. It also required that we develop a protocol for determining the required trait parameters of populations including: 1) a simple observation-measurement process easily applied empirically, in the laboratory, and possible to be applied demographically, in the field; and 2) a means of curve-fitting the Characterization measurements to the paired Monod functions (with per-resource responses and common organismal maximum growth limit) for a population's response to two resources. We have shown that we can characterize multiple populations and arrive at distinctive sets of response trait parameters. We have then shown that we can apply these parameters to our predictive formulation to give clear delineation of relative growth response, between two populations, across a broad Hutchinsonian resource space. And we have applied the Characterization and the prediction to successfully predict the outcomes, and areas of uncertain outcome, in common-media competitions of two populations.

Advantages of our approach—for which we can find no strong equivalent in the literature—include that it addresses and appears to solve several shortcomings of previous implementations of Tilman's approach including warnings dating back to his original work but never resolved for the general case—our model appears to be both simpler to use and more mechanistically realistic in our use of characterized non-linear responses, per population and per resource, rather than assumed linear responses. We also believe that we have obviated some of the complex efforts, and associated difficulties, to apply the  $R^*$  concept and its derivatives because it relies on assumptions of resource supply stability and constant inter-population effects

(such as predation or herbivory) that most often do not prevail *in natura* while our approach can deal with competition across the Hutchinsonian  $n$ -dimensional space as both resource supplies and competitive effects may vary. We would especially emphasize the ability of our model to deal with: 1) non-linear isoclines (ZNGIs or others), 2) inter-penetrating growth response surfaces which are completely outside the concepts of the simple Tilman approach, and 3) quantitative differential growth response which permits the distinction among “rapid dominance”, “slow dominance”, “periodic or transitory dominance” and “stochastic uncertainty” to be detected at any desired level.

The ability to plot the response-surface “tents” of Figure 3-3 individually, in “two-up” dual presentation, and in any of our three differential presentation (see Chapter 2) give multiple ways to achieve either insight or prediction, whichever one may consider to be the primary purpose of ecological models in general. We used our differential plots—difference-surface, shaded-difference and shaded-contour, alike—to select the two-resource points for our competition experiments—choosing both points where we expected clear dominance and points where we expected stochastic uncertainty. Aside from making successful predictions of competitive outcomes when displacement was clearly predicted the ability to quantify areas of uncertainty and related zones of transition from certainty to uncertainty to certainty—as cases may be—on any desired value of what growth difference is sensitive to stochastic effects is a unique characteristic of our model. We also believe it is significant that when response trait parameters cannot be well determined for a problem under consideration our model is capable of “fallback” to essentially the original-linear-flat Tilman presentation as a guide, perhaps, to fruitful further investigation of the case.

We focus on measurements of biomass rather than count of cells or other demographic units following the lead established by MacArthur, Monod and Tilman and their assertion, explicit or implicit, that it is really biomass, regardless of population size distribution and number of individuals, that resource mass is converted into. Our assessment of competitive outcome relied on yeast colony count because we were not looking, in the present case, for fine distinction of relative dominance but, rather, were looking for either essentially complete displacement or failure of displacement to occur. There is nothing to preclude, in other cases, testing for partial dominance or quantified coexistence by some means like differential counting of cells (with the aid of GFP, perhaps, instead of an antibiotic) or otherwise-distinguishable individuals whether by flow cytometry in microbes and plankton or by counting meso-arthropods in a soil sample.

Our model and protocols are, at present, strictly laboratory-experimental and we regard them primarily as a simulation system. As such, it can be used to investigate hypotheses of resource-dependent displacement cases, perhaps including predator-prey interactions dependent on underlying resource supplies, or evolutionary effects in isogenic or narrowly polygenic populations, or complex selection effects in broadly polygenic populations. As a basic simulation system our model opens the opportunity to extend some of the investigations initiated by Paquin and Adams (Paquin and Adams 1983a, Paquin and Adams 1983b, Adams *et al.* 1985, Adams 2004), Lenski *et al.* (Lenski 1989, Cooper *et al.* 2003, Elena and Lenski 2003), Rutgers *et al.* (1990) etc. As a system potentially capable of detecting cryptic genetic covariance and/or incorporating them at the trait parameter level (referring ahead to Chapter 4) our model may be able to offer worthwhile tests of otherwise difficult phenotypic effects.

If we may propose an extended case for application of our model we would refer to the interaction of inter- *versus* intra-population competition (as in Clark 2010), in a theoretical framework or even *in vitro* with polygenic populations and quantitative-differential genetic analysis of the survivors.

Tables

Table 3-1. Yeast Characterization Nutrient Resource Supplies.

<b>Mode</b>	<b>C, g L<sup>-1</sup></b>	<b>N, g L<sup>-1</sup></b>
	0.75	
<b>Carbon Step</b>	0.375	0.064
	0.1875	
	0.09375	
		0.032
<b>Nitrogen Step</b>	1.5	0.016
		0.008
		0.004

Table 3-2. **Typical Yeast Strain Characterization Data.**

**Vial #:** for record; **Flask vol.:** measured volume of culture from chemostat, mL to 0.5; **C:** carbon resource concentration, g L<sup>-1</sup>; **N:** nitrogen resource concentration, g L<sup>-1</sup>; **Vial Net:** culture biomass, mg to 0.005; **mg/ml:** culture density, mg mL<sup>-1</sup>; **mean:** mean of culture densities; **σ<sup>2</sup>:** standard deviation of culture densities; **Outlier:** culture density excluded by Dean-Dixon outlier test (as in Lohninger 2009), n=4, α=0.05.

Vial #	Flask vol.	C	N	Vial Net	mg/ml	mean	σ <sup>2</sup>	Outlier
601	42.0	1.5	0.032	21.670	0.5160			
602	45.0	1.5	0.032	12.905				0.2868
603	41.5	1.5	0.032	21.845	0.5264			
604	42.5	1.5	0.032	17.785	0.4185	0.4869	0.0486	
605	36.0	1.5	0.016	6.020	0.1672			
606	39.0	1.5	0.016	7.365	0.1888			
607	43.0	1.5	0.016	9.070	0.2109			
608	44.5	1.5	0.016	8.085	0.1817	0.1872	0.0158	
609	40.0	1.5	0.008	4.215	0.1054			
610	43.0	1.5	0.008	2.755	0.0641			
611	41.0	1.5	0.008	1.460	0.0356			
612	44.5	1.5	0.008	3.280	0.0737	0.0697	0.0249	
613	38.5	1.5	0.004	1.915	0.0497			
614	41.5	1.5	0.004	1.325	0.0319			
615	41.0	1.5	0.004	2.565	0.0626			
616	42.5	1.5	0.004	0.970	0.0228	0.0418	0.0154	
617	41.5	0.75	0.064	20.385	0.4912			
618	36.0	0.75	0.064	15.620	0.4339			
619	33.0	0.75	0.064	13.340	0.4042			
620	43.0	0.75	0.064	16.760	0.3898	0.4298	0.0389	
621	39.5	0.375	0.064	13.580				0.3438
622	45.0	0.375	0.064	13.505	0.3001			
623	39.0	0.375	0.064	11.665	0.2991			
624	42.0	0.375	0.064	12.520	0.2981	0.2991	0.0008	
625	47.0	0.1875	0.064	8.555	0.1820			
626	41.5	0.1875	0.064	7.575	0.1825			
627	46.0	0.1875	0.064	8.145	0.1771			
628	41.5	0.1875	0.064	6.905	0.1664	0.1770	0.0065	
629	45.0	0.09375	0.064	4.955	0.1101			
630	38.0	0.09375	0.064	0.955	0.0251			
631	43.5	0.09375	0.064	4.380	0.1007			
632	43.0	0.09375	0.064	2.070	0.0481	0.0710	0.0355	

**Table 3-3. Yeast Strains Growth Response Parameters Summary.**

**Population:** population/ strain/ isolate name; **R<sub>K</sub>:** maximum capable intrinsic growth rate; **C<sub>1C</sub>:** carbon half-saturation constant; **C<sub>1N</sub>:** nitrogen half-saturation constant; **C:N:** ratio of half-saturation constants, alias dual-limiting ratio, slope of Tilman's OPL (Optimum Proportion Line); **!R<sup>2</sup>:** Adjusted R<sup>2</sup> (correlation) of R<sub>K</sub>, C<sub>1C</sub> and C<sub>1N</sub>; **SE XX:** standard error of R<sub>K</sub>, C<sub>1C</sub> or C<sub>1N</sub>; **Msd C:N:** Monte Carlo standard deviation of C:N.

<b>Population</b>	<b>R<sub>K</sub></b>	<b>SE R<sub>K</sub></b>	<b>C<sub>1C</sub></b>	<b>SE C<sub>1C</sub></b>	<b>C<sub>1N</sub></b>	<b>SE C<sub>1N</sub></b>	<b>!R<sup>2</sup></b>	<b>C:N</b>	<b>Msd C:N</b>
<b>MRG-2</b>	0.834	0.0544	0.210	0.0379	0.0130	0.00214	0.946	16.15	4.27
<b>MRG-2N</b>	0.845	0.0430	0.223	0.0310	0.0154	0.00185	0.971	14.48	2.72
<b>MRG-8</b>	0.860	0.0358	0.216	0.0234	0.0142	0.00135	0.982	15.21	2.36
<b>MRG-8N</b>	0.929	0.0461	0.232	0.0303	0.0150	0.00173	0.974	15.47	2.67

**Table 3-4. Yeast Strains Growth Response Parameters Comparison.**

**Population:** population/ strain/ isolate name; **R<sub>K</sub>:** maximum capable intrinsic growth rate; **C<sub>1C</sub>:** carbon half-saturation constant; **C<sub>1N</sub>:** nitrogen half-saturation constant; **C:N:** ratio of half-saturation constants, alias dual-limiting ratio, slope of Tilman's OPL (Optimum Proportion Line); **Lo XX & Hi XX:** high and low values of R<sub>K</sub>, C<sub>1C</sub> and C<sub>1N</sub> 95% confidence interval; **MLo C:N & MLo C:N:** high and low values of C:N Monte Carlo 95% confidence interval. The table is arranged to place the tested pairs in adjacent rows. The shaded cells call out comparisons which are significantly different by 95% confidence intervals. Note that three of the C:N ratio pairs show significant difference although none of the response parameter pairs do so.

<b>Population</b>	<b>R<sub>K</sub></b>	<b>Lo R<sub>K</sub></b>	<b>Hi R<sub>K</sub></b>	<b>C<sub>1C</sub></b>	<b>Lo C<sub>1C</sub></b>	<b>Hi C<sub>1C</sub></b>	<b>C<sub>1N</sub></b>	<b>Lo C<sub>1N</sub></b>	<b>Hi C<sub>1N</sub></b>	<b>C:N</b>	<b>MLo C:N</b>	<b>MHi C:N</b>
<b>MRG-2</b>	0.834	0.722	0.945	0.210	0.133	0.288	0.0130	0.00865	0.0174	16.15	15.89	16.42
<b>MRG-2N</b>	0.845	0.757	0.934	0.223	0.159	0.286	0.0154	0.0116	0.0192	14.48	14.31	14.65
<b>MRG-2</b>	0.834	0.722	0.945	0.210	0.133	0.288	0.0130	0.00865	0.0174	16.15	15.89	16.42
<b>MRG-8N</b>	0.929	0.834	1.023	0.232	0.170	0.294	0.0150	0.0115	0.0186	15.47	15.30	15.63
<b>MRG-8</b>	0.860	0.822	0.9695	0.216	0.169	0.264	0.0142	0.0114	0.0169	15.21	15.07	15.35
<b>MRG-2N</b>	0.845	0.757	0.934	0.223	0.159	0.286	0.0154	0.0116	0.0192	14.48	14.31	14.65
<b>MRG-8</b>	0.860	0.822	0.9695	0.216	0.169	0.264	0.0142	0.0114	0.0169	15.21	15.07	15.35
<b>MRG-8N</b>	0.929	0.834	1.023	0.232	0.170	0.294	0.0150	0.0115	0.0186	15.47	15.30	15.63
<b>MRG-2</b>	0.834	0.722	0.945	0.210	0.133	0.288	0.0130	0.00865	0.0174	16.15	15.89	16.42
<b>MRG-8</b>	0.860	0.822	0.9695	0.216	0.169	0.264	0.0142	0.0114	0.0169	15.21	15.07	15.35

**Table 3-5. Yeast Strain MRG-2 Complete Response Parameters Data.**  
**AdjustedRSquared**

0.946367

**ANOVA Table**

	<b>DF</b>	<b>SS</b>	<b>MS</b>
<b>Model</b>	3	2.03212	0.677373
<b>Error</b>	28	0.103453	0.00369475
<b>Uncorrected Total</b>	31	2.13557	
<b>Corrected Total</b>	30	0.751379	

**ParameterConfidenceIntervalTable,  $\alpha=0.05$**

	<b>Estimate</b>	<b>Standard Error</b>	<b>Confidence Interval</b>	
<b>RK</b>	0.833635	0.0544411	0.722117	0.945152
<b>C1C</b>	0.210322	0.0379248	0.132637	0.288008
<b>C1N</b>	0.0130414	0.00214042	0.00865691	0.0174258

**ParameterTable**

	<b>Estimate</b>	<b>Standard Error</b>	<b>t Statistic</b>	<b>P-Value</b>
<b>RK</b>	0.833635	0.0544411	15.3126	3.89246×10-15
<b>C1C</b>	0.210322	0.0379248	5.54577	6.25477×10-6
<b>C1N</b>	0.0130414	0.00214042	6.0929	1.42587×10-6

**Table 3-6. Yeast Strain MRG-2N Complete Response Parameters Data.  
AdjustedRSquared**

0.971143

**ANOVA Table**

	<b>DF</b>	<b>SS</b>	<b>MS</b>
<b>Model</b>	3	1.99109	0.663697
<b>Error</b>	28	0.0532858	0.00190306
<b>Uncorrected Total</b>	31	2.04438	
<b>Corrected Total</b>	30	0.734808	

**Parameter Confidence Interval Table,  $\alpha=0.05$**

	<b>Estimate</b>	<b>Standard Error</b>	<b>Confidence Interval</b>	
<b>RK</b>	0.84548	0.0430188	0.75736	0.933601
<b>C1C</b>	0.222601	0.0309664	0.159169	0.286033
<b>C1N</b>	0.0153732	0.00184946	0.0115848	0.0191617

**Parameter Table**

	<b>Estimate</b>	<b>Standard Error</b>	<b>t Statistic</b>	<b>P-Value</b>
<b>RK</b>	0.84548	0.0430188	19.6537	$6.41057 \times 10^{-18}$
<b>C1C</b>	0.222601	0.0309664	7.18846	$7.99383 \times 10^{-8}$
<b>C1N</b>	0.0153732	0.00184946	8.31228	$4.81046 \times 10^{-9}$

**Table 3-7. Yeast Strain MRG-8 Complete Response Parameters Data.  
AdjustedRSquared**

0.982131

**ANOVA Table**

	<b>DF</b>	<b>SS</b>	<b>MS</b>
<b>Model</b>	3	2.39956	0.799853
<b>Error</b>	28	0.039363	0.00140582
<b>Uncorrected Total</b>	31	2.43892	
<b>Corrected Total</b>	30	0.80565	

**Parameter Confidence Interval Table,  $\alpha=0.05$**

	<b>Estimate</b>	<b>Standard Error</b>	<b>Confidence Interval</b>	
<b>RK</b>	0.895798	0.0358265	0.82241	0.969185
<b>C1C</b>	0.216459	0.0233999	0.168526	0.264391
<b>C1N</b>	0.0141549	0.00134917	0.0113912	0.0169185

**Parameter Table**

	<b>Estimate</b>	<b>Standard Error</b>	<b>t Statistic</b>	<b>P-Value</b>
<b>RK</b>	0.895798	0.0358265	25.0038	1.07902×10-20
<b>C1C</b>	0.216459	0.0233999	9.25043	5.22192×10-10
<b>C1N</b>	0.0141549	0.00134917	10.4915	3.30222×10-11

**Table 3-8. Yeast Strain MRG-8N Complete Response Parameters Data.  
AdjustedRSquared**

0.974457

**ANOVA Table**

	<b>DF</b>	<b>SS</b>	<b>MS</b>
<b>Model</b>	3	2.48598	0.828659
<b>Error</b>	28	0.0587085	0.00209673
<b>Uncorrected Total</b>	31	2.54469	
<b>Corrected Total</b>	30	0.853847	

**Parameter Confidence Interval Table,  $\alpha=0.05$**

	<b>Estimate</b>	<b>Standard Error</b>	<b>Confidence Interval</b>	
<b>RK</b>	0.928554	0.0461443	0.834031	1.02308
<b>C1C</b>	0.232111	0.0302732	0.170099	0.294122
<b>C1N</b>	0.0150399	0.00173464	0.0114866	0.0185931

**Parameter Table**

	<b>Estimate</b>	<b>Standard Error</b>	<b>t Statistic</b>	<b>P-Value</b>
<b>RK</b>	0.928554	0.0461443	20.1228	$3.45471 \times 10^{-18}$
<b>C1C</b>	0.232111	0.0302732	7.66721	$2.36768 \times 10^{-8}$
<b>C1N</b>	0.0150399	0.00173464	8.67033	$2.03323 \times 10^{-9}$

Table 3-9. **Results of Competitive Qualitative Outcomes.**

Two Replicates at Four Resource Competition Points for each of Four Strain Pairings

[C]: carbon resource concentration, g L<sup>-1</sup>; [N]: nitrogen resource concentration, g L<sup>-1</sup>; **Str Y**: competing strain Y; **Rrel Y**: predicted realized growth rate of Y, **Str Z**: competing strain Z; **Rrel Z**: predicted realized growth rate of Z; **ΔR**: difference of predicted realized growth rates, RrelY-RrelZ; **?Y**: visual assessment of growth on YPD plate; **?YN**: visual assessment of growth on YPD+nourseothricin plate; **1 Win**: winning strain per pair; **C Win**: consensus winning strain; **Pred**: predicted winning strain by ΔR; **Conf**: Confirmation “Y”, Weak Confirmation “W” or Contradiction “N” of Pred. Out of 16 competitive pairs our prediction was Confirmed 10 times, Weakly Confirmed 3 times and Contradicted 3 times.

[C]	[N]	Str Y	Rrel Y	Str Z	Rrel Z	ΔR	?Y	?YN	1 Win	C Win	Pred	Conf
0.2	0.01	2	0.363	2N	0.333	0.0299	++	<++	2	2	2	Y
0.2	0.01	2	0.363	2N	0.333	0.0299	++	<++	?2			
1.2	0.01	2	0.363	2N	0.333	0.0299	+	<+	2	2	2	Y
1.2	0.01	2	0.363	2N	0.333	0.0299	+	<+	?2			
0.2	0.1	2	0.407	2N	0.400	0.0073	++	++	2N	?	?2	W
0.2	0.1	2	0.407	2N	0.400	0.0073	++	<++	?2			
1.2	0.1	2	0.710	2N	0.713	-0.0028	++	<++	?	?	?	Y
1.2	0.1	2	0.710	2N	0.713	-0.0028	++	<++	?			
0.3	0.025	2	0.491	8N	0.524	-0.0333	++?	+?	?8N	8N	8N	Y
0.3	0.025	2	0.491	8N	0.524	-0.0333	++	++	8N			
1.2	0.025	2	0.549	8N	0.581	-0.0319	++	nil	2	?	8N	N
1.2	0.025	2	0.549	8N	0.581	-0.0319	+	<+	?8N			
0.3	0.1	2	0.491	8N	0.524	-0.0333	++	+	?8N	8N	8N	Y
0.3	0.1	2	0.491	8N	0.524	-0.0333	++	+	?8N			
1.2	0.1	2	0.710	8N	0.778	-0.0687	++	+	?8N	8N	8N	Y
1.2	0.1	2	0.710	8N	0.778	-0.0687	++	+	?8N			
0.3	0.025	8	0.521	2N	0.485	0.0362	<++	<+	?8	8	8	Y
0.3	0.025	8	0.521	2N	0.485	0.0362	++	+	?8			
1.2	0.025	8	0.571	2N	0.523	0.0485	+	<+	?8	8	8	Y
1.2	0.025	8	0.571	2N	0.523	0.0485	++	+	?8			
0.3	0.1	8	0.521	2N	0.485	0.0362	++	+	?8	8	8	Y
0.3	0.1	8	0.521	2N	0.485	0.0362	+	<+	?8			
1.2	0.1	8	0.759	2N	0.713	0.0467	++	<+	?8	8	8	Y
1.2		8	0.000	2N	0.000	0.0000	++	<+	?8			

[C]	[N]	Str Y	Rrel Y	Str Z	Rrel Z	$\Delta R$	?Y	?YN	1 Win	C Win	Pred	Conf
0.2	0.01	8	0.370	8N	0.372	-0.0014	+	triv	8	8	?	N
0.2	0.01	8	0.370	8N	0.372	-0.0014	++	triv	8			
1.2	0.01	8	0.370	8N	0.372	-0.0014	++	+	?	?8	?	W
1.2	0.01	8	0.370	8N	0.372	-0.0014	++	<+	8			
0.2	0.1	8	0.431	8N	0.430	0.0007	++	triv	8	8	?	N
0.2	0.1	8	0.431	8N	0.430	0.0007	++	triv	8			
1.2	0.1	8	0.759	8N	0.778	-0.0192	++	<++	8N	8N	?8N	W
1.2	0.1	8	0.759	8N	0.778	-0.0192	++	<++	8N			

Table 3-10. **Results of Competitive Quantitative Outcomes.**

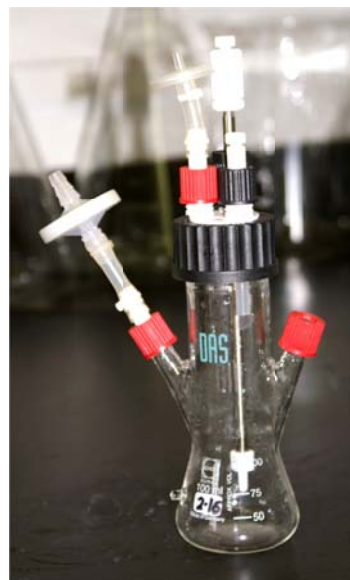
[C]: carbon resource concentration, g L<sup>-1</sup>; [N]: nitrogen resource concentration, g L<sup>-1</sup>; **Str Y**: competing strain Y; **Rrel Y**: predicted realized growth rate of Y; **Str Z**: competing strain Z; **Rrel Z**: predicted realized growth rate of Z; **Pred**: predicted winning strain by  $\Delta R$ ; **Win by Count**: winner by consensus of 8 pair-wise colony counts; **Diff**: mean pair-wise difference of 8 colony counts;  $\sigma^2$  **Diff**: standard deviation of difference; **CI 0.95**: P=0.95 confidence interval of Diff; **Diff + CI**: mean difference plus CI; **Diff - CI**: mean difference minus CI; **Win by CI**: winner or none by CI crossing 1. All four trials of eight replicates made correct predictions of dominance or not by both consensus of colony counts and computed confidence intervals.

[C]	[N]	Str Y	R <sub>rel</sub> Y	Str Z	R <sub>rel</sub> Z	$\Delta R$	Pred	Win by Count	Diff	$\sigma^2$ Diff	CI 0.95	Diff + CI	Diff - CI	Win by CI
1.2	0.08	2	0.710	8N	0.778	-0.0687	8N	8N	2.04	1.37	0.949	2.99	1.09	no cross, <b>8N</b>
1.2	0.08	8	0.759	2N	0.709	0.0507	8	8	0.693	0.190	0.132	0.825	0.561	no cross, <b>8</b>
0.7	0.08	2	0.642	2N	0.641	0.000693	?	?	0.845	0.483	0.334	1.18	0.511	cross, no win
0.2	0.01	8	0.370	8N	0.372	-0.00135	?	?	1.21	0.942	0.653	1.86	0.558	cross, no win

## Figures



(a)



(b)

Figure 3-1. **Chemostat.**

**Panel (a)** shows the complete system, open, without flasks; the flask base plate is drawn forward above the door; the feed and waste lines can be seen draped to the flask base plate; the air supply regulating manifold and flow meters can be seen with their yellow labels above the door opening; the feed (left) and waste (right) peristaltic pumps can be seen atop the cabinet. Feed and waste lines, from carboys and to disposal, are draped from the left and right sides of the cabinet.

**Panel (b)** shows a flask with closures for sterilization. The left-side arm is the air inlet with a 0.2 micron PTFE filter; the right-side arm is the sampling port with a PTFE-on-silicone septum; the headgear has a 0.2 micron filter on the air outlet, a screw connector for nutrient medium inlet with a silicone drip tube into the headspace, and a screw connector atop the waste siphon. The lower end of the waste siphon carries a 0.2 mm diam. orifice to maintain capillary closure when it is exposed to air. The penetration depth of the waste siphon is adjusted to maintain a working volume of  $50 \pm 2$  mL.

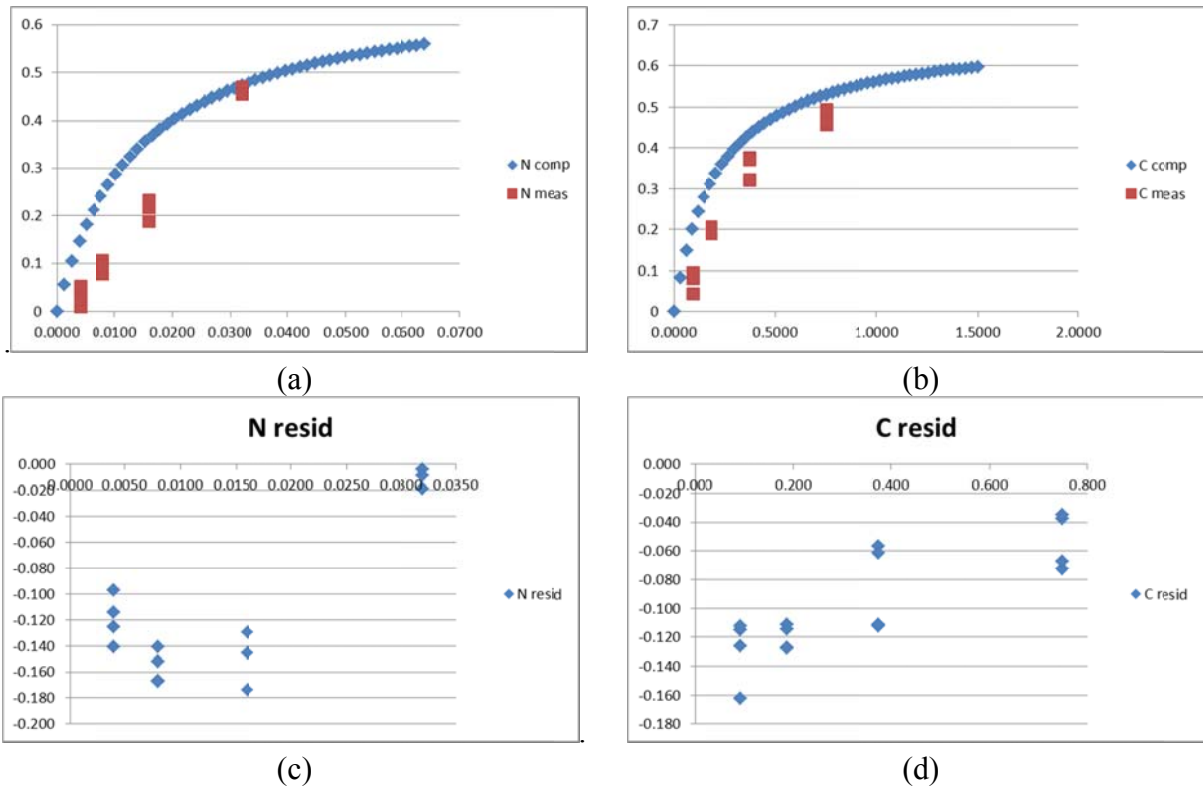


**Figure 3-2. Typical Yeast Strain Parameters Plot versus Characterization Data.** Characterization of Response Parameters for Typical Strain MRG-8. **Panel (a)**, Nitrogen response computed from fitted parameters (curve) and Characterization data points (scattered). **Panel (b)**, Carbon response computed from fitted parameters (curve) and Characterization data points (scattered). **Panel (c)**, Nitrogen response residuals at nitrogen supply values. **Panel (d)**, Carbon response residuals at carbon supply values. Goodness of fit values are given in Table 3-7. The Adjusted R-Squared for the three parameters,  $R_K$ ,  $C_{1C}$  and  $C_{1N}$ , is 0.982 as summarized in Table 3-3.

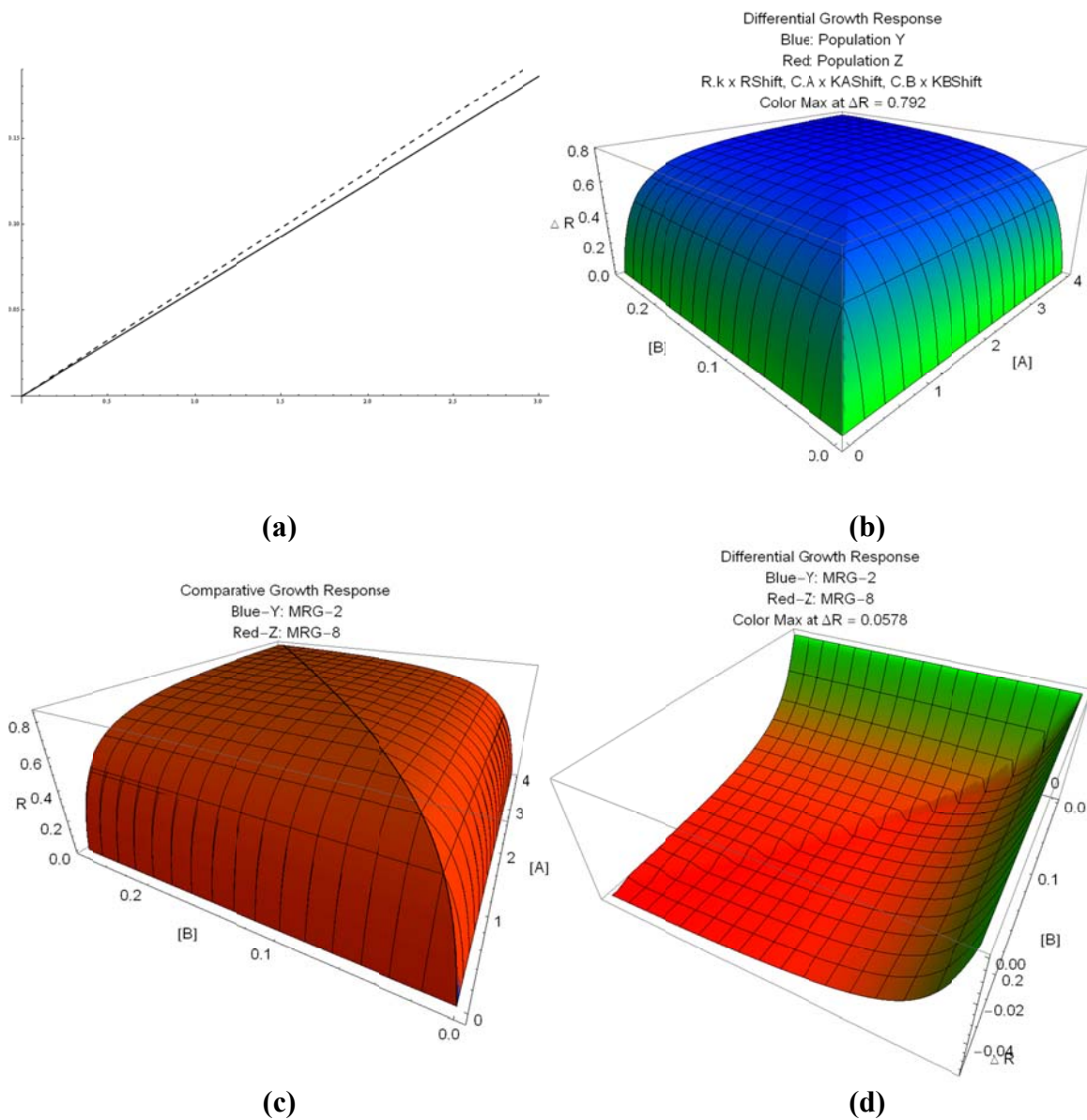


Figure 3-3. **Resource-Response Traits and Surface Plots.**

Using Trait Parameters of Experimental Strains MRG-2 and MRG-8

**Panel (a)**, Tilman OPLs (Optimum Proportion Lines) of MRG-2 (solid) and MRG-8 (dashed) (the slope of the OPL is also the dual-limiting C:N ratio), horizontal axis is carbon supply  $g L^{-1}$  and vertical axis is nitrogen supply  $g L^{-1}$ ; the OPL slopes are significantly different as shown in Table 3-4. **Panel (b)**, Response surface plot for MRG-2; **Panel (c)**, Dual-Plot Tents for MRG-2 (blue) hidden beneath MRG-8 (red); **Panel (d)**, Differential Growth Response Plot of MRG-2 (would shade to blue but generally overwhelmed) minus MRG-8 (shading to red). “Pure green” corresponds to zero difference in growth response.

## Chapter 4, Experimental Evidence that Microevolution Reshapes the Ecological Niche

### Summary

We applied our model, previously developed in Chapter 2 and tested in Chapter 3, to populations of *Saccharomyces cerevisiae* evolved from a single, isogenic, wild-type ancestor under complementary regimes of high and low carbon:nitrogen supply ratio. The evolving populations were grown under the complementary stress regimes for approx. 400 generations and then subjected to our Characterization Protocol, as used in Chapter 3. We found clear shifts as expected in descendants' growth response trait parameters for the low-supply resource in each regime and not-intuitively-expected shifts in other trait parameters including one counter-intuitive shift (compare to Adams *et al.* 1985, Zeyl 2005). We applied our predictive model to descendant *versus* ancestor and descendant *versus* descendant cases and found areas of predicted displacement, or not, robustly corresponding to what we expected from the shifted response trait parameters.

### Introduction

We have previously demonstrated in Chapter 2 that our predictive formulation of population growth response, across a Cartesian space of two resource supplies in the sense of a Hutchinsonian  $n$ -dimensional volume niche (1957) or a *resource niche* (Chase and Leibold 2003), is a valid three-dimensional extension from Tilman's *Graphical-Mechanistic Approach* (Tilman 1980). It successfully predicts growth responses of hypothetical populations (as an ecological phenomenon) from resource supply concentrations (as ecological environmental

phenomena) by organismal traits of per-resource growth response and maximum capable growth response. It is uniquely capable of detecting and quantifying intra-resource trade-offs of growth response within a single population or between competing populations and inter-resource tradeoffs between competing populations.

We further demonstrated in Chapter 3 that our formulation can successfully predict the expected outcome or uncertainty of competition between live populations in a shared environment of varying resource supplies.

The purpose of the present work, this chapter, is to predict the outcome of competition and investigate other effects between populations which have evolved, from a common ancestor, to adapt to complementarily severely restricted supplies (alias shifted resource ratios) of two essential resources. To achieve this objective we first seeded aliquots of an isogenic population of *Saccharomyces cerevisiae* to multiple parallel replicates of “low-carbon” and “low-nitrogen” nutrient resource supplies and grew them in constant-flow, chemostat mode to a point where they were expected to show distinct evolutionary adaptation to the two environments—while all resources except the “low” resource were in excess supply. We then applied our Characterization Protocol to determine the organismal traits of per-resource (C and N) growth response and the population-common organismal trait of maximum capable growth response for each population. We had no method to directly test the evolved strains against each other—they were indistinguishable by methods available to us—and the degree of change in trait parameters, particularly maximum capable growth response, precluded competition against either of our distinguishable, antibiotic-resistant isolates

## Methods

See also Appendix A, Mathematics

Our experimental ancestral population for this chapter was an isogenic strain of wild-type *Saccharomyces cerevisiae*, a unicellular yeast found widely in the natural and domesticated environment—drawn from the same source populations as in Chapter 3, see also Appendix B. For the purposes of our work, we considered an isogenic strain a population and although an oversimplification in some respects it enabled unambiguous identification of niche requirements, competitive outcomes and adaptive responses in the evolved populations.

For the work presented here we selected one of our wild-type, diploid isolates, referred to as MRG-2, (see Appendix B, Yeast Strains) as our ancestral population. Isolates master cultures were stored at  $-80\text{ }^{\circ}\text{C}$  with 1.7 mL of dense culture and 0.3 mL glycerol (15% v/v) in 2 mL Eppendorf tubes; as is standard practice for *S. cerevisiae*.

#### *Propagation of ancestral strain*

The MRG-2 isolate was sub-sampled from cryo-storage into standard media for culturing *S. cerevisiae*. Specifically, they were inoculated into YPD Broth (Y1375, Sigma-Aldrich, St. Louis, MO, USA), which at  $50\text{ g L}^{-1}$  comprises  $20\text{ g L}^{-1}$  bacteriological grade peptone,  $10\text{ g L}^{-1}$  yeast extract, and  $20\text{ g L}^{-1}$  glucose. They were then grown at  $30\text{ }^{\circ}\text{C}$  for 48 h in batch culture, prior to inoculation into the chemostats, where they could be grown continuously in log-phase under tightly-controlled resource supply rates.

Our chemostats (Figure 3-1, page 72) comprise “Multitron II” incubators (Infors HT, Bottmingen, CH) with DasGIP glassware (DasGIP AG, Jülich, DE) and “200 Series” pumps (Watson-Marlow, Wilmington, MA, USA). Each of the two chemostats maintained 16, 250 mL culture flasks concurrently at  $30\text{ }^{\circ}\text{C}$ , with gyratory agitation at 105 rpm and 25 mm throw,  $10.7\text{ mL h}^{-1}$  feed rate,  $50\pm 2\text{ mL}$  working culture volumes, and 4.69 h ( $0.213\text{ h}^{-1}$ ) culture turnover times. Each flask had separate nutrient medium supply, waste removal, and air supply. Waste

removal was siphoned at 3 times the rate of media supply, ensuring that culture volumes were maintained at 50 mL and that there was no back-flow of waste. Air supply was regulated to 0.5 L min<sup>-1</sup> and dried, de-oiled by expansion and carbon block adsorption, and filtered to 0.2 µm. The outlet filter on each flask maintained a positive pressure (≈0.1 ATM) within each flask, further preventing microbial contamination of the cultures.

Chemostat culture flasks were inoculated from the starter cultures and *S. cerevisiae* populations were grown overnight in batch culture conditions, with non-limiting nutrients. The medium (CYN5501 YNB w/o AA, w/o Ammonium phosphate, w/o Potassium Dihydrogen Phosphate and w/o Inositol; ForMedium Ltd, Norwich, UK) for these overnight cultures included 10 g L<sup>-1</sup> D-glucose monohydrate C<sub>6</sub>H<sub>12</sub>O<sub>6</sub>•H<sub>2</sub>O (49159; Sigma-Aldrich, St. Louis, MO, USA), 5 g L<sup>-1</sup> anhydrous (NH<sub>4</sub>)<sub>2</sub>SO<sub>4</sub> (A4418; Sigma-Aldrich, St. Louis, MO, USA), and 1 g L<sup>-1</sup> anhydrous KH<sub>2</sub>PO<sub>4</sub> (P9791; Sigma-Aldrich, St. Louis, MO, USA). This gave concentrations for C, N and P of 4.00 g L<sup>-1</sup> C, 1.06 g L<sup>-1</sup> N, 0.228 g L<sup>-1</sup> P and media was adjusted to pH 6.0±0.1 using NaOH. We established in preliminary experiments and development of our Characterization Protocol that culture densities in the chemostat with this media were equivalent at the stated and double concentrations of C, N and P, confirming the formulation was not growth-limiting. To invoke resource limitation we then fed the chemostat cultures with the same base medium and phosphorus but with reduced concentration of C or N.

### *Evolution environment*

The reference, “rich” formulation of our experimental culture medium provided 3.20 g L<sup>-1</sup> carbon, 1.00 g L<sup>-1</sup> nitrogen, 0.200 g L<sup>-1</sup> phosphorus and the manufacturer’s recommended concentration of “YNB” base. The phosphorus and base concentrations were held at these levels for the entire evolution process. These “rich” levels of carbon and nitrogen supply were shown

by earlier testing to be non-interfering with differential limitation of our experimental isolates. The carbon supply concentration of  $3.20 \text{ g L}^{-1}$  was also low enough that it would not drive the experimental populations into fermentative, anaerobic respiration which is generally considered to occur spontaneously at carbon concentrations in excess of  $8 \text{ g L}^{-1}$ .

The “low C” evolution medium provided  $0.0550 \text{ g L}^{-1}$  C and  $0.0470 \text{ g L}^{-1}$  N, a C:N ratio of 1.17. The “low N” medium provided  $1.80 \text{ g L}^{-1}$  C and  $0.00290 \text{ g L}^{-1}$  N, a C:N ratio of 621. The dual-limiting or “optimum” C:N ratio for the MRG-2 isolate, as determined in the work for Chapter 3, was 16.1. The C:N ratio in the “low N” environment was thus 38.5 times optimum and in the “low C” environment it was 0.076 or 1/13.8 times optimum. The ratio of the C:N ratios was 530 or 1/0.00189.

The carbon supply,  $1.80 \text{ g L}^{-1}$ , to the “Low N” environment would have been limiting with unlimited nitrogen and the nitrogen supply,  $0.0470 \text{ g L}^{-1}$ , to the “Low C” environment would have been limiting with unlimited carbon.

We ran sixteen chemostat cultures, eight “low N” or “high C:N” and eight “low C” or “low C:N” for 79 days, 404 generations at  $4.69 \text{ h}$  ( $0.213 \text{ h}^{-1}$ ) turnover. Culture samples were aseptically extracted at several checkpoints and held in our standard cryo-storage regime. When we encountered culture contamination problems at three points in the 79 day process we were able to replace-restart the contaminated cultures with saved cryo-samples. Because of culture time lost in these restarts, not all sixteen cultures ran the full 79 days. We had final evolved cultures ranging in age from 48 to 79 days, 246 to 404 generations.

While time did not permit testing every checkpoint culture for contamination as it was saved, the cultures used for restart and all of the terminal cultures were tested. We used a simple controlled process of plating our cultures of interest and four obviously, and apparently

differently, contaminated cultures saved for the purpose. Each culture was plated on standard YPD Broth (Y1375, Sigma-Aldrich, St. Louis, MO, USA) in agar medium and on a 50-50 mix of the same YPD and Mueller Hinton Broth (70192, Sigma-Aldrich, St. Louis, MO, USA) in agar medium, the latter being both known and observed to provide sensitive detection of “non-fastidious” yeasts and bacteria. Cultures whose plates of both media showed *cerevisiae*-typical growth, and nothing else, after 48 h incubation at 30 °C were considered to be uncontaminated and usable.

At the end of the evolution runs, we had eight “low N” cultures, of 56 and 67 days, 287 and 343 generations. We had eight “low C” cultures, of 48 and 79 days, 246 and 404 generations. We checked the density of each terminal culture and selected the two that showed the highest density in its evolutionary stress medium for Characterization and comparison with our growth response model. These were Desc-01 “low N” and Desc-13 “low C”.

We subjected each of the selected terminal cultures, Desc-01 and Desc-13, to our Characterization Protocol as we had previously done with the ancestor MRG-2. (See Chapter 3.)

We then applied our growth response differential analysis to the three characterized cultures, MRG-2 “Ancestor”, Desc-01 “Low N, High C:N Descendant” and Desc-13 “Low C, Low C:N Descendant”, looking for any evidence of nutrient response “tradeoff” or other change of organismal response traits.

## Results

### *Trait Parameters Comparison*

Growth response parameters for the ancestor and descendants are shown in Table 4-1 and the OPLs (Optimum Proportion Lines) of the three populations are plotted in Figure 4-1.

At this point, even before we look at the competition-prediction plots, there are several interesting changes to notice comparing each evolved population to the common ancestor:

- Both evolved populations increased their maximum capable growth response trait parameter,  $R_K$ , in addition to changing their per-resource responses.
- The Low-C evolved population improved (reduced) its half-saturation carbon response trait parameter,  $C_{IC}$ , and degraded (increased) its half-saturation nitrogen response trait parameter,  $C_{IN}$ . These two shifts combined to give a reduced optimum C:N ratio. Together, the “opposite” changes of  $C_{IC}$  and  $C_{IN}$  may be superficially intuitive as a “resource response trade-off” for “adaptation to low carbon”.
- The Low-N evolved population improved (reduced) its half-saturation nitrogen response trait parameter,  $C_{IN}$ , and also improved (reduced) its half-saturation carbon response trait parameter,  $C_{IC}$ . These two shifts combined to give a reduced optimum C:N ratio. The improved nitrogen response is superficially intuitive for “adaptation to low nitrogen” but the improved carbon response and the reduced optimum C:N ratio are definitely not.

The occurrence of increased  $R_K$  in both of our evolved strains raises the possibility that it is a “domestication” effect related to the experimental environment. In the evolutionary environments, low C and low N, with all other resources in excess supply it is difficult to propose that this change is a response to anything other than the temperature (30 °C), the continuously aerobic environment (forced air flow) or possibly pH (held at 6.0 ±0.1). Certainly, something like a transposition or epigenomic change that had been held at bay in the wild environment may have occurred in our environment. This situation could be investigated by putting all sixteen of our evolved strains through the Characterization Protocol to look for an equivalent increase of  $R_K$  in some or all of them. It could also be tested by growing a number of

replicates of the ancestral, MRG-2, strain in our environment and rich base medium, without the C and N limitations, for several hundred generations to determine whether it appears separate from the low C- and low N-related mutations.

Further, comparing the evolved descendants to each other, we also find:

- The Low-N descendant improved (reduced) its half-saturation carbon response trait parameter slightly more than did the Low-C descendant, a definitely non-intuitive result.
- The Low-N descendant does have a higher optimum C:N ratio than the low-C descendant, as intuitively expected, but being lower than the ancestor's optimum C:N ratio it is intuitively inexplicable.

Table 4-2 shows all of the trait parameters,  $R_K$ ,  $C_{IC}$ ,  $C_{IN}$ , that we measured and the optimum C:N ratio computed from the parameters, for Ancestor and Descendants with 95% confidence intervals. Full statistics from the curve-fitting program are shown in Table 4-3 through Table 4-5. It is interesting to compare the “no significant difference” inference, except for C:N ratio, to the expected results of competition shown in Figure 4-1 through Figure 4-4 and the Results section of Chapter 3. What we infer here (as discussed in Chapter 3, Results) is validation of a point long argued that “Statistical significance does not show ecological significance—and vice-versa.”

As a specific model for microbial evolution *in vitro*, these changes are strong indication that something non-intuitive, even counter-intuitive, is occurring genetically to set the new response trait parameters. These results are comparable to those in Zeyl (2004) or Adams *et al.* (1985) although that work did not follow through to an equivalent of our complete Characterization Protocol.

As a simulation model for general “polygenic species” evolution or selection *in natura*, these changes indicate that unexpected trait parameter changes, and underlying genetic effects, can be expected in genetically “narrow” populations (*e.g.* Barrett and Bell 2006) and that unexpected sub-population selection can be expected in genetically “broad” populations (see especially Clark *et al.* 2007, Clark 2010)—such as the population that would be formed simply by mixing several of the Goddard laboratory strains (see Appendix B, Yeast Strains) from which we selected our experimental populations.

Because our evolution runs were “sex free” (*i.e.*, the populations were kept, so far as we can tell, out of sexual-reproduction mode) we cannot say with certainty what would have happened if genetic recombination had occurred along with our measured response trait changes. It is accepted as safe to say that “the outcome might have been different” but any specific assertion is only speculative. What would be informative, procedurally straightforward, but very time-consuming would be to take each of our terminal populations, mix them with each other or the ancestor, drive them through a sexual-reproduction cycle to permit back-cross and recombination, then separate and characterize the resulting genetically recombined populations (compare to Paquin and Adams 1983a, Travisano *et al.* 1995, Gerrish and Lenski 1998). The result of this Characterization, comparison and prediction would be particularly interesting in comparison to Zeyl (2005) who back-crossed *S. cerevisiae* examining mutation number and size but not particularly looking at competitive ability of the crosses and definitely not looking at resource-response traits in our sense.

Results of the Characterization runs, curve-fitted growth-response parameters, for our three comparable strains are shown in Table 4-1.

Based on the curve-fitted growth-response parameters, Figure 4-2 through Figure 4-4 show selected plots of the modeled relative growth response of Ancestor *versus* High C:N Descendant; Ancestor *versus* Low C:N Descendant; and High *versus* Low C:N Descendants.

### *Response Plot Comparisons*

Following Characterization of the Desc-01 (Low N) and Desc-13 (Low C) evolved strains, and using the Characterization of the MRG-2 (ancestor) from Chapter 3, we ran our relative-growth plot *Mathematica*® (Wolfram Research 2008) program to compare predicted growth responses strain pairings across a Hutchinsonian-requirements resource space. We used all three possible pairings of the strains (MRG-2 *versus* Desc-01, MRG-2 *versus* Desc-13, and Desc-01 *versus* Desc-13). We do not show all possible plot forms from our program for each pairing but only those which we believe provide the most interesting or obvious indications.

Figure 4-2 and Figure 4-3 compare MRG-2 to the two evolved populations, Desc-01 and Desc-13 respectively. In both comparisons the increase in the maximum capable growth response trait  $R_K$  generally overrides the changes in the per-resource response trait parameters  $C_{IC}$  and  $C_{IN}$ . The Low-C descendant, D-13, does show, however, a broader area of potential coexistence, subject to stochastic effects, at low nitrogen concentrations. The maximum growth response advantage shown is 0.0516 for Desc-01 and 0.0500 for Desc-13, throughout the plotted niche range of 0 to 3.0 G L<sup>-1</sup> carbon and 0 to 0.2 g L<sup>-1</sup> nitrogen.

Figure 4-4 compares the two descendant populations, Desc-01 Low-N to Desc-13 Low-C. The dual surface plot shows the generally lower dome tent of Desc-13 penetrating (and dominating) Desc-01 in a patch “left of” the OPL ridge as the plot is viewed. Note, however that the maximum difference in realized growth response,  $R$ , is only 0.0113 throughout the plotted range—highly subject to stochastic effects in any shared environment.

### *Phenomenological Pleiotropy*

The term *pleiotropy*, properly used, applies to the field of genetics and simply means that one gene (or locus) affects more than one phenotypic trait. Most often the base term is used to mean *antagonistic pleiotropy*, where one trait is “improved” while another is “degraded”. The complement of antagonistic pleiotropy then is *synergistic pleiotropy*, where two traits are “improved”. There is a problem, however, with the idea of “improved” or “degraded” because both refer to selection in a particular environment, usually the “present” or “principal experimental” environment—ignoring that a change in the current or experimental environment can completely reverse selection for “improved” *versus* “degraded”. We will use the term *pleiotropy* in the simple sense of two trait changes from apparently one genetic event.

Since our work here did not attempt to look at specific genetic effects by genes or even by recognized loci, we prefer to use the term *phenomenological pleiotropy* for two (or more) identifiable, quantifiable trait changes which appear to have occurred at the same time. We do not attempt to distinguish among genes, loci and epigenetic phenomena nor among such things as dual effects from a single source, concurrent effects by linkage etc.

The Desc-13, low-C evolved, population showed (see Table 4-1 and Table 4-2) an increase in its nitrogen half-saturation response trait parameter,  $C_{IN}$ . Since an increase in either  $C_I$  response trait would decrease the realized growth rate,  $R$ , it would not pass competitive selection. It appears, therefore, that the increase, “degradation”, in  $C_{IN}$  must have been in the same evolutionary step as “improvement” in at least one other trait parameter—which satisfies a *phenomenological* definition of *pleiotropy*, cf. (MacLean et al. 2004, Dudley et al. 2005, Cooper et al. 2007), Table 4-6 shows the several possible sequences of trait parameters evolutionary

change which could have coupled the increase in  $C_{IN}$  with an offsetting change in one of the other trait parameters. We make the usual parsimony assumption of minimum required steps.

## Discussion

Our primary purpose in this work was to apply our model—for which we can find no strong equivalent in the literature—of population competition on two resources to new populations evolved under complementary elevated and depressed C:N resource ratios to determine the outcome of two proposed ecological scenarios: 1) the evolved population occupies less than the range of the ancestor and, through some ecological or geophysical mechanism comes into competition with the ancestor in an arbitrary resource supply regime—not necessarily either the “original” or “forcing” regime; or 2) two evolved sub-populations come into competition with each other in an arbitrary resource supply regime.

We saw in our work for Chapter 3 that supposedly minor interventions of a genome can produce phenotypic changes that are competitively significant and involve multiple growth-response traits—in terms of expected displacement or coexistence a change in realized growth rate of as little as  $\pm 0.02$ , operating over generations, can change the ecological outcome. The particular changes we saw in this work were more complex than what we saw before, typical of Zeyl (2005) contrasting Zeyl (2004) for our wild type strains. We would suspect, without having opportunity to characterize their step-wise cultures, that the serial-evolution experiments of Adams *et al.* (1985) showed apparent “reduced fitness” of successors because of genetic covariance operating on response to other than the one resource that was in deliberate low supply (see also Travisano *et al.* 1995, Cooper *et al.* 2003).

As a case of a trait change being intuitively unexpected and ecologically potentially catastrophic for an evolved population we need only note the cryptic, antagonistic

*phenomenological pleiotropy* that occurred in Descendant 13 when an increase in its half-saturation nitrogen response trait parameter, a decrease in its realized growth response to nitrogen, “hitch-hiked” on either an increase in its maximum capable growth response trait or a decrease in its half-saturation carbon response trait. This nitrogen response trait change was not under selection in the low-carbon evolutionary environment but could have severe and entirely unexpected counter-selective impact in another resource supply regime.

In a sexually reproducing population with recombination etc. the adaptive and maladaptive elements of our pleiotropic covariance might have been either linked or independent. If the two elements were linked then the net advantage of the pair might have carried the maladaptive element through succeeding generations. If the two elements were not linked then the maladaptive element would be expected to fail selection and disappear from the population. The general case of linkage includes at least three possible syndromes: close positioning of independent genes between high-probability chromosomal crossover points; positioning of independent genes within a single transposable element; and the possibility that it was just one gene that engendered the two measurable effects.

Our model, either the graphical-predictive component taken alone as for simulation of hypothetical evolutionary changes or the graphical-predictive and Characterization Protocol components taken together in an empirical environment, *in vitro* or *in natura*, is a new, unique extension of the family of Tilman-like approaches. We have a simplified formulation of the graphical-predictive core which fully incorporates asymptotic, saturating, non-linear growth response trait parameters. We have a graphical technique which applies the trait parameters and resource supply range to robustly predict growth response relationships across an entire Hutchinsonian  $n$ -dimensional space (1957) of resource supply, for a population’s *requirements*

*niche* as Chase and Leibold (2003) would call it. And we have a Characterization Protocol which can readily obtain response parameter traits from observed phenomena of resource supply and realized growth.

Our model could readily be extended to deal with response to substitutable resources, with differing responses to the same elemental resource from different source substances.

Our model could also be extended to deal with three resources such as the “big three” C:N:P. The Characterization Protocol which determines response trait parameters for one resource at a time could easily be applied in this case and Our *Mathematica*® curve-fitting program could be extended to three resources. The predictive-graphical, plot-display component would need to be modified to deal with the three pair-wise resource interactions or could be made to generate shaded-filled three-dimensional displays similar to our shaded-plane displays.

Other future work might be to sample an evolutionary sequence at finer intervals than we used for backstop purposes and determine more precisely when, in what sequence, the various selectively favorable mutations occurred and when, in what pairings, the phenomenological pleiotropic changes occurred. And a finer-grained genetic analysis of evolved populations with particular trait changes, by expression analysis or gene-reading, might shed good light on more or less commonly involved loci and modes of change.

As in the Discussion of Chapter 3, we would again propose an extended case for application of our model in investigating the interaction of inter- *versus* intra-population competition (as in Clark 2010), in a theoretical framework or even *in vitro* with polygenic populations and quantitative-differential genetic analysis of the survivors.

## Tables

Table 4-1. **Yeast Strains Growth Response Parameters Summary.**

**Population:** population/ strain/ isolate name; **R<sub>K</sub>:** maximum capable intrinsic growth rate; **C<sub>1C</sub>:** carbon half-saturation constant; **C<sub>1N</sub>:** nitrogen half- saturation constant; **C:N:** ratio of half-saturation constants, alias dual-limiting ratio, slope of Tilman's OPL (Optimum Proportion Line); **!R<sup>2</sup>:** Adjusted R<sup>2</sup> (correlation) of R<sub>K</sub>, C<sub>1C</sub> and C<sub>1N</sub>; **SE XX:** standard error of R<sub>K</sub>, C<sub>1C</sub> or C<sub>1N</sub>; **Msd C:N:** Monte Carlo standard deviation of C:N.

<b>Population</b>	<b>R<sub>K</sub></b>	<b>SE</b>	<b>C<sub>1C</sub></b>	<b>SE</b>	<b>C<sub>1N</sub></b>	<b>SE</b>	<b>C:N</b>	<b>stdev</b>	<b>!R<sup>2</sup></b>
<b>MRG-2</b>	0.834	0.0544	0.210	0.0379	0.0130	0.00214	16.15	4.27	0.946
<b>Desc-01</b>	0.868	0.0399	0.181	0.0238	0.0125	0.00146	14.48	2.65	0.976
<b>Desc-13</b>	0.871	0.0428	0.184	0.0262	0.0133	0.00168	13.83	2.76	0.971

Table 4-2. **Yeast Strains Growth Response Parameters Comparison.**

**Population:** population/ strain/ isolate name; **R<sub>K</sub>:** maximum capable intrinsic growth rate; **C<sub>1C</sub>:** carbon half-saturation constant; **C<sub>1N</sub>:** nitrogen half-saturation constant; **C:N:** ratio of half-saturation constants, alias dual-limiting ratio, slope of Tilman's OPL (Optimum Proportion Line); **Lo XX & Hi XX:** high and low values of R<sub>K</sub>, C<sub>1C</sub> and C<sub>1N</sub> 95% confidence interval; **MLo C:N & MLo C:N:** high and low values of C:N Monte Carlo 95% confidence interval. The table is arranged to place the tested pairs in adjacent rows. The shaded cells call out comparisons which are significantly different by 95% confidence intervals. Note that all three of the C:N ratio pairs show significant difference although none of the response parameter pairs do so.

<b>Population</b>	<b>R<sub>K</sub></b>	<b>Lo R<sub>K</sub></b>	<b>Hi R<sub>K</sub></b>	<b>C<sub>1C</sub></b>	<b>Lo C<sub>1C</sub></b>	<b>Hi C<sub>1C</sub></b>	<b>C<sub>1N</sub></b>	<b>Lo C<sub>1N</sub></b>	<b>Hi C<sub>1N</sub></b>	<b>C:N</b>	<b>MLo C:N</b>	<b>MHi C:N</b>
<b>MRG-2</b>	0.834	0.722	0.945	0.210	0.133	0.288	0.0130	0.00865	0.0174	16.15	15.89	16.42
<b>Desc-01</b>	0.868	0.787	0.950	0.181	0.132	0.230	0.0125	0.00951	0.0155	14.48	14.31	14.65
<b>MRG-2</b>	0.834	0.722	0.945	0.210	0.133	0.288	0.0130	0.00865	0.0174	16.15	15.89	16.42
<b>Desc-13</b>	0.871	0.784	0.959	0.184	0.131	0.238	0.0133	0.00981	0.0167	13.83	13.66	14.01
<b>Desc-01</b>	0.868	0.787	0.950	0.181	0.132	0.230	0.0125	0.00951	0.0155	14.48	14.31	14.65
<b>Desc-13</b>	0.871	0.784	0.959	0.184	0.131	0.238	0.0133	0.00981	0.0167	13.83	13.66	14.01

**Table 4-3. Yeast Strain MRG-2 (Ancestor) Complete Response Parameters Data. AdjustedRSquared**

0.946367

**ANOVA Table**

	<b>DF</b>	<b>SS</b>	<b>MS</b>
<b>Model</b>	3	2.03212	0.677373
<b>Error</b>	28	0.103453	0.00369475
<b>Uncorrected Total</b>	31	2.13557	
<b>Corrected Total</b>	30	0.751379	

**Parameter Confidence Interval Table,  $\alpha=0.05$**

	<b>Estimate</b>	<b>Standard Error</b>	<b>Confidence Interval</b>	
<b>RK</b>	0.833635	0.0544411	0.722117	0.945152
<b>C1C</b>	0.210322	0.0379248	0.132637	0.288008
<b>C1N</b>	0.0130414	0.00214042	0.00865691	0.0174258

**Parameter Table**

	<b>Estimate</b>	<b>Standard Error</b>	<b>t Statistic</b>	<b>P-Value</b>
<b>RK</b>	0.833635	0.0544411	15.3126	3.89246×10-15
<b>C1C</b>	0.210322	0.0379248	5.54577	6.25477×10-6
<b>C1N</b>	0.0130414	0.00214042	6.0929	1.42587×10-6

**Table 4-4. Yeast Strain Descendant-01 Complete Response Parameters Data.  
AdjustedRSquared**

0.976033

**ANOVATable**

	<b>DF</b>	<b>SS</b>	<b>MS</b>
<b>Model</b>	3	2.65693	0.885643
<b>Error</b>	29	0.0589894	0.00203412
<b>Uncorrected Total</b>	32	2.71592	
<b>Corrected Total</b>	31	0.762527	

**ParameterConfidenceIntervalTable,  $\alpha=0.05$**

	<b>Estimate</b>	<b>Standard Error</b>	<b>Confidence Interval</b>	
<b>RK</b>	0.86837	0.0398899	0.786786	0.949954
<b>C1C</b>	0.181011	0.0237608	0.132415	0.229607
<b>C1N</b>	0.0125035	0.00146227	0.0095128	0.0154942

**ParameterTable**

	<b>Estimate</b>	<b>Standard Error</b>	<b>t Statistic</b>	<b>P-Value</b>
<b>RK</b>	0.86837	0.0398899	21.7692	1.63065×10-19
<b>C1C</b>	0.181011	0.0237608	7.61805	2.12556×10-8
<b>C1N</b>	0.0125035	0.00146227	8.55073	2.02821×10-9

**Table 4-5. Yeast Strain Descendant-13 Complete Response Parameters Data.  
AdjustedRSquared**

0.971345

**ANOVA Table**

	<b>DF</b>	<b>SS</b>	<b>MS</b>
<b>Model</b>	3	2.65681	0.885602
<b>Error</b>	28	0.0705916	0.00252113
<b>Uncorrected Total</b>	31	2.7274	
<b>Corrected Total</b>	30	0.735571	

**Parameter Confidence Interval Table,  $\alpha=0.05$**

	<b>Estimate</b>	<b>Standard Error</b>	<b>Confidence Interval</b>	
<b>RK</b>	0.871355	0.0427877	0.783708	0.959001
<b>C1C</b>	0.184406	0.0262283	0.13068	0.238133
<b>C1N</b>	0.0132597	0.00168252	0.00981317	0.0167061

**Parameter Table**

	<b>Estimate</b>	<b>Standard Error</b>	<b>t Statistic</b>	<b>P-Value</b>
<b>RK</b>	0.871355	0.0427877	20.3646	$2.52428 \times 10^{-18}$
<b>C1C</b>	0.184406	0.0262283	7.03081	$1.20052 \times 10^{-7}$
<b>C1N</b>	0.0132597	0.00168252	7.88083	$1.38847 \times 10^{-8}$

Table 4-6. **Phenomenological Pleiotropy for Descendant-13.**

Possible Sequences Involving Cryptic Antagonistic Pleiotropy

$R_K$ ,  $C_{1C}$ ,  $C_{1N}$  and  $R$  are the usual Monod symbols. Shaded cells indicate possible pairings of  $C_{1N}$  with another parameter in a possible (cryptic antagonistic) pleiotropic step. Evolutionary selection is based on  $R$  (computed as in the low-C evolution medium where the strain evolved) which must always increase. A step with no increase in  $R$  would not pass selection. A step where  $C_{1N}$  alone increased would cause a decrease in  $R$  and so would not pass selection.  $C_{1N}$  must have increased at the same time some other trait parameter(s) changed to provide, together, an increase in  $R$ . Our parsimony assumption is that the number of steps is the minimum required for the total observed change.

$R_K$	$C_{1C}$	$C_{1N}$	$R$
0.834	0.210	0.0130	0.173
0.871	0.210	0.0130	0.181
0.871	0.184	0.0133	0.200
0.834	0.210	0.0130	0.173
0.871	0.210	0.0133	0.181
0.871	0.184	0.0133	0.200
0.834	0.210	0.0130	0.173
0.834	0.184	0.0130	0.192
0.871	0.184	0.0133	0.200
0.834	0.210	0.0130	0.173
0.834	0.184	0.0133	0.192
0.871	0.184	0.0133	0.200

## Figures

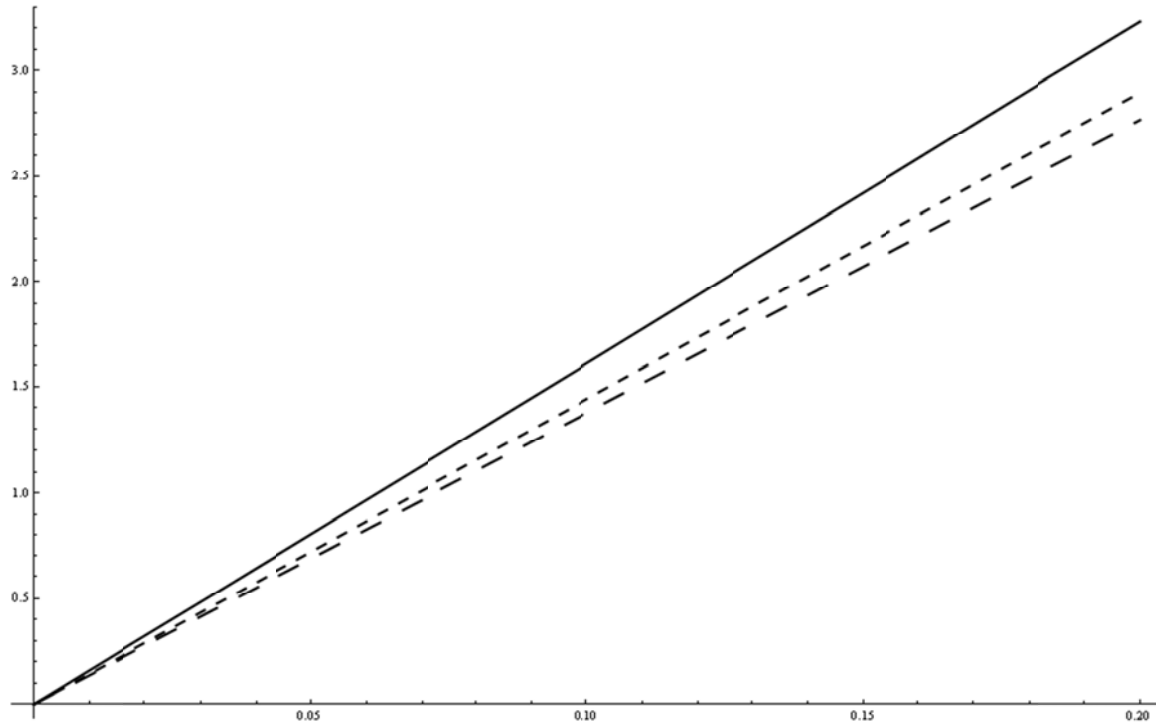


Figure 4-1. **OPLs for Ancestor and Descendant Populations.**

**Solid line**, ancestor MRG-2; **Long-dash line**, low-C evolved Descendant-13; **Short-dash line**, low-N evolved Descendant-01; Nitrogen concentration 0 to 0.20 mg L<sup>-1</sup>; Carbon concentration 0 to 3.3 mg L<sup>-1</sup>. The naïve expectation for the shift of Desc-13's OPL (long dashes) would be "downward", as it did move, indicating its ability to achieve *its* maximum growth response with less carbon, a lower optimum C:N ratio. This plot, however, says nothing about what Desc-13's maximum capable growth response *is*. The naïve expectation for the shift of Desc-01's OPL (short dashes) would be "upward", contrary to what it actually did, expecting the ability to achieve maximum growth with less nitrogen, a higher optimum C:N ratio. Desc-01, however, increased its maximum capable growth response,  $R_K$ , to the extent that it displaced the ancestor MRG-2 strain in the nitrogen-limited evolutionary environment regardless of how its OPL shifted. All three of the lines are significantly different as shown in Table 4-2.

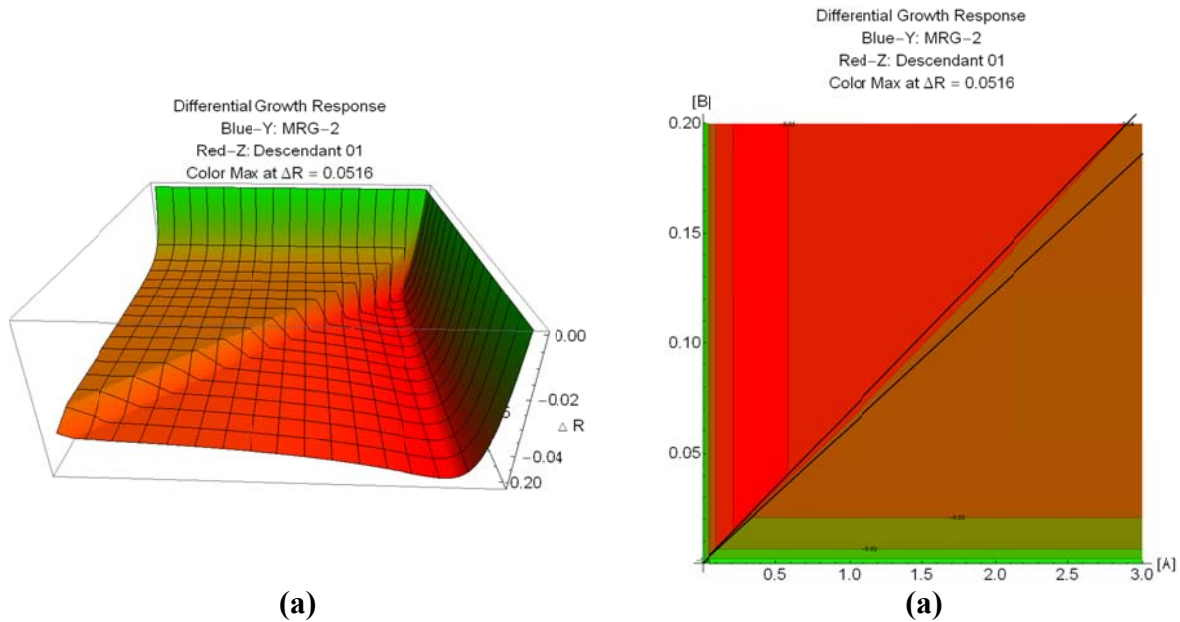


Figure 4-2. **Differential growth Response, MRG-2 versus Desc-01.**

Differential, Relative Growth Response of Strains MRG-2 (blue) *versus* Desc-01 (red)

**Panel (a)** is our Differential Surface Plot showing the relative growth responses of the two populations across the C:N resource space. There is no area where the ancestor dominates the descendant. Also note that, unlike some of our other example plots, there is virtually no area where dominance would be likely subject to stochastic effects—the differential response moves very rapidly to its maximum value of 0.0516, and remains greater than the stochastic-susceptible boundary value of 0.02 out to carbon supply level that would be expected to cause fermentative, anaerobic respiration and out to nitrogen supply level that would, carbon supply permitting, drive both populations to their maximum capable growth at which the descendant would remain clearly dominant (plots to these extreme ranges are not shown). **Panel (b)** is our Differential Shaded-Contour Plot, showing constant-difference isoclines, the contour lines, from which quantitative values of  $\Delta R$  can be read.

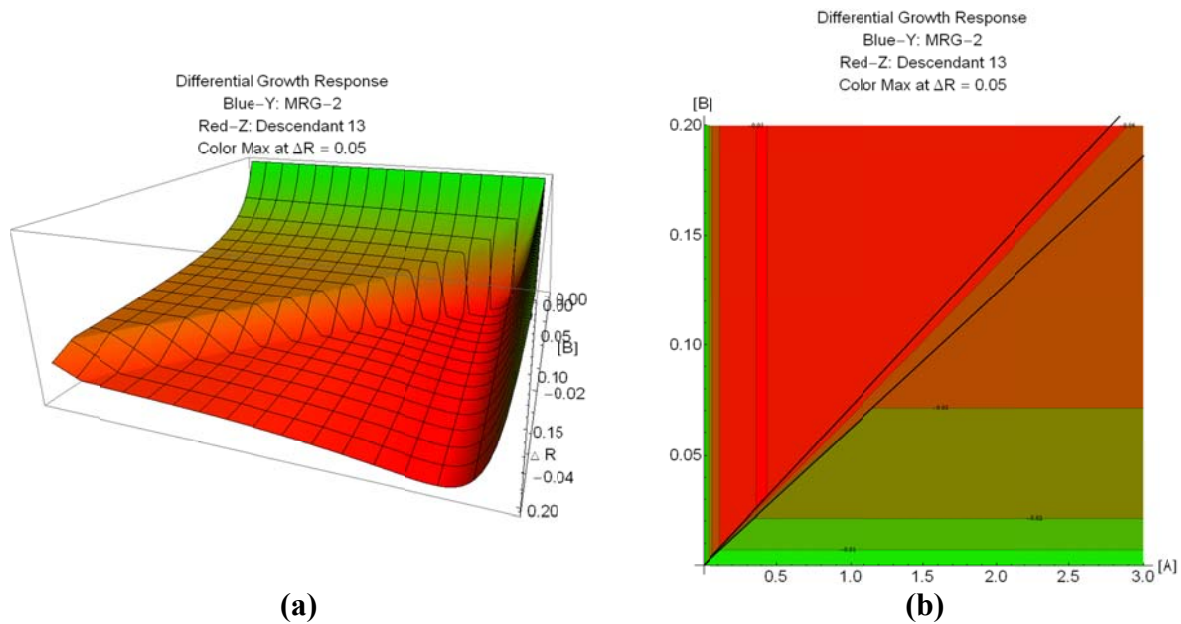


Figure 4-3. **Differential Growth Response, MRG-2 versus Desc-13.**

Differential, Relative Growth Response of Strains MRG-2 (blue) *versus* Desc-13 (red)

**Panel (a)** is our Differential Surface Plot showing the relative growth responses of the two populations across the C:N resource space. There is no area where the ancestor clearly dominates the descendant but there is an area where dominance would be likely subject to stochastic effects—the differential response in the range of  $0.07 \text{ mg L}^{-1}$  nitrogen or less is below the stochastic-susceptible boundary value of 0.02 out to a carbon supply level that would be expected to cause fermentative, anaerobic respiration. **Panel (b)** is our Differential Shaded-Contour Plot equivalent to Panel (a), showing constant-difference isoclines, the contour lines, from which quantitative values of  $\Delta R$  can be read.

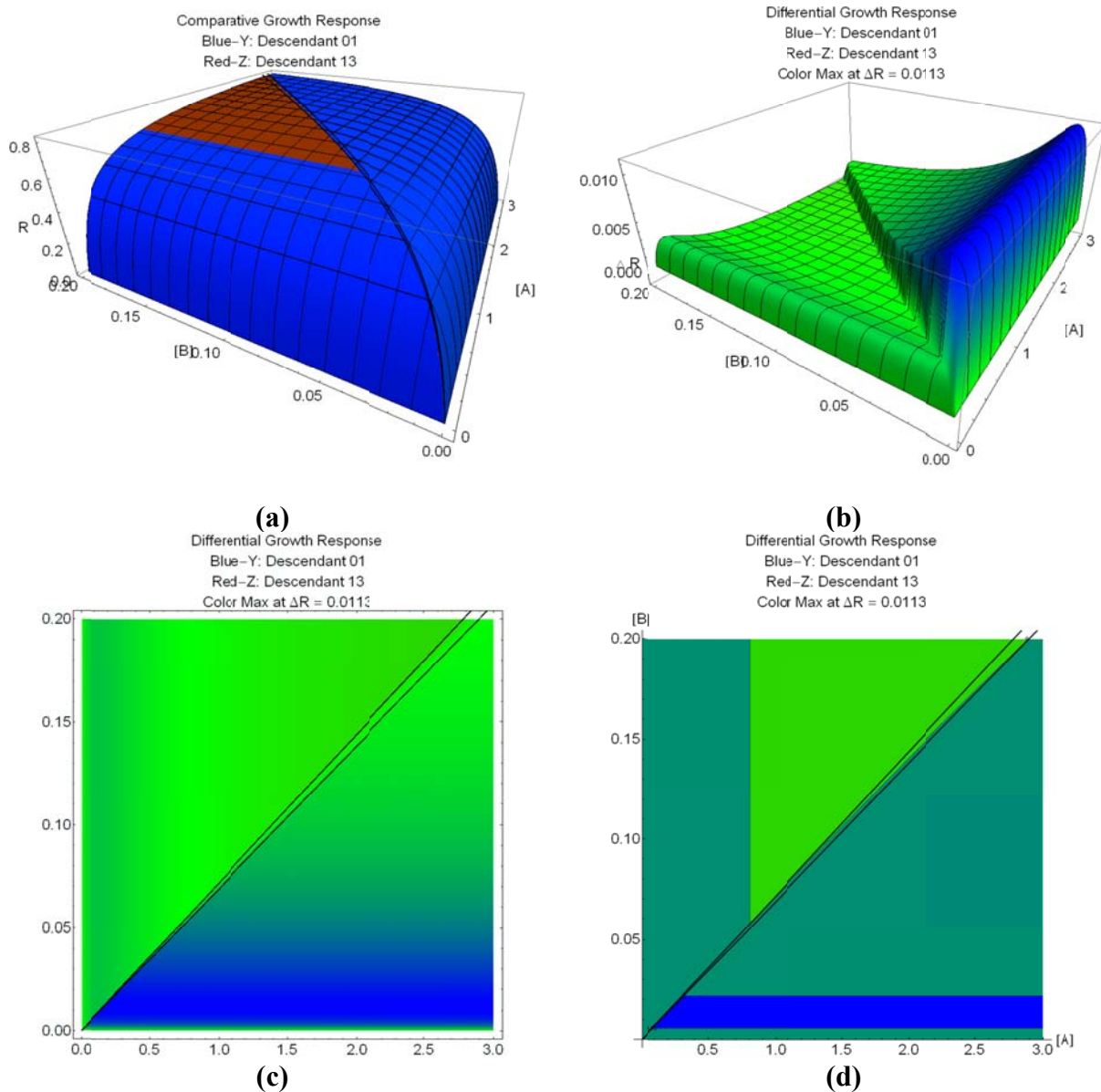


Figure 4-4. **Growth Response Comparison Plots, Desc-01 versus Desc-13.**

Our Full Set of Growth Response Plots for Desc-01 (blue) versus Desc-13 (red)

**Panel (a)** is our Dual Surface Plot, of the two populations' individual response surfaces. As can be seen from the way in which the red tent of Desc-13 "pops up" through the blue tent of Desc-01, the relationship of these two evolved strains is going to be very different from what might be inferred from comparison of their OPLs (compare to Figure 4-1) and is not going to look like a simplistic Tilman-form plot. **Panel (b)** is our Differential Surface Plot showing the relative growth responses of the two populations across the C:N resource space. There is no area where the Desc-13 clearly dominates Desc-01 but there is a large area where dominance would be likely subject to stochastic effects—the "mostly green" area. **Panel (c)**, is our Differential Shaded Plot which provides a continuous analog to a simple Tilman plot. **Panel (d)** is our Differential Shaded-Contour Plot equivalent showing Tilman-like constant-difference isoclines, the contour lines, which can be located automatically or by specification (such as drawing a pair

at  $-0.02 < R < 0.02$  to bound the stochastically sensitive range) from which quantitative values of  $\Delta R$  can be read.

## Chapter 5, Conclusions

Our conclusions from this work fall into three contexts: validity of the model itself as an experimental or investigative tool; implications of our model system for further *in vitro* research in ecological genetics; and implications of what we have found, or what we might find in further work, for ecological concerns *in natura* of continuing and expected environmental change.

### Validity

We believe we have robustly tested and clearly supported the principal hypothesis of the present work:

*A population's ecological niche is reshaped by evolution in response to changes in its ecological environment but trait changes which are adaptive under immediate selection may be accompanied by others which can be either adaptive or maladaptive in other environments.*

We have shown that the Hutchinsonian, ecological, requirements niches (Chase and Leibold 2003, Holt et al. 2005) of our evolved populations exhibited adaptive changes in obviously related single traits when subjected to environments of significantly non-optimum resource supply ratios. We have shown that, at the same time, traits not obviously related to the applied stress also changed in an adaptive direction (Travisano 1997). And we have further shown that, again at the same time, traits intuitively counter-related to the applied stress changed in a direction which would be maladaptive (Travisano et al. 1995, Vasi and Lenski 1999) in either the ancestral, normative environment or in credibly likely subsequent changed environments.

We detected these obvious, non-obvious and cryptic changes and were able to predict their likely effect on population competition by our new modeling approach which exhibits five particular attributes:

- it is formulated to predict populations' response relationships and likely competitive outcomes across an entire  $n$ -dimensional Hutchinsonian space of resource availability or other effects—as in the post-Hutchinson concept of the *requirements niche*;
- it is formulated without regard to development over time and thus reduces the number of parameters required “external” or “internal” to the model;
- it formulates populations' response functions in terms of inherent, organismal traits, rather than in terms of only observed, demographic variables;
- it is formulated in terms of individual populations' responses from which competitive relationships may be determined, rather than in terms of demographic relationships between populations; and
- it is formulated in a way which can detect the effects of underlying subtle, cryptic and non-intuitive genetic covariance.

Our model system also includes a Characterization Protocol for determining experimental populations' response traits, both the common inherent growth response limit and per-resource growth responses for use in our formulation.

Finally, our model system includes a display, plotting, component which represents populations' responses in readily interpreted qualitative (for insight) and quantitative (for prediction) form. It represents a Hutchinson-like two-dimensional (*cf.*  $n$ -dimensional (Hutchinson 1957)) Cartesian resource supply space with a third dimension of populations' individual or relative responses. While our formulation can be mathematically extended to

concurrently deal with more than two resources, the difficulties of simultaneously displaying or perceiving more than three graphic dimensions would require recasting our plot forms to some dimensionally merged or selected-projected form.

The details we observed in our evolved populations, trait changes from their common ancestor, covered the range of possibilities addressed in our principal hypothesis. Both the quantitative and qualitative results of our model showed that it can be applied to experimental populations *in vitro* for both prediction and insight in investigation of population-organismal response trait parameters and trait changes in evolution or selection scenarios. The qualitative results of our model show that it can be applied to hypothesized scenarios *in natura* as well as *in vitro*.

### Research

In the context of further *in vitro* research in ecological genetics (or genetic ecology), we see lines of research where our model may be applied like that reported with *E. coli* (Travisano et al. 1995, Xu et al. 1996, Travisano 1997, Papadopoulos et al. 1999, Cooper et al. 2003, Remold and Lenski 2004, Perfeito et al. 2007), with *S. cerevisiae* (Adams et al. 1985, Chesson 2000b, Szafranec et al. 2001, Boer et al. 2003, Andalis et al. 2004, Wu et al. 2004, Zeyl 2005, Zhenqiong et al. 2005, Cooper et al. 2007, Louis 2009, Hall and Joseph 2010) and with rotifers (Ciros-Perez et al. 2001, Fussmann et al. 2005). All of this work deals with finding correlation between a population's gene pool (often isogenic at the beginning) and population competitive performance or metabolic response, usually after evolution or genetic manipulation.

While there are, now, fast techniques such as micro-arrays, rapid sequencing or rapid sub-sequence identification for distinguishing genomic changes in experimental populations there has been no fast, reliable method employed to date for fast characterization of a population

on multiple resource response traits or for determination of competitive outcomes, especially across resource space.

We believe that our Characterization Protocol, model and graphical presentation offer (as a suite) an effective and efficient way to obtain more thorough and more meaningful comparison of populations' growth or metabolic traits for correlation-comparison-contrast with genetic processes. This advantage should apply in either of the two common viewpoints of these research tracks: discovery of genetic events underlying "forced" or selected ecological changes; and evaluation of ecological effects resulting from experimental genetic manipulations.

We also believe that there is ecological research where genetic analysis is not a major concern, such as in the general study of biodiversity (Buckling et al. 2003, Brown et al. 2004, Holt et al. 2005, Clark et al. 2007, Shou et al. 2007, Martinez-Abraín 2008, Shores et al. 2008, Fraser et al. 2009, Clark 2010) where our model's ability to map inter-species relationships across resource space as a simulation system may offer worthwhile insight.

### Environmental Change

The most important thing our work has shown in the context of environmental change is that both not-obviously directed adaptive changes and cryptic maladaptive changes must be expected from evolution under selection by changes of resource availability. The possible responses of a species or population to large-area change, whether in climate or resource supplies or any other factor are often described as "change, move or die". When the response which emerges is "change", the first change may be by variation from available genetic traits but when available recombinant alternatives are exhausted, drawn to their limits of availability, then the "change" response must become "evolve". If a population is large enough (and the reproduction rate is high enough) the likelihood of adaptive genetic change, generating a more capable

phenotype, becomes high enough that adaptive evolution can be expected (Elena and Lenski 2003, De Visser and Rozen 2005, Hermisson and Pennings 2005).

A common fallacy of expectation of “directed evolution”, however, is to overlook the possibility of changes that are not “under pressure” in the strict sense of the “adverse” aspect of the present environmental change (Bloom and Arnold 2009). We have shown that even in simple cases, such as our *S. cerevisiae* under stress from only a shift in the ratio of two resources, both non-obvious adaptive and cryptic maladaptive effects must be expected. These effects may lead to entirely unexpected competitive relationships—with populations which evolved (or not) under other changed ecological regimes, when the forcing change is rolled back (or long cyclical), when the subject or another population chooses the “move” response to the change...

When and as original, evolving or evolved populations, or proxies, are available and accessible to be characterized our system can be directly applied but otherwise it can be used in simulation of change scenarios to the extent they can be reliably predicted.

In all, our new model appears to have affirmed our principal hypothesis, to offer answers not previously available in ecological research into population competition, and to provide linkage to genetics research in stress-survival, resistance and competition.

## Works Cited

- Adams, J. 2004. Microbial evolution in laboratory environments. *Research in Microbiology* **155**:311-318.
- Adams, J., C. Paquin, P. W. Oeller, and L. W. Lee. 1985. Physiological Characterization of Adaptive Clones in Evolving Populations of the Yeast, *Saccharomyces-Cerevisiae*. *Genetics* **110**:173-185.
- Andalis, A. A., Z. Storchova, C. Styles, T. Galitski, D. Pellman, and G. R. Fink. 2004. Defects arising from whole-genome duplications in *Saacharomyces cerevisiae*. *Genetics* **167**:1109-1121.
- Barrett, R. D. H. and G. Bell. 2006. The dynamics of diversification in evolving *Pseudomonas* populations. *Evolution* **60**:484-490.
- Bell, G. 2001. Neutral Macroecology. *Science* **293**:2413-2418.
- Berendse, F. 1994. Competition between Plant-Populations at Low and High Nutrient Supplies. *Oikos* **71**:253-260.
- Bloom, J. D. and F. H. Arnold. 2009. In the light of directed evolution: Pathways of adaptive protein evolution. *Proceedings of the National Academy of Sciences* **106**:9995-10000.
- Boer, V. M., J. H. de Winde, J. T. Pronk, and M. D. W. Piper. 2003. The genome-wide transcriptional responses of *Saccharomyces cerevisiae* grown on glucose in aerobic chemostat cultures limited for carbon, nitrogen, phosphorus, or sulfur. *Journal of Biological Chemistry* **278**:3265-3274.
- Brown, J. H., J. F. Gillooly, A. P. Allen, V. M. Savage, and G. B. West. 2004. Toward a metabolic theory of ecology. *Ecology* **85**:1771-1789.
- Buckling, A., M. A. Wills, and N. Colegrave. 2003. Adaptation limits diversification of experimental bacterial populations. *Science* **302**:2107-2109.
- Cerucci, M., G. K. Jalgama, and R. B. Ambrose. 2010. Comparison of the Monod and Droop Methods for Dynamic Water Quality Simulations. *Journal of Environmental Engineering-Asce* **136**:1009-1019.
- Chase, J. M. 2007. Drought mediates the importance of stochastic community assembly. *Proceedings of the National Academy of Sciences* **104**:17430-17434.
- Chase, J. M. and M. A. Leibold. 2003. *Ecological niches : linking classical and contemporary approaches*. University of Chicago Press, Chicago.
- Chesson, P. 1991. A need for niches? *Trends in Ecology & Evolution* **6**:26-28.

- Chesson, P. 2000a. General Theory of Competitive Coexistence in Spatially-Varying Environments. *Theoretical Population Biology* **58**:211-237.
- Chesson, P. 2000b. MECHANISMS OF MAINTENANCE OF SPECIES DIVERSITY. *Annual Review of Ecology and Systematics* **31**:343-366.
- Chisholm, R. A. and M. A. Burgman. 2004. THE UNIFIED NEUTRAL THEORY OF BIODIVERSITY AND BIOGEOGRAPHY: COMMENT. *Ecology* **85**:3172-3174.
- Ciros-Perez, J., M. J. Carmona, and M. Serra. 2001. Resource competition between sympatric sibling rotifer species. *Limnology and Oceanography* **46**:1511-1523.
- Clark, D. R. 2001. Growth rate relationships to physiological, indices of nutrient status in marine diatoms. *Journal of Phycology* **37**:249-256.
- Clark, J. S. 2010. Individuals and the Variation Needed for High Species Diversity in Forest Trees. *Science* **327**:1129-1132.
- Clark, J. S., M. Dietze, S. Chakraborty, P. K. Agarwal, I. Ibanez, S. LaDeau, and M. Wolosin. 2007. Resolving the biodiversity paradox. *Ecology Letters* **10**:647-659.
- Condit, R., N. Pitman, E. G. Leigh, Jr., J. Chave, J. Terborgh, R. B. Foster, P. Nunez, S. Aguilar, R. Valencia, G. Villa, H. C. Muller-Landau, E. Losos, and S. P. Hubbell. 2002. Beta-Diversity in Tropical Forest Trees. *Science* **295**:666-669.
- Cooper, T. F., E. A. Ostrowski, and M. Travisano. 2007. A negative relationship between mutation pleiotropy and fitness effect in yeast. *Evolution; International Journal Of Organic Evolution* **61**:1495-1499.
- Cooper, T. F., D. E. Rozen, and R. E. Lenski. 2003. Parallel changes in gene expression after 20,000 generations of evolution in *Escherichia coli*. *Proceedings of the National Academy of Sciences of the United States of America* **100**:1072.
- De Visser, J. and D. E. Rozen. 2005. Limits to adaptation in asexual populations. *Journal of Evolutionary Biology* **18**:779-788.
- Di Stefano, J. 2004. A confidence interval approach to data analysis. *Forest Ecology and Management* **187**:173-183.
- Duboc, P. and U. von Stockar. 1998. Dual limitations: Kinetic and stoichiometric analysis. *Thermochimica Acta* **309**:121-128.
- Dudley, A. e. M., D. M. Janse, A. Tanay, R. Shamir, and G. M. Church. 2005. A global view of pleiotropy and phenotypically derived gene function in yeast. *Molecular Systems Biology* **1**:E1-E11.
- Elena, S. F. and R. E. Lenski. 2003. Microbial genetics: Evolution experiments with microorganisms: the dynamics and genetic bases of adaptation. *Nature Reviews Genetics* **4**:457.
- Elton, C. S. 1927. *Animal Ecology*. Sidgwick and Jackson, London.
- Ferenci, T. 1999. 'Growth of bacterial cultures' 50 years on: towards an uncertainty principle instead of constants in bacterial growth kinetics. *Research in Microbiology* **150**:431-438.

- Fraser, C., E. J. Alm, M. F. Polz, B. G. Spratt, and W. P. Hanage. 2009. The Bacterial Species Challenge: Making Sense of Genetic and Ecological Diversity. *Science* **323**:741-746.
- Fussmann, G. F., S. P. Ellner, N. G. Hairston, L. E. Jones, K. W. Shertzer, and T. Yoshida. 2005. Ecological and evolutionary dynamics of experimental plankton communities. *Advances in Ecological Research*, Vol. 37: Population Dynamics and Laboratory Ecology **37**:221-243.
- Gause, G. F. 1936. *The Struggle for Existence*. Williams and Wilkins, Baltimore.
- Gerrish, P. and R. Lenski. 1998. The fate of competing beneficial mutations in an asexual population. *Genetica* **102-103**:127-144.
- Goddard, M. R. 2006. personal communication, Yeast Strains Transmittal etc.
- Goddard, M. R. 2008. Quantifying the Complexities of *Saccharomyces cerevisiae*'s Ecosystem Engineering via Fermentation. *Ecology* **proof**.
- Goddard, M. R. and M. A. Bradford. 2003a. The adaptive response of a natural microbial population to carbon- and nitrogen-limitation. *Ecology Letters* **6**:594-598.
- Goddard, M. R. and M. A. Bradford. 2003b. The adaptive response of a natural microbial population to carbon- and nitrogen-limitation. *Ecology Letters* **6**:594.
- Goldberg, D. E. 1996. Competitive ability: Definitions, contingency and correlated traits. *Philosophical Transactions of the Royal Society of London Series B-Biological Sciences* **351**:1377-1385.
- Graham, M. H. and M. S. Edwards. 2001. Statistical significance versus fit: estimating the importance of individual factors in ecological analysis of variance. *Oikos* **93**:505-513.
- Grinnell, J. 1917. The niche-relationships of the California Thrasher. *Auk* **34**:427-433.
- Grover, J. P. 1997. *Resource competition*. 1st edition. Chapman & Hall, London ; New York.
- Hall, A. R. and N. Colegrave. 2007. How does resource supply affect evolutionary diversification? *Proceedings of the Royal Society B-Biological Sciences* **274**:73-78.
- Hall, D. W. and S. B. Joseph. 2010. A High Frequency of Beneficial Mutations Across Multiple Fitness Components in *Saccharomyces cerevisiae*. *Genetics* **185**:1397-1409.
- Hermisson, J. and P. S. Pennings. 2005. Soft sweeps: Molecular population genetics of adaptation from standing genetic variation. *Genetics* **169**:2335-2352.
- Higuera-Guisset, J., J. Rodriguez-Viejo, M. Chacon, F. J. Munoz, N. Vignes, and J. Mas. 2005. Calorimetry of microbial growth using a thermopile based microreactor. *Thermochemica Acta* **427**:187-191.
- Holt, R. D., M. Barfield, and R. Gomulkiewicz. 2005. Theories of Niche Conservatism and Evolution -- Could Exotic Species be Potential Tests? Pages 259-290 *in* D. F. Sax, J. J. Stachowicz, and S. D. Gaines, editors. *Species Invasions: Insights into Ecology, Evolution, and Biogeography*. Sinauer Associates, Sunderland, Mass.
- Holt, R. D., J. Grover, and D. Tilman. 1994. SIMPLE RULES FOR INTERSPECIFIC DOMINANCE IN SYSTEMS WITH EXPLOITATIVE AND APPARENT COMPETITION. *American Naturalist* **144**:741-771.

- Hoskisson, P. A. and G. Hobbs. 2005. Continuous culture - making a comeback? *Microbiology-Sgm* **151**:3153-3159.
- Hsu, S. B., K. S. Cheng, and S. P. Hubbell. 1981. Exploitative Competition of Microorganisms for 2 Complementary Nutrients in Continuous Cultures. *Siam Journal on Applied Mathematics* **41**:422-444.
- Hsu, S. B., S. Hubbell, and P. Waltman. 1977. Mathematical-Theory for Single-Nutrient Competition in Continuous Cultures of Microorganisms. *Siam Journal on Applied Mathematics* **32**:366-383.
- Hubbell, S. P. 2001. *The unified neutral theory of biodiversity and biogeography*. Princeton University Press, Princeton, N.J.
- Hubbell, S. P. and L. Borda-de-Água. 2004. THE UNIFIED NEUTRAL THEORY OF BIODIVERSITY AND BIOGEOGRAPHY: REPLY. *Ecology* **85**:3175-3178.
- Hutchinson, G. E. 1957. Concluding Remarks. Page 437 *in* Cold Spring Harbor Laboratory, editor. *Population Studies: Animal Ecology and Demography*, Cold Spring Harbor Symposia on Quantitative Biology XXII. Cold Spring Harbor Laboratory Press, Woodbury, NY.
- Hutchinson, G. E. 1959. Homage to Santa-Rosalía or Why Are There So Many Kinds of Animals. *American Naturalist* **93**:145-159.
- Hutchinson, G. E. 1978. *An introduction to population ecology*. Yale University Press, New Haven.
- Leibold, M. A. 1995. THE NICHE CONCEPT REVISITED - MECHANISTIC MODELS AND COMMUNITY CONTEXT. *Ecology* **76**:1371-1382.
- Leibold, M. A. 1996. A graphical model of keystone predators in food webs: Trophic regulation of abundance, incidence, and diversity patterns in communities. *American Naturalist* **147**:784-812.
- Leibold, M. A. 1998. Similarity and local co-existence of species in regional biotas. *Evolutionary Ecology* **12**:95-110.
- Lenski, R. E. 1989. ARE SOME MUTATIONS DIRECTED. *Trends in Ecology & Evolution* **4**:148-150.
- Levert, J. M. and J. L. Xia. 2001. Modeling the growth curve for *Spirulina* (*Arthrospira*) *maxima*, a versatile microalga for producing uniformly labelled compounds with stable isotopes. *Journal of Applied Phycology* **13**:359-367.
- Levin, S. A. 1970. Community Equilibria and Stability, and an Extension of the Competitive Exclusion Principle. *The American Naturalist* **104**:413.
- Lohninger, H. 2009. *Fundamentals of Statistics*.
- Lokshina, L. Y., V. A. Vavilin, R. H. Kettunen, J. A. Rintala, C. Holliger, and A. N. Nozhevnikova. 2001. Evaluation of kinetic coefficients using integrated Monod and Haldane models for low-temperature acetoclastic methanogenesis. *Water Research* **35**:2913-2922.
- Louis, E. J. 2009. Evolutionary genetics: Origins of reproductive isolation. *Nature* **457**:549-550.

- MacArthur, R. H. 1958. Population Ecology of Some Warblers of Northeastern Coniferous Forests. *Ecology* **39**:599-619.
- MacArthur, R. H. 1972. Geographical ecology; patterns in the distribution of species. Harper & Row, New York,.
- MacLean, R. C., G. Bell, and P. B. Rainey. 2004. The evolution of a pleiotropic fitness tradeoff in *Pseudomonas fluorescens*. *Proceedings of the National Academy of Sciences of the United States of America* **101**:8072-8077.
- Maguire, B., Jr. 1973. Niche Response Structure and the Analytical Potentials of Its Relationship to the Habitat. *The American Naturalist* **107**:213-246.
- Mankad, T. and E. B. Nauman. 1992. MODELING OF MICROBIAL-GROWTH UNDER DUAL LIMITATIONS. *Chemical Engineering Journal and the Biochemical Engineering Journal* **48**:B9-B11.
- Martinez-Abraín, A. 2007. Are there any differences? A non-sensical question in ecology. *Acta Oecologica-International Journal of Ecology* **32**:203-206.
- Martinez-Abraín, A. 2008. Statistical significance and biological relevance: A call for a more cautious interpretation of results in ecology. *Acta Oecologica-International Journal of Ecology* **34**:9-11.
- Milbrink, G., M. L. Kruse, and J. Bengtsson. 2003. Competitive ability and life history strategies in four species of *Daphnia*: *D-obtusa*, *D-magna*, *D-pulex* and *D-longispina*. *Archiv Fur Hydrobiologie* **157**:433-453.
- Miller, T. E., J. H. Burns, P. Munguia, E. L. Walters, J. M. Kneitel, P. M. Richards, N. Mouquet, and H. L. Buckley. 2005. A critical review of twenty years' use of the resource-ratio theory. *American Naturalist* **165**:439-448.
- Monod, J. 1949. THE GROWTH OF BACTERIAL CULTURES. *Annual Review of Microbiology* **3**:371-394.
- Nakagawa, S. and I. C. Cuthill. 2007. Effect size, confidence interval and statistical significance: a practical guide for biologists. *Biological Reviews* **82**:591-605.
- Papadopoulos, D., D. Schneider, J. Meier-Eiss, W. Arber, R. E. Lenski, and M. Blot. 1999. Genomic evolution during a 10,000-generation experiment with bacteria. *Proceedings of the National Academy of Sciences of the United States of America* **96**:3807-3812.
- Paquin, C. and J. Adams. 1983a. Frequency of Fixation of Adaptive Mutations Is Higher in Evolving Diploid Than Haploid Yeast Populations. *Nature* **302**:495-500.
- Paquin, C. E. and J. Adams. 1983b. Relative Fitness Can Decrease in Evolving Asexual Populations of *S-Cerevisiae*. *Nature* **306**:368-371.
- Perfeito, L., L. Fernandes, C. Mota, and I. Gordo. 2007. Adaptive mutations in bacteria: High rate and small effects. *Science* **317**:813-815.
- Poilpre, E., D. Tronquit, G. Goma, and V. Guillou. 2002. On-line estimation of biomass concentration during transient growth on yeast chemostat culture using light reflectance. *Biotechnology Letters* **24**:2075-2081.

- Price, N. M. and F. M. M. Morel. 1991. Colimitation of Phytoplankton Growth by Nickel and Nitrogen. *Limnology and Oceanography* **36**:1071-1077.
- Pulliam, H. R. 2000. On the relationship between niche and distribution. *Ecology Letters* **3**:349-361.
- Raich, J. W., A. E. Russell, K. Kitayama, W. J. Parton, and P. M. Vitousek. 2006. TEMPERATURE INFLUENCES CARBON ACCUMULATION IN MOIST TROPICAL FORESTS. *Ecology* **87**:76-87.
- Remold, S. K. and R. E. Lenski. 2001. Contribution of individual random mutations to genotype-by-environment interactions in *Escherichia coli*. *Proceedings of the National Academy of Sciences of the United States of America* **98**:11388-11393.
- Remold, S. K. and R. E. Lenski. 2004. Pervasive joint influence of epistasis and plasticity on mutational effects in *Escherichia coli*. *Nature Genetics* **36**:423-426.
- Replansky, T., V. Koufopanou, D. Greig, and G. Bell. 2008. *Saccharomyces sensu stricto* as a model system for evolution and ecology. *Trends in Ecology & Evolution* **23**:494-501.
- Rutgers, M., P. A. Balk, and K. Vandam. 1990. Quantification of Multiple-Substrate Controlled Growth - Simultaneous Ammonium and Glucose Limitation in Chemostat Cultures of *Klebsiella-Pneumoniae*. *Archives of Microbiology* **153**:478-484.
- Shoresh, N., M. Hegreness, and R. Kishony. 2008. Evolution exacerbates the paradox of the plankton. *Proceedings of the National Academy of Sciences* **105**:12365-12369.
- Shou, W. Y., S. Ram, and J. M. G. Vilar. 2007. Synthetic cooperation in engineered yeast populations. *Proceedings of the National Academy of Sciences of the United States of America* **104**:1877-1882.
- Stephens, P. A., S. W. Buskirk, and C. M. del Rio. 2007. Inference in ecology and evolution. *Trends in Ecology & Evolution* **22**:192-197.
- Sterner, R. W. and J. J. Elser. 2002. *Ecological Stoichiometry: The Biology of Elements from Molecules to the Biosphere*. Princeton University Press, Princeton.
- Szafranec, K., R. H. Borts, and R. Korona. 2001. Environmental stress and mutational load in diploid strains of the yeast *Saccharomyces cerevisiae*. *Proceedings of the National Academy of Sciences of the United States of America* **98**:1107-1112.
- Tang, Y. J. J., A. L. Meadows, and J. D. Keasling. 2007. A kinetic model describing *Shewanella oneidensis* MR-1 growth, substrate consumption, and product secretion. *Biotechnology and Bioengineering* **96**:125-133.
- Tilman, D. 1980. Resources: A Graphical-Mechanistic Approach to Competition and Predation. *American Naturalist* **116**:362-393.
- Tilman, D. 1981. Tests of Resource Competition Theory Using Four Species of Lake Michigan Algae. *Ecology* **62**:802-815.
- Tilman, D. 1982. *Resource competition and community structure*. Princeton University Press, Princeton, N.J.
- Tilman, D. 1988. *Plant strategies and the dynamics and structure of plant communities*. Princeton University Press, Princeton, N.J.

- Travisano, M. 1997. Long-term experimental evolution in *Escherichia coli*. 5. Environmental constraints on adaptation and divergence. *Genetics* **146**:471-479.
- Travisano, M., F. Vasi, and R. E. Lenski. 1995. Long-Term Experimental Evolution in *Escherichia-Coli*. 3. Variation among Replicate Populations in Correlated Responses to Novel Environments. *Evolution* **49**:189-200.
- Vasi, F. K. and R. E. Lenski. 1999. Ecological strategies and fitness tradeoffs in *Escherichia coli* mutants adapted to prolonged starvation. *Journal of Genetics* **78**:43-49.
- Velicer, G. J. 1999. Pleiotropic effects of adaptation to a single carbon source for growth on alternative substrates. *Applied and Environmental Microbiology* **65**:264-269.
- Velicer, G. J. and R. E. Lenski. 1999. Evolutionary trade-offs under conditions of resource abundance and scarcity: Experiments with bacteria. *Ecology* **80**:1168-1179.
- Weiherr, E. and P. A. Keddy. 1999. Ecological assembly rules : perspectives, advances, retreats. Cambridge University Press, Cambridge [England] ; New York, NY, USA.
- WERNER BioAgents. 2009. clonNAT + Plasmid pYL16. Meisenweg 7/ OT Cospeda, 07751 Jena, Germany.
- Wiegand, T., C. V. S. Gunatilleke, I. A. U. N. Gunatilleke, and A. Huth. 2007. How individual species structure diversity in tropical forests. *Proceedings of the National Academy of Sciences* **104**:19029-19033.
- Williams, C. B. 1964. Patterns in the balance of nature and related problems in quantitative ecology. Academic Press, London, New York,.
- Wolfram Research, Inc. 2008. Mathematica. Wolfram Research, Inc., Champaign, Illinois.
- Wu, J., N. S. Zhang, A. Hayes, K. Panoutsopoulou, and S. G. Oliver. 2004. Global analysis of nutrient control of gene expression in *Saccharomyces cerevisiae* during growth and starvation. *Proceedings of the National Academy of Sciences of the United States of America* **101**:3148-3153.
- Xu, W. Z., A. Kashiwagi, T. Yomo, and I. Urabe. 1996. Fate of a mutant emerging at the initial stage of evolution. *Researches on Population Ecology* **38**:231-237.
- Zeyl, C. 2004. Capturing the adaptive mutation in yeast. *Research in Microbiology* **155**:217-223.
- Zeyl, C. 2005. The number of mutations selected during adaptation in a laboratory population of *Saccharomyces cerevisiae*. *Genetics* **169**:1825-1831.
- Zeyl, C. and J. A. G. M. DeVisser. 2001. Estimates of the Rate and Distribution of Fitness Effects of Spontaneous Mutation in *Saccharomyces cerevisiae*. *Genetics* **157**:53-61.
- Zhenqiong, G., L. David, D. Petrov, T. Jones, R. W. Davis, and L. M. Steinmetz. 2005. Elevated evolutionary rates in the laboratory strain of *Saccharomyces cerevisiae*. *Proceedings of the National Academy of Sciences of the United States of America* **102**:1092-1097.
- Zinn, M., B. Witholt, and T. Egli. 2004. Dual nutrient limited growth: models, experimental observations, and applications. *Journal of Biotechnology* **113**:263-279.

## Appendix A, Mathematics

### Introduction

We designed our model to permit prediction of individual and relative growth responses of two competing populations across a range of Hutchinsonian requirements niches, a Cartesian space of environmental supply, of two co-limiting, essential resources. When the relative growth responses of the populations are combined with expected environmental supply of the resources it is possible to predict the outcome of competition between the populations: stable equilibrium (*i.e.*, coexistence), dynamic equilibrium (*i.e.*, cyclic coexistence) or non-equilibrium (*i.e.*, displacement).

The general form of our model is based on Tilman's *Graphical-Mechanistic Approach* (1980) which was based *inter alia* on niche theory of MacArthur (1972) and Maguire (1973), both of which acknowledged Lotka and Volterra (ca. 1920s). We needed to correct deficiencies in Tilman's original model as he suggested (1981, 1982) and as noted, more in application than in fundamentals, by Miller *et al.* (2005). We adopted Monod's model (1949), sometimes called the Michaelis-Menten model, of population growth response on a single limiting resource, extended with von Liebig's *Law of the Minimum* (ca. 1840s) (as in Tilman 1980, p. 367, eqn. 2). We also took guidance from others such as Sterner and Elser (2002) and Chase and Leibold (2003).

We wanted to make the model as mechanistic-realistic as possible without making it unreasonably complex for implementation in the laboratory or the field and, finally, we wanted to take advantage of mathematical software not available thirty or even ten years ago.

We adopted *Mathematica*®, version 7 (Wolfram Research 2008) as our software system.

We discuss our model here in four aspects: Formulation Selection, Response Prediction, Population Response Measurement, and Response Traits Curve Fitting.

### Formulation Selection

It has been shown, discussed and recommended, *e.g.* (Hsu et al. 1977, Tilman 1981, Grover 1997) that population growth response modeling across any “wide” range of a resource supply requires a non-linear, asymptotic formulation. Linear increase of the supply of a limiting resource gives an asymptotic (*i.e.* “saturating” to a limit) increase in intrinsic growth rate, which is necessarily nonlinear, and not an indefinite (*i.e.* without limit) increase, the unavoidable behavior of a linear formulation.

Linear approximations have been useful in “near zero supply” simulations as in the basic form of Tilman’s *Graphical-Mechanistic Approach* (1980) or in the simplified examples of Chase and Leibold (2003) but simply do not work well elsewhere.

Our justification for choosing Monod’s (1949) (asymptotic, nonlinear) function as the mathematical core of our model is, first, the fact that it is widely recognized as a reference model, *e.g.* (Ferenci 1999, Levert and Xia 2001, Lokshina et al. 2001, Higuera-Guisset et al. 2005, Tang et al. 2007, Cerucci et al. 2010) for work similar to ours—affording a basis for comparability—and, second, the fact that it is easy to comprehend, parameterize and apply—helping to achieve our objective of a simple model with no more parameters than necessary

The canonical form of the Monod equation is the simple hyperbola:

$$y = \alpha x / (\beta + x) \quad (1)$$

Here, considering only Cartesian first quadrant (*i.e.*  $x > 0, y > 0$ ),  $y$  is the “response”,  $x$  is the “supply”,  $y = \alpha$  (Greek alpha) is the “asymptotic limit” parameter and  $x = \beta$  (Greek beta) is the “characteristic” parameter. There are other asymptotic expressions, such as the simple exponential or hyperbolic sigmoid which could be used in place of the simple hyperbola but none offers the prospect of more precise curve-fitting to a population’s observed growth response or easier comprehension and application.

### Response Prediction

The Monod equation specifies a population’s realized intrinsic growth response phenomenon,  $R$ , on a resource as:

$$R = \frac{dN/dt}{N} = R_k \frac{C}{C_1 + C} \quad (2)$$

This is Monod’s equation 2 (1949 pg 343) where  $N$  is the population size by mass (Monod’s *density*),  $t$  is time,  $R_k$  is the population maximum intrinsic growth response,  $C_1$  is the resource supply concentration required to achieve one-half  $R_k$ , (which we call the *half-saturation constant*) and  $C$  is the instant resource supply concentration. This formulation applies to a population for any one resource when all other resources are “in large excess” (*ibid.*, p. 379) which is the same as saying that the one resource is solely growth-limiting. We note that  $C$  and  $R$  are *ecological phenomena*, empirically or demographically observable, while  $C_1$  and  $R_k$  are *organismal traits*, inherent to the population.

When a population is limited by multiple essential resources (*i.e.*, neither can substitute for the other), all other resources being in excess supply, its growth response obeys von Liebig’s

*Law of the Minimum* (compare to Tilman 1980, p. 367, eqn. 2) and the realized growth response of the population is the minimum of the per-resource growth responses. Using Monod's notation and two resources, **A** and **B**, we have:

$$R_{A,B} = \min \left[ R_{KA} \frac{C_A}{C_{1A}+C_A}, R_{KB} \frac{C_B}{C_{1B}+C_B} \right] \quad ()$$

where *min* is the arithmetic *minimum of* operator.

But since  $R_K$  is a trait common to the organism-population,  $R_{KA} = R_{KB}$  and we can reduce to:

$$R = R_k \min \left[ \frac{C_A}{C_{1A}+C_A}, \frac{C_B}{C_{1B}+C_B} \right] \quad ()$$

For two populations, **Y** and **Z**, in a common environment we can formulate the per-population growth responses as:

$$R_Y = R_{KY} \min \left[ \frac{C_A}{C_{1AY}+C_A}, \frac{C_B}{C_{1BY}+C_B} \right] \quad ()$$

$$R_Z = R_{KZ} \min \left[ \frac{C_A}{C_{1AZ}+C_A}, \frac{C_B}{C_{1BZ}+C_B} \right] \quad ().$$

So the relative (*i.e.*, differential) growth response,  $R_{rel}$ , is:

$$R_{rel} = R_{KY} \min \left[ \frac{C_A}{C_{1AY}+C_A}, \frac{C_B}{C_{1BY}+C_B} \right] - R_{KZ} \min \left[ \frac{C_A}{C_{1AZ}+C_A}, \frac{C_B}{C_{1BZ}+C_B} \right] \quad ().$$

This is the essential formulation used in our plotting code. It is also possible and more or less straightforward to formulate and plot relative Darwinian fitness or other expressions from the two growth responses.

### Plotting Code and Examples

The following figures illustrate our growth response computation and plotting scheme, using trait parameters of selected experimental populations in a carbon- and nitrogen-limiting-resource space:

Figure A-0-1 is the entire *Mathematica*® code for generating all four of our plot forms for a pair of populations. Figure A-0-2 isolates the essential functions and math for the “Differential Surface” plot form.

Figure A-0-3 (a) shows a single population’s dome tent shape of the realized growth response *phenomenon*,  $\mathbf{R}$ , generated from the non-linear per-resource response *traits*,  $\mathbf{C}_{IC}$  and  $\mathbf{C}_{IN}$ , (giving the curved sides) and the asymptotic approach to the maximum capable growth response *trait*,  $\mathbf{R}_K$ . Figure A-0-3 (b) shows the intersecting, inter-penetrating dome tents of two populations.

Figure A-0-3 (c) shows the relative growth response of two populations as a three-dimensional projected surface.

Figure A-0-4 (a) shows the growth response of a single population as a stepped-shaded, contour-line plot. Figure A-0-4 (b) shows the relative growth response of a pair of populations in the same form, similar to a simple Tilman-like plot with constant-difference isoclines. Figure A-0-4 (c) shows the relative growth response of two populations as a shaded surface.

### Population Response Measurement

Predicting populations’ growth responses, graphically or in any other way, requires that we obtain values of the response trait parameters  $\mathbf{R}_K$ ,  $\mathbf{C}_{IA}$  and  $\mathbf{C}_{IB}$  for each population. In our present experimental regime dealing with carbon- and nitrogen-limited growth responses the  $\mathbf{A}$  and  $\mathbf{B}$  subscripts become  $\mathbf{C}$  and  $\mathbf{N}$ .

We subject each population to be “characterized”, as we call the process, to resource-limited growth under conditions of “high N, stepped C” and “high C, stepped N” with the base medium and other nutrient resources, including P, in excess supply. Each of the two limited-

growth conditions includes four different, known limiting concentrations of the “stepped” nutrient resource while the “high” resource is provided at a known non-interfering concentration.

This process gives us eight data points for which we run four replicates each. Four of the data points are  $(R, C_{High}, C_{Nstep})$  and four are  $(R, C_{Cstep}, C_{Nhigh})$ . We use these eight data points, replicated four times for thirty-two triples, as input to our curve-fitting algorithm.

### Response Statistics

Recapping our discussion Chapter 3...

An overarching problem with statistical analysis of our results is that we are not dealing with conventional hypothesis testing (except, perhaps, in our direct competitions) or conventional statistical inference. We have no single parameters which are independently derived from our Characterization Protocol and the multiple data values per test point  $(R, C_C, C_N)$ . The multiple parameters we need  $(R_K, C_{IC}, C_{IN})$  for maximum capable growth response and per-resource growth response can only be determined by simultaneous curve-fitting to a single equation.

If we were to attempt to fit each per-resource response,  $C_{IC}$  and  $C_{IN}$ , from our data sets or any other measurement scheme, individually (*i.e.* without simultaneous  $R_K$ ) we would be left with a linear relationship as our only alternative and we know from numerous sources previously cited *e.g.* (Ferenci 1999, Levert and Xia 2001, Lokshina et al. 2001, Higuera-Guisset et al. 2005, Tang et al. 2007, Cerucci et al. 2010) that that is not a viable option.

If we were to attempt to fit each per-resource response,  $C_{IC}$  or  $C_{IN}$ , with  $R_K$  independent of the other per-resource response, we would be virtually certain to arrive at two values for  $R_K$ , as if  $R_{KC}$  and  $R_{KN}$ , which we know from several of the immediate prior citations as well as from Grover (1997) is not realistically applicable. Simply put, if we provide a single population with

sufficient supply of all resources that no further increase of any resource provides any greater growth response, then we have reached a population limit to growth rate. This can be verified by decreasing each resource, one at a time, to establish a limiting growth value for each (non-substitutable) resource and these limits will be found to be all at the same maximum growth response. So we must, in the end, fit all three of our parameters for each population,  $R_K$ ,  $C_{IC}$ ,  $C_{IN}$ , simultaneously to the single Monod-and-von Leibig formulation.

We are in the situation of having no “independent variables” or “additive variables” statistical analysis available. We rely, instead, on confidence interval comparison for whatever meaning there may be to “significant difference” between competing populations’ values of each of our three parameters. Our curve-fitting program and its core *Mathematica*® function, *NonlinearModelFit[]*, provide an ANOVA table for the objective variable  $x$ , our realized-observed  $R$ , but have no equivalent of independent or additive behavior to determine customary, per-variable error, residual statistics. The program does provide Standard Error, Confidence Interval (95%), t-Statistic and P-value per fitted parameter but while these are comparable to the usual statistics they are not the same and are not related by any simple function.

In Chapter 3 we discuss one example of graphical fit and residuals plot of  $C_{IC}$  and  $C_{IN}$ , for one of our populations, as if these parameters had been individually determined. The fit and residuals for  $C_{IC}$  look good but those for  $C_{IN}$  do not. If we had recognized this syndrome early in our sequence of experiments we might have extended our range of  $C_N$ , nitrogen supply concentration, to higher values to obtain a better-appearing fit but we chose to stay with a consistent set of test points. It is not clear, however, that the  $C_{IN}$  fit would have “looked” any better by curve or by residuals as the entire fit can only deal with all three parameters.

The OPL slopes for the several populations show significant difference between all but one of the competing pairs, which runs counter to customary suspicion of “statistics of statistics”, *i.e.* because the OPL slope is a ratio of two fitted parameters which, themselves, do not appear to be significantly different. We analyzed the OPL slopes by a Monte Carlo process of dithering each of the OPL components,  $C_{IC}$  and  $C_{IN}$ , 1,000 times by its Standard Error on a Normal Distribution, taking the ratio of each pair of dithered values, and performing a simple analysis of Mean, Variance and Confidence Interval (95%) of the 1,000 ratios.

### Response Traits Curve Fitting

The general objective of curve-fitting an array of data points,  $(R, C)$ , to a function  $R = f(C, (R_K, C_1))$  such as Monod's,  $R = R_K C / (C_1 + C)$ , is conceptually and practically simple so long as there is a continuous derivative,  $f'$ , and can be accomplished with a number of readily available software tools. Our function to be fitted, however, is a discontinuous combination of Monod and von Leibig,  $R = R_K \min [ C_A / (C_{1A} + C_A), C_B / (C_{1B} + C_B) ] - \text{Flow}$ , and is itself discontinuous so it has no continuous derivative. The addition of the **Flow** term in curve-fitting places the Monod growth-response function into the context of the continuous-flow, chemostat culture mode where **Flow** is the proportional rate of flow-through per time, also known as dilution rate, which is equivalent to an intrinsic mortality rate which operates against the intrinsic growth rate,  $R_K$ , to give the realized growth rate and thus the standing biomass of the culture.

While our adopted software tool, *Mathematica*®, has several ways to do curve-fitting, even its most-capable, self-adapting curve-fitting function, *NonlinearModelFit*[], cannot deal with functions which lack a continuous derivative. It was necessary to re-cast our discontinuous function:

$$R_{A,B} = R_K \min \left[ \frac{C_A}{C_{1A}+C_A}, \frac{C_B}{C_{1B}+C_B} \right] - \text{Flow} \quad ()$$

to a continuous and continuous-derivative function, let's call it  $\mathbf{G}$ :

$$R_{A,B} = R_K \mathbf{G} \left[ \frac{C_A}{C_{1A}+C_A}, \frac{C_B}{C_{1B}+C_B} \right] - \text{Flow} \quad ()$$

which would behave as the min operator of a sum of continuous etc. functions,  $\mathbf{G}_L$  and  $\mathbf{G}_R$  where  $\mathbf{R}$  and  $\mathbf{L}$  indicate “left” and “right” (see next):

$$R_{A,B} = R_K \left[ G_L \left( \frac{C_A}{C_{1A}+C_A} - \text{Flow} \right) + G_R \left( \frac{C_B}{C_{1B}+C_B} - \text{Flow} \right) \right] \quad ()$$

which would behave as if it were doubly continuous.

The basic Monod function on a single supply variable is shown in Figure 2-1 (page 31).

The Monod-form functions on  $C_A$  and  $C_B$  are twice-continuous so the key, then, was to find  $\mathbf{G}_L$ ,  $\mathbf{G}_R$  as twice-continuous functions which would multiply the function on  $C_A$  by  $\mathbf{1}$  where we want its values to apply, by  $\mathbf{0}$  elsewhere, and would complementarily multiply the function on  $C_B$  by  $\mathbf{1}$  and  $\mathbf{0}$ . Figure A-0-5 shows what we would like to accomplish for Monod-equation curve-fitting.

We settled on the simple hyperbolic sigmoid function and its complement as our  $\mathbf{G}_L$ ,  $\mathbf{G}_R$  pair:

$$G_L = \frac{1}{1+e^x} \quad ()$$

$$G_R = 1 - \frac{1}{1+e^x} \quad ().$$

Obviously, the sum of these two equations is unity, as required. The “crossover” from 0 to 1 and 1 to 0 can be made “steeper” by adding a “steepness factor”,  $\mathbf{S}$ :

$$G_L = \frac{1}{1+e^{Sx}} \quad ()$$

$$G_R = 1 - \frac{1}{1+e^{Sx}} \quad ().$$

And the crossover  $x$  value can be offset from zero by adding an “offset” term,  $\mathbf{O}$ :

$$G_L = \frac{1}{1+e^{S(x-o)}} \quad ()$$

$$G_R = 1 - \frac{1}{1+e^{S(x-o)}} \quad ().$$

Figure A-0-6 shows application of this “sigmoid switch” to intersecting, complementary linear functions.

Our complete curve-fit target function with adaptive computation of  $O$  as  $O_A$  and  $O_B$ , corresponding to  $G_L$  and  $G_R$  in equation (), looks like this:

$$R_{A,B} = R_K \left[ \frac{1}{1+e^{S(x-O_A)}} \frac{C_A}{C_{1A}+C_A} + \left( 1 - \frac{1}{1+e^{S(x-O_B)}} \right) \frac{C_B}{C_{1B}+C_B} \right] \quad ().$$

There is, as is common in curve-fitting to complicated functions, a key “trick” to be applied, ensuring in our situation that the crossover point of the two Monod functions—the offset value,  $O$ , in equation ()—remains “between” the highest values of  $C_{1A}$  and  $C_{1B}$ . This is particularly complicated in our code by the fact that we are not really working on a common abscissa, *i.e.*, because we are actually working with two axes,  $C_A$  and  $C_B$ . Our self-adaptive computation of, effectively,  $O_A$  and  $O_B$  is shown in the *Mathematica*® code. Our entire approach works because the *NonlinearModelFit[]* function iterates-approximates the entire argument function and not just some abstracted-extracted “core” as some curve-fitting functions do.

Figure A-0-7 is the entire *Mathematica*® code of our curve-fitting program. The input file is a “.csv” (comma-separated values) form of  $(C_A, C_B, R)$  triplets from the Characterization Protocol (chemostat) run and the output is fitted trait parameters  $R_K$ ,  $C_{1A}$  and  $C_{1B}$ . Note that although our terminology in this paper has been normalized to match Monod’s, much of our *Mathematica*® code, as here, still employs an earlier terminology—which should, nevertheless, be comprehensible in reference to the Monod terminology.

Figure A-0-8 is the complete output, including diagnostics and redundancies for programmer-operator’s review, of a Characterization run of one of our experimental populations.

Figure A-0-9 is the essential, core setup of the *NonlinearModelFit[]* function in our *Mathematica*® code, annotated to explain at least some of what is happening. It includes the adaptive-offset computation,  $\mathbf{O}_A$  and  $\mathbf{O}_B$  in equation () above, for the two ecological variables,  $C_A$  and  $C_B$ .

#### *Goodness of fit*

Our curve-fitting code provides estimated goodness-of-fit values along with the fitted parameters. The report, including the fitted parameters, is shown in Figure A-0-8 with a full set of curve-fitting output.

## Figures

### **Begin Figure A-1.**

```
(* Alternative Population Parameters Set 1 *)  
PopName1 = "MRG-2" ;  
RK1 = 0.833635 ;  
C1C1 = 0.210322 ;  
C1N1 = 0.0130414 ;
```

```
(* Alternative Population Parameters Set 3 *)  
PopName3 = "MRG-2N" ;  
RK3 = 0.845480 ;  
C1C3 = 0.222601 ;  
C1N3 = 0.0153732 ;
```

```
(* Alternative Population Parameters Set 2 *)  
PopName2 = "MRG-8" ;  
RK2 = 0.859798 ;  
C1C2 = 0.216459 ;  
C1N2 = 0.0141549 ;
```

```
(* Alternative Population Parameters Set 5 *)  
PopName5 = "Descendant 01" ;  
RK5 = 0.868370 ;  
C1C5 = 0.181011 ;  
C1N5 = 0.0125035 ;
```

```
(* Alternative Population Parameters Set 6 *)  
PopName6 = "Descendant 13" ;  
RK6 = 0.871355 ;  
C1C6 = 0.184406 ;  
C1N6 = 0.0132597 ;
```

```
(* Alternative Population Parameters Set 4 *)  
PopName4 = "MRG-8N" ;  
RK4 = 0.928554 ;  
C1C4 = 0.232111 ;  
C1N4 = 0.0150399 ;
```

```
(* "Null" Population Parameters Set *)  
PopNameNN = "Null" ;  
RKNN = 0.0000001 ;  
C1CNN = 0.0000001 ;  
C1NNN = 0.0000001 ;
```

```
(* supply concentration ranges from zero *)
```

```

CChi=4.0 ;
CNhi=4.0/15.0 ;

(* Plot Control and Display Values *)
Clear [ Ppoints , Pwidth ] ;

(* evaluate/plot initial _ points per axis *)
Ppoints = 100 ;

(* plot _ inches wide at _ dpi *)
Pwidth = 3 * 300 ;

(*
... Select a Pair to Plot ...
#1 MRG-2  RK1=0.833635  C1C1=0.210322  C1N1=0.0130414  C:N=16.13
#2 MRG-2N  RK3=0.845480  C1C3=0.222601  C1N3=0.0153732
C:N=14.48
#3 MRG-8  RK2=0.859798  C1C2=0.216459  C1N2=0.0141549  C:N=15.29
#4 Desc-01  RK5=0.868370  C1C5=0.181011  C1N5=0.0125035
C:N=14.48
#5 Desc-13  RK6=0.871355  C1C6=0.184406  C1N6=0.0132597
C:N=13.91
#6 MRG-8N  RK4=0.928554  C1C4=0.232111  C1N4=0.0150399
C:N=15.43
*)

Clear [ RKY , C1CY , C1NY , RKZ , C1CZ , C1NZ ] ;

PopNameY = PopName4 ;
RKY = RK4 ;
C1CY = C1C4 ;
C1NY = C1N4 ;

PopNameZ = PopName6 ;
RKZ = RK6 ;
C1CZ = C1C6 ;
C1NZ = C1N6 ;
Plots

(* Dual Surface Plot *)
Show [

Plot3D [
[[ RKY Min [ C1C/(C1C+C1CY) , C1N/(C1N+C1NY) ] ,
RKZ Min [ C1C/(C1C+C1CZ) , C1N/(C1N+C1NZ) ] ]],
[[ C1C , 0 , CChi ]], [[ C1N , 0 , CNhi ]],
Exclusions -> None ,
LabelStyle -> [[ 25 , FontFamily -> "Helvetica" ]], PlotLabel ->

```

```

Style [ "Comparative Growth Response\nBlue-Y: "<> PopNameY <>
"\nRed-Z: " <> PopNameZ , 25 , FontFamily -> "Helvetica" ] ,
AxesLabel -> [[ " [ A ] " , " [ B ] " , "R" ]] ,
AxesEdge -> [[ [[ -1 , -1 ]] , [[ -1 , -1 ]] , [[ -1 , 1 ]] ]] ,
PlotPoints -> Ppoints ,
ImageSize -> [[ Pwidth , Pwidth ]] ,
ViewPoint -> [[ -1.0` , -0.5 , 0.5` ]] ,
PlotStyle -> [[ RGBColor [ 0 , 0.25 , 1 ] , RGBColor [ 1 , 0.25
, 0 ] ]] ] ,

```

```

ParametricPlot3D [
[[ C1C , C1NY / C1CY C1C , RKY C1C/(C1C+C1CY) ]] ,
[[ C1C , 0 , CChi ]] ,
Exclusions -> None ,
PlotPoints -> Ppoints ,
ImageSize -> [[ Pwidth , Pwidth ]] ,
PlotStyle -> [[ Black , Thick ]] ] ,

```

```

ParametricPlot3D [
[[ C1C , C1NZ / C1CZ C1C , RKZ C1C/(C1C+C1CZ) ]] ,
[[ C1C , 0 , CChi ]] ,
Exclusions -> None ,
PlotPoints -> Ppoints ,
ImageSize -> [[ Pwidth , Pwidth ]] ,
PlotStyle -> [[ Black , Thick ]] ] ]

```

```

(* Differential Surface *)
Clear [ ColorScale ] ;
ColorScale = Max [ Abs [ MaxValue [ [[ RKY Min [ C1C/(C1C
+C1CY),C1N/(C1N+C1NY) ] - RKZ Min [
C1C/(C1C+C1CZ),C1N/(C1N+C1NZ) ] , 0 <= C1C <= CChi , 0 <= C1N <=
CNhi
]] , [[ C1C , C1N ]] ] ] , Abs [ MinValue [ [[ RKY Min [
C1C/(C1C+C1CY),C1N/(C1N+C1NY) ] - RKZ Min [
C1C/(C1C+C1CZ),C1N/(C1N+C1NZ) ] , 0 <= C1C <= CChi , 0 <= C1N <=
CNhi ]] , [[ C1C , C1N ]] ] ] ] ;

```

```

Plot3D [
[[ RKY Min [ C1C/(C1C+C1CY),C1N/(C1N+C1NY) ] -
RKZ Min [ C1C/(C1C+C1CZ),C1N/(C1N+C1NZ) ] ]] ,
[[ C1C,0,CChi ]] , [[ C1N,0,CNhi ]] ,
Exclusions -> None ,
LabelStyle -> [[ 25 , FontFamily -> "Helvetica" ]] ,PlotLabel ->
Style [ "Differential Growth Response\nBlue-Y: "<> PopNameY <>
"\nRed-Z: " <> PopNameZ <> "\nColor Max at ΔR = " <> ToString [
NumberForm [ ColorScale , 3 ] ] , 25 , FontFamily -> "Helvetica"
] ,

```

```

AxesLabel-> [[ " [ A ] ", " [ B ] ", "Δ R" ] ] ,
AxesEdge-> [[ [[ -1,-1 ] ] , [[ -1,-1 ] ] , [[ -1,1 ] ] ] ] ,
PlotPoints->Ppoints,
ImageSize-> [[ Pwidth,Pwidth ] ] ,
ViewPoint-> [[ -1.0^, -1.0, 0.5^ ] ] ,
ColorFunction-> Function [ [[ x, y, z ] ] ,
  RGBColor [ Max [ 0, -(z/ColorScale) ] , 1 - Abs [ z/ColorScale
] ,
  Max [ 0, z/ColorScale ] ] ] ,
ColorFunctionScaling->False ]

(* Differential Density *)
Clear [ ColorScale ] ;
ColorScale = Max [ Abs [ MaxValue [ [[ RKY Min [
C1C/(C1C+C1CY), C1N/(C1N+C1NY) ] - RKZ Min [
C1C/(C1C+C1CZ), C1N/(C1N+C1NZ) ] , 0 ≤ C1C ≤ CChi , 0 ≤ C1N ≤
CNhi
]] , [[ C1C , C1N ] ] ] ] , Abs [ MinValue [ [[ RKY Min [
C1C/(C1C+C1CY), C1N/(C1N+C1NY) ] - RKZ Min [
C1C/(C1C+C1CZ), C1N/(C1N+C1NZ) ] , 0 ≤ C1C ≤ CChi , 0 ≤ C1N ≤
CNhi ] ] , [[ C1C , C1N ] ] ] ] ] ;

Show [

  DensityPlot [
    RKY Min [ C1C/(C1C+C1CY), C1N/(C1N+C1NY) ] -
    RKZ Min [ C1C/(C1C+C1CZ), C1N/(C1N+C1NZ) ] ,
    [[ C1C,0,CChi ] ] , [[ C1N,0,CNhi ] ] ,
    Exclusions -> None ,
    LabelStyle -> [[ 25 , FontFamily -> "Helvetica" ] ] , PlotLabel ->
    Style [ "Differential Growth Response\nBlue-Y: "<> PopNameY <>
"\nRed-Z: " <> PopNameZ <> "\nColor Max at ΔR = " <> ToString [
NumberForm [ ColorScale , 3 ] ] ] , 25 , FontFamily -> "Helvetica"
] ,
    AxesLabel-> [[ " [ A ] ", " [ B ] " ] ] ,
    PlotPoints->Ppoints,
    ImageSize-> [[ Pwidth,Pwidth ] ] ,
    ColorFunction-> Function [ [[ z ] ] ,
      RGBColor [ Max [ 0, -(z/ColorScale) ] , 1 - Abs [ z/ColorScale
] ,
      Max [ 0, z/ColorScale ] ] ] ,
    ColorFunctionScaling->False ] ,

  Plot [
    [[ C1NY / C1CY C1C ] ] ,
    [[ C1C , 0 , CChi ] ] ,
    Exclusions -> None ,

```

```

PlotPoints -> Ppoints ,
ImageSize -> [[ Pwidth , Pwidth ] ] ,
PlotStyle -> [[ Black , Thick ] ] ] ,

Plot [
  [[ C1NZ / C1CZ C1C ] ] ,
  [[ C1C , 0 , CChi ] ] ,
Exclusions -> None ,
PlotPoints -> Ppoints ,
ImageSize -> [[ Pwidth , Pwidth ] ] ,
PlotStyle -> [[ Black , Thick ] ] ] ]

(* Differential Contour *)
Clear [ ColorScale ] ;
ColorScale = Max [ Abs [ MaxValue [ [[ RKY Min [
C1C/(C1C+C1CY),C1N/(C1N+C1NY) ] - RKZ Min [
C1C/(C1C+C1CZ),C1N/(C1N+C1NZ) ] , 0 ≤ C1C ≤ CChi , 0 ≤ C1N ≤
CNhi
]] , [[ C1C , C1N ] ] ] ] , Abs [ MinValue [ [[ RKY Min [
C1C/(C1C+C1CY),C1N/(C1N+C1NY) ] - RKZ Min [
C1C/(C1C+C1CZ),C1N/(C1N+C1NZ) ] , 0 ≤ C1C ≤ CChi , 0 ≤ C1N ≤
CNhi ] ] , [[ C1C , C1N ] ] ] ] ] ;

Show [

ContourPlot [
  RKY Min [ C1C/(C1C+C1CY),C1N/(C1N+C1NY) ] -
  RKZ Min [ C1C/(C1C+C1CZ),C1N/(C1N+C1NZ) ] ,
  [[ C1C,0,CChi ] ] , [[ C1N,0,CNhi ] ] ,
Exclusions -> None ,
Contours -> [[ -0.1 , -0.05 , -0.04 , -0.03 , -0.02 , -0.01 , 0 ,
0.01 , 0.02 , 0.03 , 0.04 , 0.05 , 0.1 ] ] ,
ContourLabels -> All ,
LabelStyle -> [[ 25 , FontFamily -> "Helvetica" ] ] ,
PlotLabel -> Style [ "Differential Growth Response\nBlue-Y: "<>
PopNameY <> "\nRed-Z: " <> PopNameZ <> "\nColor Max at ΔR = " <>
ToString [ NumberForm [ ColorScale , 3 ] ] , 25 , FontFamily ->
"Helvetica" ] ,
Frame -> False ,
Axes -> True ,
AxesLabel-> [[ " [ A ] " ," [ B ] " ] ] ,
PlotPoints->Ppoints,
ImageSize-> [[ Pwidth,Pwidth ] ] ,
Contours-> 16 ,
ContourLabels -> False ,
ColorFunction-> Function [ [[ z ] ] ,
  RGBColor [ Max [ 0 , -(z/ColorScale) ] , 1 - Abs [ z/ColorScale

```

```

] ,
  Max [ 0, z/ColorScale ] ] ] ,
ColorFunctionScaling->False ] ,

Plot [
  [[ C1NY / C1CY C1C ]] ,
  [[ C1C , 0 , CChi ]] ,
Exclusions -> None ,
PlotPoints -> Ppoints ,
ImageSize -> [[ Pwidth , Pwidth ]] ,
PlotStyle -> [[ Black , Thick ]] ] ] ,

Plot [
  [[ C1NZ / C1CZ C1C ]] ,
  [[ C1C , 0 , CChi ]] ,
Exclusions -> None ,
PlotPoints -> Ppoints ,
ImageSize -> [[ Pwidth , Pwidth ]] ,
PlotStyle -> [[ Black , Thick ]] ] ]

```

Figure A-1. **Growth Response Plot Code, *Mathematica*®**  
**Begins on page 123.**

This is the entire *Mathematica*® code of our growth response plotting program. It is “front-loaded” with the parameters of our six experimental populations used in this work, which may be setup for any desired demonstration combination. *Note:* The *Mathematica*® code characters “left curly bracket” and “right curly bracket” have been replaced by double characters `[[` and `]]`, respectively, to eliminate interference with our word processor and bibliography manager programs.

“ColorScale” variable captures the maximum absolute difference to be plotted.

```
ColorScale =
Max [
  Abs [
    MaxValue [
]] RKY Min [ C1C/(C1C +C1CY) ,C1N/(C1N+C1NY) ] -
      RKZ Min [ C1C/(C1C+C1CZ) ,C1N/(C1N+C1NZ) ] ,
      0 <= C1C <= CChi , 0 <= C1N <= CNhi ]] ,
]] C1C , C1N ]]
]
] ,
Abs [
  MinValue [
]] RKY Min [ C1C/(C1C+C1CY) ,C1N/(C1N+C1NY) ] -
      RKZ Min [ C1C/(C1C+C1CZ) ,C1N/(C1N+C1NZ) ] ,
      0 <= C1C <= CChi , 0 <= C1N <= CNhi ]] ,
]] C1C , C1N ]]
]
]
] ;
```

“Plot3D” function generates the plot.

```
Plot3D [
]] RKY Min [ C1C/(C1C+C1CY) ,C1N/(C1N+C1NY) ] -
  RKZ Min [ C1C/(C1C+C1CZ) ,C1N/(C1N+C1NZ) ] ]] ,
]] C1C,0,CChi ]] , ]] C1N,0,CNhi ]] ,
```

“ColorFunction” colors the surface from red through green to blue as the response difference value  $z$  runs from “minus ColorScale” through zero to “plus ColorScale”

```
ColorFunction-> Function [ ]] x, y, z ]] ,
RGBColor [ Max [ 0, -(z/ColorScale) ] ,
  1 - Abs [ z/ColorScale ] ,
  Max [ 0, z/ColorScale ] ] ] ,
```

#### Figure A-2. Growth Response Plot Code, Annotated Section

This is the section of our *Mathematica*® growth response plotting program which generates the differential surface plot. Key computations are noted. **Note:** The *Mathematica*® code characters “left curly bracket” and “right curly bracket” have been replaced by double characters `[[` and `]]`, respectively, to eliminate interference with our word processor and bibliography manager programs.

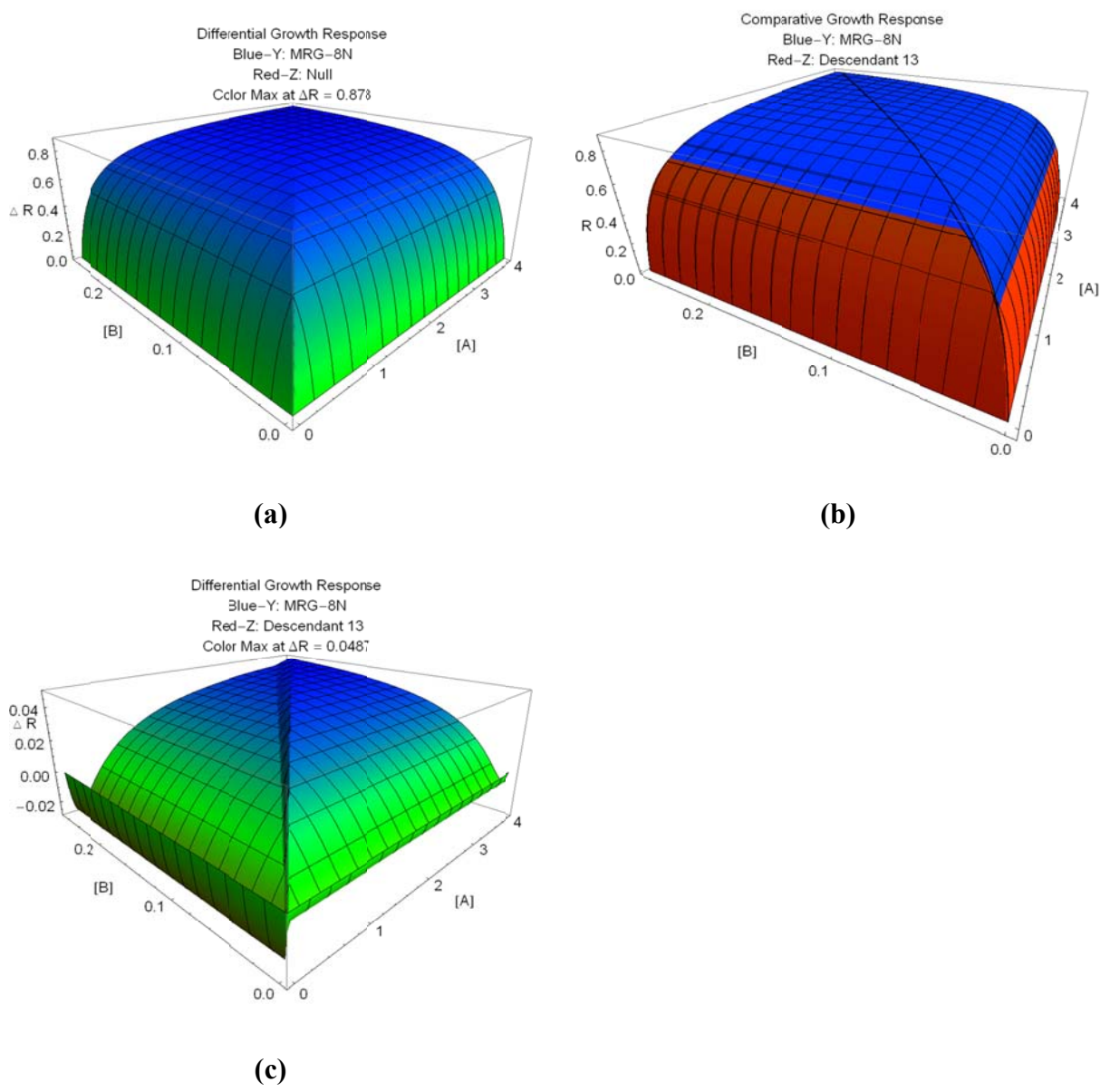


Figure A-3. **Response Surface Plots**

**Panel (a)** shows the “dome tent” growth response surface of a single population across a resource space, shading from zero growth in “full green” to maximum plotted response (0.876) in “full blue”. The OPL follows the “ridge” of the tent. Quantitative values of the response can be read from the grid-mesh lines and the vertical scale. **Panel (b)** plots the surfaces of two populations simultaneously and shows a “punch through” relationship of the surfaces when one population (blue) has a higher maximum growth capability,  $R_K$ , but steeper per-resource responses,  $C_{IA}$  and  $C_{IB}$ , than the other. **Panel (c)** shows the qualitative and quantitative difference of the same two populations’ growth responses. Areas of strong or weak dominance, likely coexistence and stochastic sensitivity of the response relationship can be located.

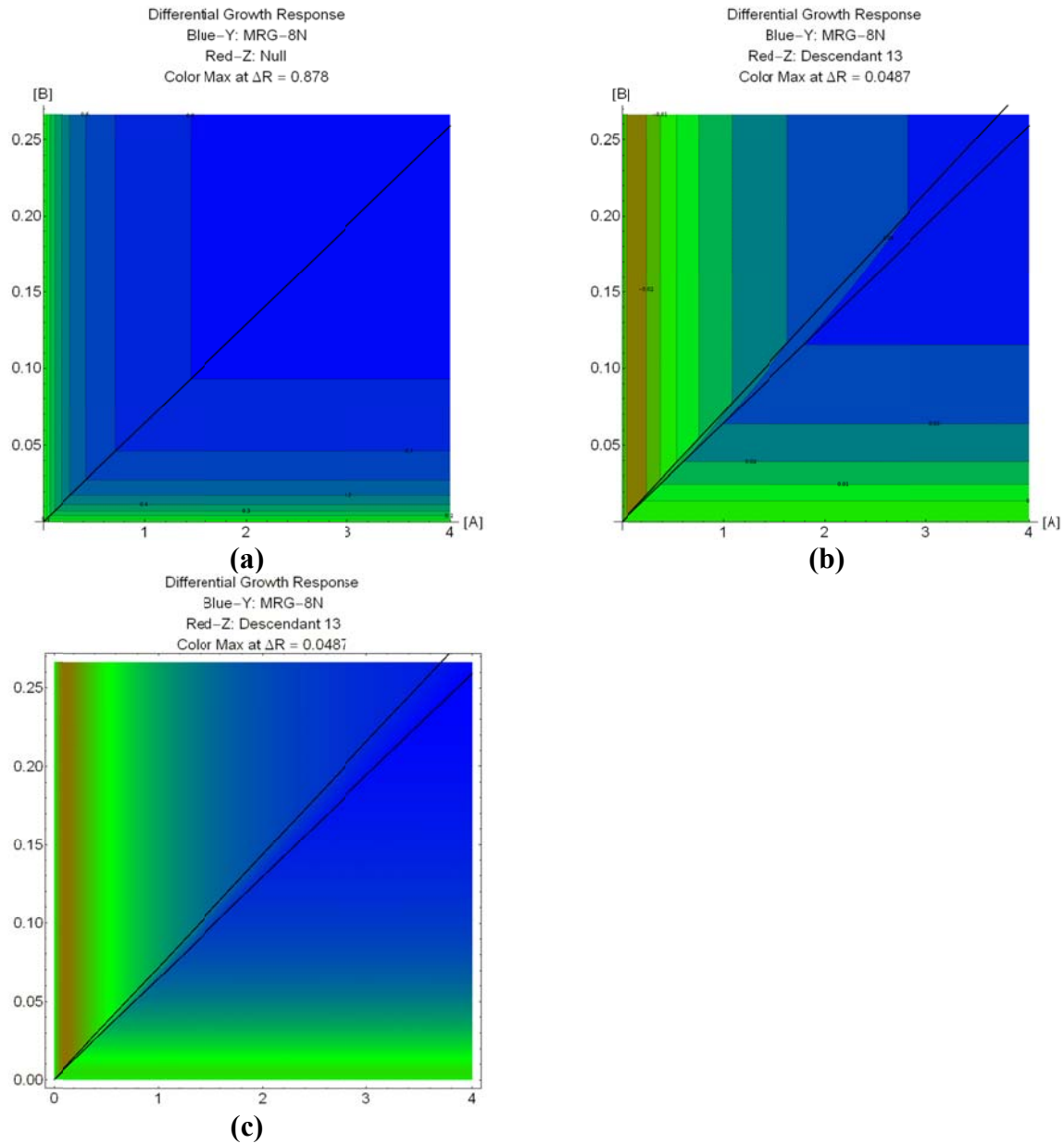


Figure A-4. **Shaded and Contour Response Plots**

**Panel (a)** is a shaded contour plot of a single population's dome tent response surface, shaded green to blue from zero to maximum plotted growth response and partitioned with contour lines. This plot gives both the impression of surface shape, useful when comparing plots for multiple populations, and quantitative values of growth response. The contour lines can be specified individually when particular growth isoclines are of interest or in logarithmic or linear spacing when specific intervals are of interest. **Panel (b)** is a shaded contour plot of the same data as in Figure A-0-3 (c), difference in growth response of two populations, from which the differential response may be read quantitatively. "Full blue" indicates dominance by one population (example, strain MRG-8N) while "full red" indicates dominance by the other population (strain Desc-13) and "full green" indicates zero difference in growth response. **Panel (c)** removes the contour lines from Panel (b) and presents the differential response as continuous shading to permit more insight at some expense of specificity.

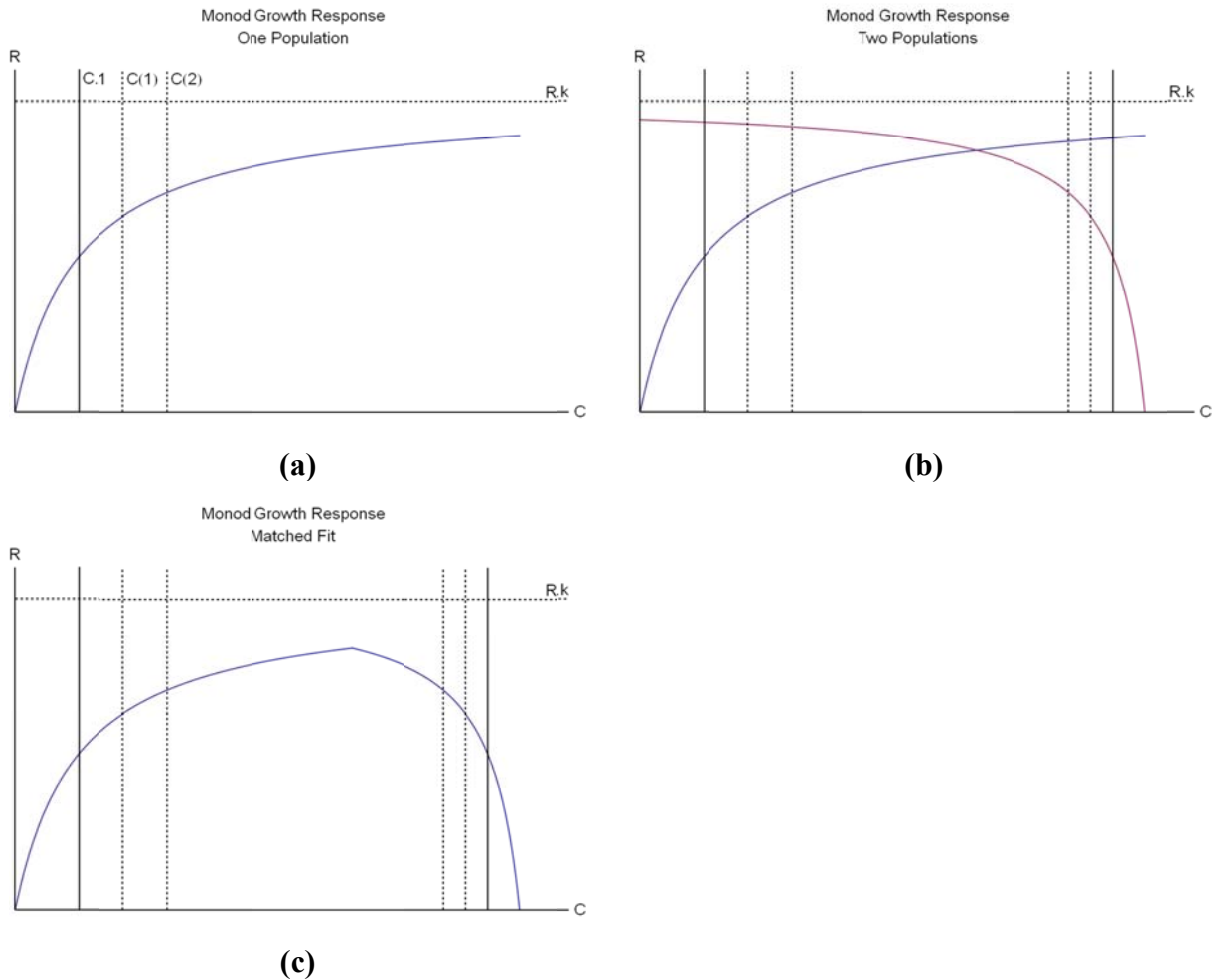


Figure A-5. **Monod Curve Fitting**

**Panel (a)** shows a single Monod response curve in coordinates of  $C$ , resource supply, and  $R$ , realized response. The population characteristics to be determined are  $R_k$ , maximum capable growth rate, and  $C_1$ , half-saturation constant for the resource. We have measured realized growth rate,  $R$ , at two supply points,  $C(1)$  and  $C(2)$  of the single resource. Fitting to this single curve requires no legerdemain. **Panel (b)** shows two such Monod response curves to be fitted from measured responses on supply points of two resources—one increasing left-to-right and the other increasing right-to-left. The view is as if we were in Figure 2-2 or Figure 3-3 (a) looking from the origin outward along the *OPL* ridge of the dome tent. We need to fit the pair of curves, “below” their intersection, to the population common  $R_k$  and two, per-resource, values of  $C_1$ . **Panel (c)** is the fit we need to achieve, where the portion of each curve “above” their intersection has been eliminated as if by the arithmetic *min*, “minimum of”, operator in whatever formula we may be using for the individual curves.

Figure A-0-7 presents the complete Mathematica® code and Figure A-0-9 presents the core Mathematica® code, annotated, in which we achieve this curve-fitting with assistance of the Sigmoid Switch of Figure A-0-6.

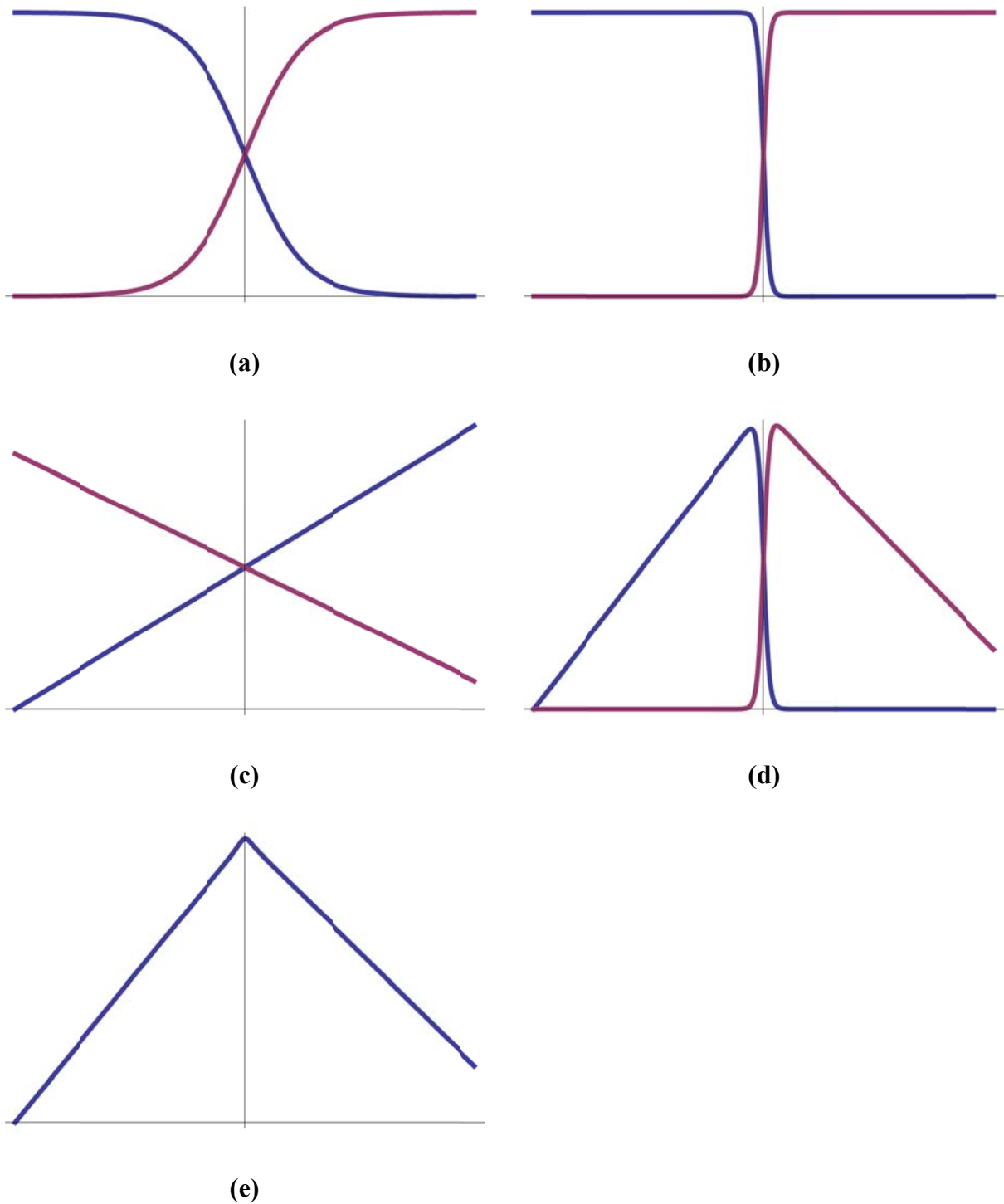


Figure A-6. **Sigmoid Switch**

**Panel (a)** shows the elementary hyperbolic sigmoid function,  $\frac{1}{1+e^{-x}}$ , and its complement,  $\frac{e^{-x}}{1+e^{-x}}$ . Adding a “steepness” parameter,  $S$ , and a “crossover” parameter,  $O$ , produces  $\frac{1}{1+e^{-S(x-O)}}$  and  $\frac{e^{-S(x-O)}}{1+e^{-S(x-O)}}$ . **Panel (b)** shows our essential ledgerdmain of applying a

large steepness parameter,  $S$ , to make the “crossover valley” become “narrower”. The crossover point remains at  $x=0$ . The sum of the two curves remains, of course equal to  $I$ . **Panel (c)** shows a pair of simple, “counter-sloping” functions to which we wish to apply the arithmetic *min*, “minimum of”, operator intending a result which looks like (e). **Panel (d)** shows the individual products of multiplying the “ascending” line of (c) by the “left” sigmoid of (b) and the “descending” line of (c) by the “right” sigmoid of (b). The “high” side of each line has been suppressed by the complementary sigmoids as the “crossover” point, now  $O=0$ , is the same for the lines and the sigmoids. **Panel (e)** shows the sum of the products from (d). The “peak” of the sum is, visibly, slightly “rounded” but can be made as “sharp” as desired by an appropriate value of  $S$ , the steepness parameter. It is trivial here to shift the crossover of the sigmoids to match the crossover of the source functions by solving for the intersection value,  $x$ , of the source functions and setting the sigmoids’  $O$  parameter to that value.

Figure A-0-7 presents the complete *Mathematica*® code and Figure A-0-9 presents the core *Mathematica*® code, annotated, in which we use this Sigmoid Switch to achieve the curve-fitting shown in Figure A-0-5.

**Begin Figure A-7.**

```

CLEAR [ InFileName ] ;
Print [
"===== " ]
;
Print [ "Use this button to select the file for the Population."
]
InFileName = "*.csv";
FileNameSetter [ Dynamic [ InFileName ] ]
Print [
"===== " ]
;
=====
Use this button to select the file for the Population.
Browse...
=====
Print [
"===== " ]
;
Print [ "----- Population data file ",InFileName ] ;
Clear [ DataMatrix ] ;
DataMatrix = Import [ InFileName , "Data" ] ;
Print [ "----- Population data " ] ;
DataMatrix
Print [
"===== " ]
;

Flow=1/4.69;
SS = 1000 ;
Clear [ RK,C1C,C1N,CC,CN ] ;

FitOutput =
NonlinearModelFit [
DataMatrix,
[[
((1-1/(1+E^(SS (C1C/C1N-CC/CN )/(C1C/C1N))))
*
(( RK CC)/(CC+C1C )-Flow)
+
(1-1/( 1+ E^( SS (C1N/C1C-CN/CC)/(C1N/C1C))))
*
(( RK CN)/(CN+C1N)-Flow)),
RK>0, C1C >0, C1N>0
]],
[[ RK, C1C , C1N ]],
[[ CC , CN ]]
```

```

]

Print [ "----- BestFitParameters" ] ;
sRK = RK /. FitOutput [ "BestFitParameters" ] [ [ 1 ] ] ;
sC1C = C1C /. FitOutput [ "BestFitParameters" ] [ [ 2 ] ] ;
sC1N = C1N /. FitOutput [ "BestFitParameters" ] [ [ 3 ] ] ;
CNRatio = sC1C / sC1N ;

Print [ "----- Maximum Capable Intrinsic Growth Rate" ]
sRK

Print [ "----- Carbon Half-Max Concentration" ]
sC1C

Print [ "----- Nitrogen Half-Max Concentration" ]
sC1N

Print [ "----- Dual-Limiting C:N Ratio" ]
CNRatio

Print [ "----- RSquared" ] ; FitOutput [ "RSquared" ]

Print [ "----- AdjustedRSquared" ] ; FitOutput [
"AdjustedRSquared" ]

Print [ "----- AIC" ] ; FitOutput [ "AIC" ]

Print [ "----- ANOVATable" ] ; FitOutput [ "ANOVATable" ]

Print [ "----- ParameterConfidenceIntervalTable" ] ; FitOutput [
"ParameterConfidenceIntervalTable" ]

Print [ "----- ParameterTable" ] ; FitOutput [ "ParameterTable"
]

Print [
"===== " ]
;

```

**Figure A-7. Curve-Fitting Code**

**Begins on page 135.**

This is the entire *Mathematica*® code of our growth response curve-fitting program. The essential core of this code is presented with annotation in Figure A-0-9.

**Note:** The *Mathematica*® code characters “left curly bracket” and “right curly bracket” have been replaced by double characters `[[` and `]]`, respectively, to eliminate interference with our word processor and bibliography manager programs.

**Begin Figure A-8.**

```
=====
----- Population data file G:\- Research\Characterization\101-
102 MRG 2.csv
```

```
----- Population data
[[ [[ 1.5,0.032,0.515952 ]], [[ 1.5,0.032,0.286778 ]], [[
1.5,0.032,0.526386 ]], [[ 1.5,0.032,0.418471 ]], [[
1.5,0.016,0.167222 ]], [[ 1.5,0.016,0.188846 ]], [[
1.5,0.016,0.21093 ]], [[ 1.5,0.016,0.181685 ]], [[
1.5,0.008,0.105375 ]], [[ 1.5,0.008,0.0640698 ]], [[
1.5,0.008,0.0356098 ]], [[ 1.5,0.008,0.0737079 ]], [[
1.5,0.004,0.0497403 ]], [[ 1.5,0.004,0.0319277 ]], [[
1.5,0.004,0.062561 ]], [[ 1.5,0.004,0.0228235 ]], [[
0.75,0.064,0.491205 ]], [[ 0.75,0.064,0.433889 ]], [[
0.75,0.064,0.404242 ]], [[ 0.75,0.064,0.389767 ]], [[
0.375,0.064,0.300111 ]], [[ 0.375,0.064,0.299103 ]], [[
0.375,0.064,0.298095 ]], [[ 0.1875,0.064,0.182021 ]], [[
0.1875,0.064,0.18253 ]], [[ 0.1875,0.064,0.177065 ]], [[
0.1875,0.064,0.166386 ]], [[ 0.09375,0.064,0.110111 ]], [[
0.09375,0.064,0.0251316 ]], [[ 0.09375,0.064,0.10069 ]], [[
0.09375,0.064,0.0481395 ]]] ]]
```

```
=====
FittedModel [

$$\left(1 - \frac{1}{1 + e^{62.0065(\ll 19 \gg - \ll 1 \gg)}}\right) \left(-0.21322 + \frac{0.833635 \text{ kSupC}}{0.210322 + \text{kSupC}}\right) + \left(1 - \frac{1}{1 + e^{\ll 1 \gg}}\right) (-0.21322 + \ll 1 \gg)$$

]
```

```
----- BestFitParameters
----- Maximum Capable Intrinsic Growth Rate
0.833635
----- Carbon Half-Max Concentration
0.210322
----- Nitrogen Half-Max Concentration
0.0130414
----- Dual-Limiting C:N Ratio
16.1273

----- RSquared
0.951557

----- AdjustedRSquared
0.946367

----- AIC
FittedModel::constr: The property values (Raich et al.) assume
```

an unconstrained model. The results for these properties may not be valid, particularly if the fitted parameters are near a constraint boundary.

-80.8072

----- ANOVATable

FittedModel::constr: The property values [[ ANOVATable ]] assume an unconstrained model. The results for these properties may not be valid, particularly if the fitted parameters are near a constraint boundary.

```
[[
[[ , DF, SS, MS ]] ,
[[ Model, 3, 2.03212, 0.677373 ]] ,
[[ Error, 28, 0.103453, 0.00369475 ]] ,
[[ Uncorrected Total, 31, 2.13557, ]] ,
[[ Corrected Total, 30, 0.751379, ]]
]]
```

----- ParameterConfidenceIntervalTable

FittedModel::constr: The property values [[ ParameterConfidenceIntervalTable ]] assume an unconstrained model. The results for these properties may not be valid, particularly if the fitted parameters are near a constraint boundary.

```
[[
[[ , Estimate, Standard Error, Confidence Interval ]] ,
[[ RK, 0.833635, 0.0544411, [[ 0.722117,0.945152 ]] ]] ,
[[ C1C, 0.210322, 0.0379248, [[ 0.132637,0.288008 ]] ]] ,
[[ C1N, 0.0130414, 0.00214042, [[ 0.00865691,0.0174258 ]] ]]
]]
```

----- ParameterTable

FittedModel::constr: The property values [[ ParameterTable ]] assume an unconstrained model. The results for these properties may not be valid, particularly if the fitted parameters are near a constraint boundary.

```
[[
[[ , Estimate, Standard Error, t Statistic, P-Value ]] ,
[[ RK, 0.833635, 0.0544411, 15.3126, 3.89246×10-15 ]] ,
[[ C1C, 0.210322, 0.0379248, 5.54577, 6.25477×10-6 ]] ,
[[ C1N, 0.0130414, 0.00214042, 6.0929, 1.42587×10-6 ]]
]]
```

=====

### Figure A-8. Curve-Fitting Output

**Begins on page 137.**

This is the complete output, including the experimental data matrix, individually computed values and generated output from the *NonlinearModelFit[]* function for curve-fitting for a

typical yeast strain. This output includes warning diagnostics from *Mathematica*® which we always check for applicability to each run. We did find that the first Characterization Protocol (chemostat) run of our evolved descendant strain *Desc-01* (see Chapter 4) had a fatal interference with the initial value of one resource at one test point so we repeated the run for that strain with a different set of test points.

**Note:** The *Mathematica*® code characters “left curly bracket” and “right curly bracket” have been replaced by double characters `[[` and `]]`, respectively, to eliminate interference with our word processor and bibliography manager programs.

**Begin Figure A-9.**

```
FitOutput =
  NonlinearModelFit [
```

*DataMatrix* is loaded earlier in the program with the ([C],[N],R) triplets from the Characterization Protocol chemostat run. Variables *SS* and *Flow* are set earlier.

```
DataMatrix,
[[
```

The function to be fitted...

```
((1-1/(1+E^(SS(C1C/C1N-CC/CN)/(C1C/C1N))))
*
((RK CC)/(CC+C1C)-Flow)
+
(1-1/(1+E^(SS(C1N/C1C-CN/CC)/(C1N/C1C))))
*
((RK CN)/(CN+C1N)-Flow)),
```

The function (in Monod's formulation) to which we would like to fit the data points is:

$$R = R_k \min \left[ \frac{C_A}{C_{1A}+C_A}, \frac{C_B}{C_{1B}+C_B} \right] - Flow \quad ()$$

The *min* (minimum of) operator, however, is incompatible with the curve-fitting function which is intended to be used with doubly continuous functions (*f* and *f'* both continuous) but, in reality, requires only that the objective function *behave as if it were* doubly continuous. So we fit to the following function which behaves as if it were doubly continuous for benefit of the underlying successive-approximation algorithm of the *NonlinearModelFit[]* function:

$$R = \text{SigC} R_k \frac{C_C}{C_{1C}+C_C} + \text{SigN} R_k \frac{C_N}{C_{1N}+C_N} - Flow \quad ()$$

*SigC* and *SigN* are complementary (“high left” and “high right”) computations of the hyperbolic sigmoid such that the “limiting, less than crossover” *C* (carbon) or *N* (nitrogen) term is multiplied by 1 and the “non-limiting, greater than crossover” term is multiplied by zero. *I.e.*, this formula “end-runs” the curve-fitting algorithm by simulating the *min* operator with a doubly continuous complete function.

The elementary form of the sigmoid function is  $y = \frac{1}{1+e^x}$  or  $y = \frac{1}{1+e^{1(x-0)}}$  which we say has its “crossover” point at  $x=0$  and “steepness” factor of *I*. This can be expanded to  $y = \frac{1}{1+e^{S(x-0)}}$  with a crossover point at  $x=0$  and steepness *S*. We set the variable *SS* to our desired steepness factor at the front of our program. The crossover point is re-computed with every iteration (for each data point) of the solution (on the “carbon side” shown here) as  $O = (C_{1C}/C_{1N} - C_C/C_N)/(C_{1C}/C_{1N})$  which compares the estimated *C:N* response ratio to the instant *C:N* supply ratio. The result of complementary (and asymptotic) multiplier terms is that only per-resource-limiting data points affect the per-resource response calculation.

These constraints are functionally unnecessary, making no difference whatsoever in the output, but appear to reduce the number of iterations required for solution.

```
RK>0, C1C >0, C1N>0
```

```
]] ,
```

The solution variables, to be solved for, are  $R_K$ ,  $C_{IC}$  and  $C_{IN}$ .

```
[[ RK, C1C , C1N ]] ,
```

Variable values to be taken from DataMatrix are  $C_C$  and  $C_N$ . The objective variable ( $R$  in our case) is always the last column of the matrix.

```
[[ CC , CN ]]
```

We have found that the solution frequently does not find stable convergence but “dithers” about the final solution, apparently due to our asymptotic crossover function. Repeated testing with manual intervention to the program has shown that closest-to-convergence is usually achieved in about 100 iterations and never in more than 250 iterations. Several examinations, by manual intervention to the program, have found no more than 1 part per million dither of the solution value in any of the three fitted parameters after 250 iterations. For simplicity we have chosen to set a limit to the number of iterations and for safety margin we have set the limit at 1000 iterations.

```
( * , MaxIterations → 1000,
```

We will show this output from *NonlinearModelFit*] along with the other data specified in Figure A-0-7.

```
RegressionReport → [[ SummaryReport , FitOutput ,  
ParameterConfidenceRegion , FitResiduals ]] *)  
]
```

### Figure A-9. Curve-Fitting Code, Annotated Core Begins on page 140.

This code is the core of our curve-fitting algorithm, including our use of the hyperbolic-asymptote “switch function”.

Figure A-0-5 shows the problem of intersecting response curves and Figure A-0-6 shows the idea of how we apply the sigmoid switch to solve the problem.

**Note:** The *Mathematica*® code characters “left curly bracket” and “right curly bracket” have been replaced by double characters `[[` and `]]`, respectively, to eliminate interference with our word processor and bibliography manager programs.

## Appendix B, Yeast Strains

Our “MRG” original yeast cultures were received 13 Feb 2006 from Prof. Matthew Goddard, University of Auckland, NZ, (Goddard 2006).

Quoting Prof. Goddard’s letter of transmittal:

“Each of the strains was isolated from a barrel ferment of Chardonnay juice from Kumeu River in Auckland. These are all from natural ferments, *i.e.*, no commercial microbes have been added to the juice.

“The Internal Transcribed Spacer One, 5.8S ribosomal gene and Internal Transcribed Spacer Two regions of each of these strains have been amplified by PCR. The PCR amplicon was then cut with specific restriction endonucleases and all gave the pattern distinctive for [*Saccharomyces*] *cerevisiae*. One of the members of this distinctive pattern group was two-way sequenced and has a DNA sequence identical to that of *S. cerevisiae*.

“These strains were then micro-satellite typed at six loci and the result of this is [Table B-1]. ...you can see that each strain has one for each of the *a* and *alpha* alleles which is strongly suggesting that these are all diploids. Each of the eight is unique with respect to the remaining five loci - this indicates that each has a different genotype. I've tried to pick a range - for example you have some that appear completely homozygous (type 7) and some that are heterozygous at the five non-MAT loci (type 9) and others that are in between.”

From other communication with Prof. Goddard we have that these cultures are fewer than fifty generations removed from the barrel ferment and have never been subjected to growth-limiting media.

Tables

**Table B-1. Yeast Strains Characteristics.**

Genotyped Characteristics of Our Yeast Strains as Reported by Goddard

**Type** is Goddard’s identifying number; **091-Ned**, **035-Fam**, **276-Hex**, **009-Fam** and **160-Hex** are typed microsatellite loci; **alpha-Fam** and **a-Hex** are the mating type locus; “**Type 2**” and “**Type 8**” are the isolates we selected to use as experimental strains **MRG-2** and **MRG-8**, respectively.

<b>Type</b>	<b>091-Ned</b>	<b>035-Fam</b>	<b>276-Hex</b>	<b>009-Fam</b>	<b>160-Hex</b>	<b>alpha-Fam</b>	<b>a-Hex</b>
1	249	337.5	395	434 454.5	466	468.5	492
2	249	358.5	427	422.5 451.5	446.5 451.5	468.5	492
3	249	358.5	427	422.5 452	451.5	468.5	492
6	296	337.5	395	434.5 454.5	466	468.5	492
7	318	358.5	447	451.5	475	468.5	492
8	248.5 296.5	337.5	395	434 454	466	468.5	492
9	249 263	336 358.5	430 437	419.5 451.5	447 451.5	468.5	492
23	318 339.5	336 358.5	427	449 451.5	469	468.5	492

## Appendix C, Biomass and Other Measurements Calibrations

Throughout our work we follow the lead of Monod (1949), MacArthur (1972) and others (Adams et al. 1985, Poilpre et al. 2002, Zinn et al. 2004) in using biomass, reported in **mg mL<sup>-1</sup>**, as our measure of population size, Monod's *density*, *N*. We also used, however, measurements of cell count, measured as **cells mL<sup>-1</sup>**, or optical density, measured as Nephelometric Turbidity Units, **NTU**—both of which we convert to our standard reporting unit of **mg mL<sup>-1</sup>**.

This table gives coefficients for quick conversion among observed and reported measures. Multiply the unit in the top row by the coefficient at the intersection to get the unit in the left column:

	<b>mg mL<sup>-1</sup></b>	<b>(10<sup>6</sup> cells) mL<sup>-1</sup></b>	<b>NTU</b>
<b>mg mL<sup>-1</sup></b>		0.0127	0.000892
<b>(10<sup>6</sup> cells) mL<sup>-1</sup></b>	78.5		0.0717
<b>NTU</b>	1120.	13.9	

We determined biomass density by separating and drying the mass from a known culture volume as described in Chapter 3. We determined cell count from a sample of a culture by a standard hemocytometer under 400 diameters magnification. We determined optical density by a T100 Turbidity Meter (Oakton Instruments, Vernon Hills, IL, USA). Our most common method of population determination in the work reported here was direct measurement of biomass—as for our Characterization Protocol. Our second method was conversion of optical density to biomass—as for equalizing inoculation of two strains into competition medium.

T Table C-1 through Table C-3 show our calibration formulae, linear fit parameters and data from early culture runs for the three conversions among measurement and reporting units.

Tables

Table C-1. **Calibration: NTU Density versus Mass Density.**

$$[mg\ mL^{-1}] = 0.00892 [NTU]$$

$$[NTU] = 1120 [mg\ mL^{-1}]$$

Linear estimate of  $y = m \cdot x + 0 : (mg\ mL^{-1}) = m (NTU)$ . **se**, standard error of  $m$ ;  $r^2$ , correlation coefficient; **F**, F statistic; **ss.reg**, regression sum of squares; **se.y**, standard error of  $y$  estimate; **df**, degrees of freedom; **ss.resid**, residual sum of squares.

<b>m</b>	0.000892381			
<b>se</b>	2.50901E-05			
<b>r<sup>2</sup></b>	0.971582594	0.066641828	<b>se.y</b>	
<b>F</b>	1265.018891	37	<b>df</b>	
<b>ss.reg</b>	5.618117509	0.164321932	<b>ss.resid</b>	

**Vol.:** culture sample volume, mL; **Vial Net:** culture sample dry mass, mg; **Mass:** culture sample density, mg mL<sup>-1</sup>; **NTU:** turbidity.

<u>Vol.</u>	<u>Vial Net</u>	<u>Mass</u>	<u>NTU</u>	<u>Vol.</u>	<u>Vial Net</u>	<u>Mass</u>	<u>NTU</u>
39.0	6.0	0.154	44.9	37.5	4.1	0.109	88.30
36.0	5.8	0.161	58.3	38.0	6.0	0.158	167.00
39.0	6.9	0.177	79.2	36.0	6.6	0.183	210.00
36.0	6.4	0.178	65.4	36.0	6.6	0.183	213.00
38.0	27.5	0.724	721	35.0	6.5	0.186	212.00
37.0	27.9	0.754	860	39.0	13.1	0.336	419.00
36.0	28.3	0.786	792	36.0	12.9	0.358	432.00
40.0	34.5	0.862	901	36.5	14.9	0.408	510.00
35.0	2.9	0.083	42.90	35.0	18.2	0.520	658.00
36.5	3.2	0.088	41.00	38.0	21.9	0.576	774.00
36.5	3.6	0.099	59.50	37.0	23.6	0.638	793.00
34.0	4.4	0.129	30.00	37.0	24.3	0.657	847.00
41.5	6.9	0.166	149.00				
40.0	6.8	0.170	118.00				
37.0	7.0	0.189	171.00				
39.5	8.1	0.205	143.00				
38.0	12.2	0.321	260.00				
39.5	13.0	0.329	288.00				
35.0	12.2	0.349	299.00				
37.5	13.4	0.357	295.00				
32.5	14.0	0.431	483.00				
40.0	17.4	0.435	497.00				
35.0	15.4	0.440	500.00				
40.0	2.9	0.073	66.80				
41.5	3.5	0.084	80.40				
35.0	3.8	0.109	88.10				

Table C-2. **Calibration: Mass Density versus Count.**

$$[\text{cell mL}^{-1}] = 78.5 \cdot 10^6 [\text{mg mL}^{-1}]$$

$$[\text{mg mL}^{-1}] = 0.0127 \cdot 10^{-6} [\text{cell mL}^{-1}]$$

Linear estimate of  $y = m \cdot x + 0 : ( ( 10^6 \text{ cell} ) \text{ mL}^{-1} ) = m ( \text{mg mL}^{-1} )$ . See Table C-1 for labels.

<b>m</b>	78.4733398			
<b>se</b>	2.46398347			
<b>r2</b>	0.891066131	13.28761107	<b>se.y</b>	
<b>F</b>	1014.305296	124	<b>df</b>	
<b>ss.reg</b>	179086.3597	21893.5154	<b>ss.resid</b>	

**Vol.:** culture sample volume, mL; **Vial Net:** culture sample dry mass, mg; **Mass:** culture sample density, mg mL<sup>-1</sup>; **Cell Count:** cell density (10<sup>6</sup> cells) mL<sup>-1</sup>;

<u>Vol.</u>	<u>Vial Net</u>	<u>Mass</u>	<u>Cell Count</u>	<u>Vol.</u>	<u>Vial Net</u>	<u>Mass</u>	<u>Cell Count</u>
48.5	9.3	0.192	1.86	23.0	3.0	0.130	7.07
50.0	10.0	0.200	2.07	41.5	7.9	0.190	7.64
48.0	10.3	0.215	2.93	51.0	17.6	0.345	7.71
40.5	5.3	0.131	3.14	22.0	3.0	0.136	7.96
42.0	7.7	0.183	3.14	36.0	5.8	0.161	8.3
41.0	9.6	0.234	3.21	40.0	9.6	0.240	8.43
42.0	9.2	0.219	3.57	49.0	14.5	0.296	9.07
43.0	10.4	0.242	3.71	37.0	13.1	0.354	9.27
47.5	8.0	0.168	3.79	49.0	14.8	0.302	9.43
46.0	7.1	0.154	4.00	44.5	7.7	0.173	9.55
40.0	3.3	0.082	4.07	36.0	6.4	0.178	9.65
34.0	4.4	0.129	4.10	39.0	6.9	0.177	9.85
48.0	9.6	0.200	4.14	46.0	11.9	0.259	10.14
42.0	10.9	0.260	4.29	43.0	7.9	0.184	10.30
46.0	9.0	0.196	4.36	48.0	13.9	0.290	10.33
42.0	6.0	0.143	4.69	22.0	3.0	0.136	10.83
43.0	9.6	0.223	4.86	37.0	13.5	0.365	10.84
39.0	7.6	0.195	5.07	42.0	11.3	0.269	10.86
45.0	13.2	0.293	5.21	22.0	1.8	0.082	11.62
48.0	10.3	0.215	5.71	50.0	17.1	0.342	11.71
47.0	12.1	0.257	5.79	48.0	13.4	0.279	12.21
44.0	15.1	0.343	6.14	40.5	25.8	0.637	12.7
35.0	2.9	0.083	6.25	44.0	9.6	0.218	12.75
36.5	3.2	0.088	6.30	46.5	6.7	0.144	13.05
45.0	9.8	0.218	6.45	40.0	6.8	0.170	13.20
36.0	4.5	0.125	6.63	49.0	13.5	0.276	13.21
41.5	10.5	0.253	6.64	41.5	6.9	0.166	13.35
39.0	6.0	0.154	6.75	48.0	14.3	0.298	13.79
36.5	3.6	0.099	7.00	39.5	8.1	0.205	14.00
40.5	4.7	0.116	7.00	48.0	11.9	0.248	14.36

<b>Vol.</b>	<b>Vial Net</b>	<b>Mass</b>	<b>Cell Count</b>
46.0	7.9	0.172	14.45
37.0	7.0	0.189	14.90
39.5	7.1	0.180	15.68
39.0	5.5	0.141	15.71
47.0	11.5	0.245	16.14
45.0	13.6	0.302	16.79
44.5	13.9	0.312	17.14
49.0	14.0	0.286	17.40
36.5	24.0	0.658	17.6
43.0	10.1	0.235	17.90
42.0	9.5	0.226	19.00
51.0	17.4	0.341	19.00
43.0	9.7	0.226	19.10
37.5	13.4	0.357	19.25
43.0	9.8	0.228	20.00
21.0	7.5	0.357	20.01
43.0	11.9	0.277	20.33
44.0	15.7	0.357	21.00
35.0	12.2	0.349	21.05
45.0	14.8	0.329	21.73
38.0	12.2	0.321	22.30
39.5	13.0	0.329	23.05
22.0	6.6	0.300	23.45
41.5	18.6	0.448	24.17
46.0	14.5	0.315	24.25
20.0	8.2	0.410	25.08
44.5	16.0	0.360	25.35
43.0	18.7	0.435	26.65
37.0	12.5	0.338	26.88
41.5	15.5	0.373	27.40
40.0	17.4	0.435	28.00
42.5	13.4	0.315	29.10
22.0	7.5	0.341	29.28
47.0	16.6	0.353	29.30
43.0	17.7	0.412	29.40
46.0	18.9	0.411	29.95
44.5	19.9	0.447	30.45
43.0	15.9	0.370	31.15
49.5	16.9	0.341	31.80
44.0	20.3	0.461	32.05
46.0	23.0	0.500	32.45
35.0	15.4	0.440	32.75
43.0	18.0	0.419	32.95
42.0	31.5	0.750	33.25
44.5	17.5	0.393	33.80

<b>Vol.</b>	<b>Vial Net</b>	<b>Mass</b>	<b>Cell Count</b>
46.0	21.4	0.465	36.06
21.0	14.0	0.667	37.35
32.5	14.0	0.431	40.75
44.0	24.7	0.561	45.30
48.0	30.2	0.629	46.25
22.0	13.8	0.627	47.84
21.0	18.7	0.890	49.29
29.0	19.4	0.669	56.24
27.5	18.7	0.680	56.64
20.0	9.9	0.495	71.54
37.0	23.7	0.641	87.22
36.5	21.7	0.595	97.27
49.0	43.4	1.550	101.37
20.0	24.2	1.210	109.42
49.0	38.2	1.317	110.52
48.0	37.4	1.438	118.08
34.0	47.5	1.397	127.80
40.0	53.6	1.340	139.68
29.5	38.9	1.319	146.68
36.0	49.7	1.381	146.99

Table C-3. **Calibration: NTU Density versus Count.**

$$[\text{cell mL}^{-1}] = 0.0717 \cdot 10^6 [\text{NTU}]$$

$$[\text{NTU}] = 13.9 \cdot 10^{-6} [\text{cell mL}^{-1}]$$

Linear estimate of  $y = m \cdot x + 0 : ( ( 10^6 \text{ cell} ) \text{ mL}^{-1} ) = m \cdot ( \text{NTU} )$ . See Table C-1 for labels.

<b>m</b>	0.071708435			
<b>se</b>	0.003307867			
<b>r2</b>	0.961140601	3.964434385	<b>se.y</b>	
<b>F</b>	469.9422046	19	<b>df</b>	
<b>ss.reg</b>	7385.95944	298.6180598	<b>ss.resid</b>	

**NTU:** turbidity; **Cell Count:** ( $10^6$  cells)  $\text{mL}^{-1}$ ;

<u>NTU</u>	<u>Cell Count</u>
30.00	4.10
41.00	6.30
42.90	6.25
44.9	6.75
58.3	8.3
59.50	7.00
65.4	9.65
79.2	9.85
118.00	13.20
143.00	14.00
149.00	13.35
171.00	14.90
260.00	22.30
288.00	23.05
295.00	19.25
299.00	21.05
483.00	40.75
497.00	28.00
500.00	32.75
519	33.25